

AFML-TR-74-189

Part II

AD A021512

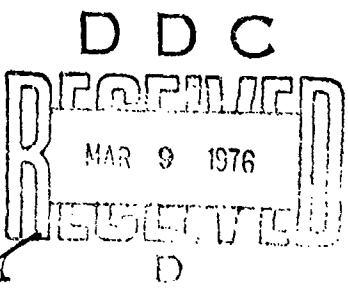
**ANALYSIS OF FILM THICKNESS EFFECT
IN SLOW-SPEED LIGHTLY-LOADED
ELASTOHYDRODYNAMIC CONTACTS**
Part II. Measurement of Film Thicknesses
in Vacuum.

SOUTHWEST RESEARCH INSTITUTE

JANUARY 1976

TECHNICAL REPORT AFML-TR-74-189, Part II
REPORT FOR PERIOD JULY 1974 -- JUNE 1975

Approved for public release; distribution unlimited




AIR FORCE MATERIALS LABORATORY
AIR FORCE WRIGHT AERONAUTICAL LABORATORIES (AFSC)
Air Force Systems Command
Wright-Patterson Air Force Base, Ohio 45433

NOTICE

When Government drawings, specifications, or other data are used for any purpose other than in connection with a definitely related Government procurement operation, the United States Government thereby incurs no responsibility nor any obligation whatsoever; and the fact that the government may have formulated, furnished, or in any way supplied the said drawings, specifications, or other data, is not to be regarded by implication or otherwise as in any manner licensing the holder or any other person or corporation, or conveying any rights or permission to manufacture, use, or sell any patented invention that may in any way be related thereto.

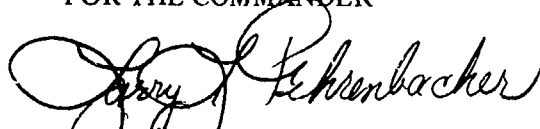
This report has been reviewed by the Information Office (OI) and is releasable to the National Technical Information Office (NTIS). At NTIS, it will be available to the general public, including foreign nations.

This technical report has been reviewed and is approved.



WAYNE E. WARD
Project Engineer

FOR THE COMMANDER



LARRY L. FEHRENBACHER, Major, USAF
Chief, Lubricants and Tribology Branch
Nonmetallic Materials Division

Copies of this report should not be returned unless return is required by security considerations, contractual obligations, or notice on a specific document.

SECURITY CLASSIFICATION OF THIS PAGE (When Data Entered)

REPORT DOCUMENTATION PAGE		READ INSTRUCTIONS BEFORE COMPLETING FORM
1. REPORT NUMBER AFML TR-74-189 (REVISED) - PT-2	2. GOVT ACCESSION NO.	3. PERFORMING ORG. REPORT NUMBER RS-632 (SWRI)
4. TITLE (and Subtitle) ANALYSIS OF FILM THICKNESS EFFECT IN SLOW-SPEED LIGHTLY-LOADED ELASTO- HYDRODYNAMIC CONTACTS, Part II. Measurement of Film Thicknesses in Vacuum.	5. TYPE OF REPORT & PERIOD COVERED Final July 1, 1974-June 15, 1975	6. CONTRACT OR GRANT NUMBER(s) F33615-73-C-5123
7. AUTHOR(s) J. C. Tyler → R. D. Brown, H. J. Carper P. M. Ku	8. PERFORMING ORGANIZATION NAME AND ADDRESS Southwest Research Institute 8500 Culebra Road San Antonio, Texas 78284	9. PROGRAM ELEMENT, PROJECT, TASK NUMBER AF- Project No. 7343 Task No. 734303
10. CONTROLLING OFFICE NAME AND ADDRESS Air Force Materials Laboratory (MBT) Air Force Systems Command Wright-Patterson Air Force Base, Ohio 45433	11. MONITORING AGENCY NAME & ADDRESS (if different from Controlling Office) Final r. 1 Jul 74 - 15 Jun 75	12. NUMBER OF PAGES 124
13. SECURITY CLASS. (of this report) UNCLASSIFIED		14. DECLASSIFICATION DOWNGRADING SCHEDULE
15. DISTRIBUTION STATEMENT (of this Report) Approved for public release; distribution unlimited.		
16. DISTRIBUTION STATEMENT (of the abstract entered in Block 20, if different from Report) 1-1211 p.		
17. SUPPLEMENTARY NOTES		
18. KEY WORDS (Continue on reverse side if necessary and identify by block number) Bearings Space Accelerated Test Lubricants Elastohydrodynamics Lubrication Vacuum		
19. ABSTRACT (Continue on reverse side if necessary and identify by block number) This report presents a summary of the second year's effort in a two-year program to study the influence of oil film thickness on bearing-lubricant life expectancy in despin mechanical assembly-type bearings operating in vacuum. Results of elastohydrodynamic film thickness measurements made by the optical interference technique in a SwRI optical tester are presented for seven oils, some of which have been employed in actual space flight hardware. These results show that the special oils formulated for vacuum		

DD FORM 1473 EDITION OF 1 NOV 65 IS OBSOLETE

UNCLASSIFIED

SECURITY CLASSIFICATION OF THIS PAGE (When Data Entered)

328200716

BLOCK 20. ABSTRACT (Continued)

use behave in a manner similar to ordinary straight mineral oils. Extensive experimental EHD film thickness data were obtained for DMA-type bearings operating in a vacuum and lubricated with various oils, and these results are presented and discussed. These film thickness measurements were made using a race displacement technique developed during the first year's work at SwRI. The measurements show that, in general, lubricant starvation occurs in the bearings with the result that the EHD film thicknesses are less than those predicted by the theoretical equations for flooded EHD lubrication. The results from long-term tests with DMA-type bearings operating in vacuum are also presented. Two bearing failures occurred and these failures are attributed to problems associated with lubrication of the interfaces between the retainer and the other bearing components. Examination of the bearings after test termination reveals that substantially full EHD lubrication (not flooded, but separation of bearing surfaces) at the ball-race contacts apparently prevailed for the duration of the tests.

UNCLASSIFIED

FOREWORD

This report was prepared by Southwest Research Institute, 8500 Culebra Road, San Antonio, Texas, under Contract F33615-73-C-5123. The contract was initiated under Project No. 7343, "Aerospace Lubricants," Task No. 734303. The work was administered by the Lubricants and Tribology Branch, Nonmetallic Materials Division, Air Force Materials Laboratory, Air Force Systems Command, Wright-Patterson Air Force Base, Ohio. The project engineers were Dr. M. Rivera, Dr. W. E. Ward, and Mr. R. J. Benzing, AFML/MBT.

Acknowledgment is given to Mr. Harold Haufler of SwRI for assisting in the development of the test facilities and also for conducting the experiments and participating in the analysis of the test data.

The report is issued in two parts: Part I, Development of Film Thickness Measurement Technique, and Part II, Measurement of Film Thicknesses in Vacuum. Part I was published in December 1974; Part II is contained herein.

Part II of the report covers the period of July 1, 1974, through June 15, 1975, and was submitted by the authors in September 1975.

The contractor's report number is RS-632.

ACCESSION for	
NTIS	White Section <input checked="" type="checkbox"/>
DDC	Diff. Section <input type="checkbox"/>
UNANNOUNCED	<input type="checkbox"/>
JUSTIFICATION.....	
BY.....	
DISTRIBUTION/AVAILABILITY CODES	
Dist.	AVAIL. and/or SPECIAL
A	

DDC
RECEIVED
MAR 9 1976
D

TABLE OF CONTENTS

	<u>Page</u>
I. INTRODUCTION	1
1. Objectives and Scope	1
2. Prior Accomplishments — Part I Review	2
II. TEST MATERIALS AND EQUIPMENT	3
1. Test Bearings	3
2. Test Oils	4
3. Bearing Test Rig and Associated Instrumentation	5
III. TASK I — DEVELOPMENT OF AN EXPERIMENTAL TECHNIQUE FOR FILM THICKNESS MEASUREMENT IN SLOW-SPEED LIGHTLY-LOADED ELASTOHYDRO- DYNAMIC CONTACTS	11
1. General	11
2. Optical EHD Film Thickness Results	16
IV. TASK II — EXPERIMENTAL MEASUREMENTS OF FILM THICKNESS IN TYPICAL DESPIN MECHANICAL ASSEM- BLY BEARINGS OPERATING IN A SIMULATED SPACE ENVIRONMENT	27
1. General	27
2. Development of Computer Program to Analyze Test Results	29
3. Experimental Test Results	31
V. TASK III — ANALYSIS OF INFLUENCE OF LUBRICANT FILM THICKNESS ON BEARING LIFE EXPECTANCY IN A SIMULATED SPACE ENVIRONMENT	49
1. General	49
2. Presentation of Experimental Results from Long-Duration Bearing Tests	52
VI. CONCLUSIONS AND RECOMMENDATIONS	66
1. Conclusions	66
2. Recommendations	68

TABLE OF CONTENTS (Cont'd)

	<u>Page</u>
APPENDIXES	
A Development of Film Thickness-Bearing Race Displacement Equations Used in Computer Programs	70
B Listing for Task II Data Reduction Program	80
C Sample Printout of Task II Data	93
D Listing of Task III Data Reduction Program	97
E Task III Data	109
LIST OF REFERENCES	124

LIST OF ILLUSTRATIONS

<u>Figure</u>		<u>Page</u>
1	Bearing Test Rig	6
2	Three Test Rigs Attached to Vacuum Facility	9
3	Closeup of Test Rig Attached to Vacuum Chamber	10
4	Dimensionless Central-Region Oil Film Thickness for SwRI Oil B in Pure Rolling	13
5	Dimensionless Minimum Oil Film Thickness for SwRI Oil B in Pure Rolling	14
6	Dimensionless Central-Region Oil Film Thickness for Four Formulations of Apiezon C	17
7	Dimensionless Central-Region Oil Film Thickness for Apiezon A	18
8	Dimensionless Central-Region Oil Film Thickness for Nye 860-2	19
9	Dimensionless Central-Region Oil Film Thickness for Seven Oils	21
10	Dimensionless Minimum Oil Film Thickness for Four Formulations of Apiezon C	22
11	Dimensionless Minimum Oil Film Thickness for Apiezon A	23
12	Dimensionless Minimum Oil Film Thickness for Nye 860-2	25
13	Dimensionless Minimum Oil Film Thickness for Seven Oils	26
14	Dimensionless Prepumpdown Oil Film Thicknesses for Standard Bearings Having Thick Initial Film of BBRC 36233	34

LIST OF ILLUSTRATIONS (Cont'd)

<u>Figure</u>		<u>Page</u>
15	Dimensionless Oil Film Thicknesses for Standard Bearings Having Thick Initial Film of Low-Viscosity Oil	38
16	Dimensionless Oil Film Thicknesses for Standard Bearings Having Thick Initial Film of Intermediate-Viscosity Oil	39
17	Dimensionless Oil Film Thicknesses for Standard Bearings Having Thick Initial Film of High-Viscosity Oil	40
18	Dimensionless Oil Film Thicknesses for Standard Bearings Having Thick Initial Film of Intermediate-Viscosity Oil Containing Antiwear Additive ZDP	42
19	Dimensionless Oil Film Thicknesses for Standard Bearings Having Thick Initial Film of Intermediate-Viscosity Oil Containing No Antiwear Additive	43
20	Dimensionless Oil Film Thicknesses for Standard Bearings Having Thin Initial Film of Intermediate-Viscosity Oil	44
21	Dimensionless Oil Film Thicknesses for Rough Bearings Having Thick Initial Film of Intermediate-Viscosity Oil	46
22	Dimensionless Oil Film Thicknesses for Rough Bearings Having Thin Initial Film of Intermediate-Viscosity Oil	47
23	Measured Variables for Endurance Test Using DMA Bearings Lubricated with Thick Initial Oil Film of Apiezon A and Having Low Λ_m	53
24	Measured Variables for Endurance Test Using DMA Bearings Lubricated with Thick Initial Oil Film of Apiezon A and Having Medium Λ_m	54

LIST OF ILLUSTRATIONS (Cont'd)

<u>Figure</u>		<u>Page</u>
25	Measured Variables for Endurance Test Using DMA Bearings Lubricated with Thick Initial Oil Film of BBRC 36233 and Having High Λ_m	55
26	View of Wedged Cage After Endurance Test "Lock Up"	58
27	Ball Track in Outer Race of Forward Bearing	61
28	Ball Track in Inner Race of Forward Bearing	62
29	Flake of Debris Deposited in Ball Pocket of Forward Bearing Cage	63
30	Four Oil-Impregnated Reservoirs as Removed from Test Rig	64
31	Schematic Drawing Showing Axially Displaced Bearing Race	71

LIST OF TABLES

<u>Table</u>		<u>Page</u>
1	Bearing Test Rig Parts List	7
2	Summary of Task II Tests	35
3	Summary of Task III Tests	51

SECTION I

INTRODUCTION

1. Objectives and Scope

As specified in the Statement of Work of Contract F33615-73-C-5123, the objectives of the proposed program are: (a) to determine the oil film thickness in an axially-loaded, angular-contact ball bearing under conditions typified by a despin mechanical assembly (DMA), and (b) to define the influence of oil film thickness on lubricant and bearing performance in long-life DMA systems.

In order to accomplish these objectives, the Statement of Work outlines three major tasks, as follows:

Task I — Development of an experimental technique for film thickness measurement in slow-speed, lightly-loaded elastohydrodynamic contacts.

Task II — Experimental measurements of film thickness in typical despin mechanical assembly bearings operating in a space (vacuum) environment.

Task III — Analysis of the influence of film thickness on lubricant film performance and bearing life expectancy in a space (vacuum) environment.

This report is issued in two parts: Part I, Development of Film Thickness Measurement Technique, and Part II, Measurement of Film Thicknesses in Vacuum. Part I of the report, submitted in July 1974 and published in December 1974,⁽¹⁾ was concerned principally with the work done under Task I, i.e., the development of a technique uniquely applicable to the measurement of the oil film thickness in angular-contact bearings, as are typically employed in DMA's. It also outlined the test plans for Tasks II and III. Part II of the report, submitted herewith, will present the results of the Tasks II and III tests, together with further analysis of the Task I results. Briefly, Task II involves film thickness measurements in typical DMA bearings in a simulated space (vacuum) environment, and Task III entails selected long-duration bearing tests in a simulated space (vacuum) environment. The objectives of Task II are to apply the basic technique developed in Task I to typical DMA bearings and to examine how the oil film thickness varies with lubricant formulations and operating conditions. The objectives of Task III are to generate experimental data relating the oil film thickness to bearing performance and to provide a realistic foundation for the development of accelerated tests for bearing life prediction.

Since this part of the report is a continuation of Part I, much of the material contained in Part I will not be repeated herein, but will be summarized or referenced for the sake of completeness.

2. Prior Accomplishments — Part I Review

Part I of this report described the experimental and analytical work performed on the development of a technique to measure the oil film thickness in an actual bearing operating in vacuum. Preliminary tests with actual bearings showed that the technique, involving the measurement of the displacement of the bearing race due to the development of elastohydrodynamic oil films at the ball-race conjunctions, was feasible. In addition to these preliminary bearing tests, extensive measurements of the elastohydrodynamic oil film thickness were made by both the displacement technique and the optical interference technique in a SwRI optical EHD tester. These measurements were made and compared using six different test oils, some of which have been employed in actual space flight hardware. These results indicated a need for further measurements and analyses, which will be reported in Section III herein.

SECTION II

TEST MATERIALS AND EQUIPMENT

1. Test Bearings

The test bearings selected for use in this program were discussed in Section II, Part I of this report. They were manufactured by the Marlin-Rockwell Company (MRC) and are typical DMA bearings, ABEC-7 grade, angular-contact ball bearings with a counterbored inner race, 100-mm bore, and a contact angle of $26^\circ \pm 1^\circ$. The surface finish of the balls in all test bearings was approximately $0.025 \mu\text{m}$ ($1 \mu\text{in.}$). However, as requested by SwRI, some bearings were to have a "standard" surface finish on the races and others were to have a race surface finish approximately twice the "standard." According to the information supplied by MRC, the "standard" race finish was approximately $0.102 \mu\text{m}$ ($4 \mu\text{in.}$) transverse (across the grinding marks), and the rougher race finish was approximately $0.204 \mu\text{m}$ ($8 \mu\text{in.}$) transverse. This roughness variation was to be employed to determine the effect of surface finish on the measured oil film thickness and on the bearing life in Tasks II and III.

Upon receipt of the test bearings from MRC, they were not disassembled, but were shipped directly to Ball Brothers Research Corporation (BBRC) for special application of the test lubricants. When the bearings were returned from BBRC to SwRI, they again were not disassembled prior to being used for testing in order to minimize the possibility of contamination. Consequently, it was not possible to check the surface roughness of the bearing races until after completion of the Task II tests and after termination of two of the Task III endurance tests.

The post-test surface roughness measurements were made on one "standard" bearing and one rough bearing, using a Talysurf surface finish measuring instrument equipped with a curved-surface attachment. These measurements showed that the inner-race surface roughness of the rough bearing was not much different from that of the standard bearing. The measurements were made using two wave "cutoff" lengths. The longer wave "cutoff" length of 0.076 cm (0.03 in.) gave an average value over a longer distance across the bearing race and consequently included an additional amount contributed by any waviness of the surface. The wave "cutoff" length of 0.025 cm (0.01 in.) was only $1/3$ as long and would exclude much of the waviness, unless the frequency of waviness is extremely high. It was found that the longer wave "cutoff" length gave surface finish values about 3 to 7 times those given by the shorter wave "cutoff" length. Therefore, it is concluded that the race surfaces have an appreciable amount of waviness that contributes to the surface roughness reading when using the longer wave "cutoff" length. The values that were obtained using

the two wave "cutoff" lengths along with the race surface finish values furnished by MRC are as follows:

	Bearing Inner-Race Roughness, μm ($\mu\text{in.}$)	
	<u>Standard finish</u>	<u>Rough finish</u>
SwRI 0.076 cm wave "cutoff" length	0.335 (13.20)	0.422 (16.62)
SwRI 0.025 cm wave "cutoff" length	0.087 (3.44)	0.062 (2.42)
MRC information	0.102 (4)	0.204 (8)

As seen from these data there is a significant difference in the values obtained by the two organizations. Further examination of the graphic traces obtained by both MRC and SwRI when traversing the bearing race surfaces led to the conclusion that the MRC values are probably more indicative of the true surface character. The MRC traces are more consistent and uniform and do indeed show that the amplitude of the stylus trace for the rough bearings is about twice that of the standard bearings. Consequently it was decided to accept the MRC roughness values for the purposes of the present study.

These measurements do show that surface roughness values obtained at different laboratories using different measuring instruments can vary considerably, thus making it a very controversial subject. Of course the width and length of the penetrating stylus will also influence the surface roughness information obtained. Discrepancies in measured surface roughness values at different laboratories using different measuring instruments is not new and certainly deserves further study to resolve these differences.

Based on the MRC measured data, the effect of ball-race composite surface roughness on the oil film thicknesses in EHD conjunctions in bearings, which is one of the variables to be investigated in Task II can be made in this study. Also, the three different Λ ratios (ratio of oil film thickness to ball-race composite surface roughness) will lend themselves to analysis in the Task III tests. Details of these results will be discussed in Sections IV and V herein.

2. Test Oils

Six different test oils were employed in this program, with emphasis being placed on several space-proven ones. These oils were supplied and applied to the test bearings by Ball Brothers Research Corporation (BBRC), which organization served as a subcontractor to SwRI in this program.

In addition to the six test oils, data on the elastohydrodynamic film thickness behavior of a straight mineral oil, SwRI Oil B, obtained in a previous SwRI program, (2) are cited for comparison.

The properties of the seven oils were discussed in detail in Section II, Part I of this report, and will not be repeated here.

3. Bearing Test Rig and Associated Instrumentation

A cross-section of the bearing test rig is shown in Figure 1 and a complete parts list keyed to the drawing is given in Table 1. There have been a few modifications made to the original design as presented in Section II, Part I of this report. Therefore, a revised drawing and parts list are presented herein for the sake of clarity.

Four identical bearing test rigs were fabricated; three were used for the long-duration tests in Task III and one for the short-duration tests in Task II. The test bearings (33) are mounted on a shaft (4) and axially preloaded by means of the diaphragm (7) which is deflected a selected distance by the bearing preload ring (10). Diaphragm load/deflection calibration was determined by using deadweights and a dial indicator. At a load of 890 N (200 lb) the axial deflection is 0.86 mm (0.034 in.). Rotary motion is imparted to the shaft by means of a magnetic coupling consisting of an inner magnet (22) and an outer magnet (23) which is mounted on the shaft of a variable speed DC motor (51). Motor speed is indicated by means of a magnetic pickup activated by a 60-tooth gear (not shown in Fig. 1) mounted on the motor shaft. Bearing temperatures are measured by means of 1/16-in. diameter sheathed thermocouples (32) which contact the outer ring of each bearing.

The technique employed for measuring oil film thickness in these tests consists of measuring the axial movement of the floating bearing by means of a linear variable differential transformer (LVDT). The LVDT components consist of a core (14) attached to the bearing cartridge (5) that carries the floating bearing and a winding (20) that is attached to the retainer plate (15).

For lubrication, the test bearings are initially coated with a film of oil and the bearing cages are impregnated with the same oil. Also, for some tests, impregnated reservoirs (16) are installed within the bearing chamber.

A photograph of the three long-duration test rigs used in Task III, as attached to the 1200 l/s ion pump, is shown in Figure 2. Much of the instrumentation employed is also shown in the photograph. Figure 3 illustrates a closeup view of one of the test rigs. Details of the instrumentation and vacuum systems employed are given in Section II, Part I of the report.

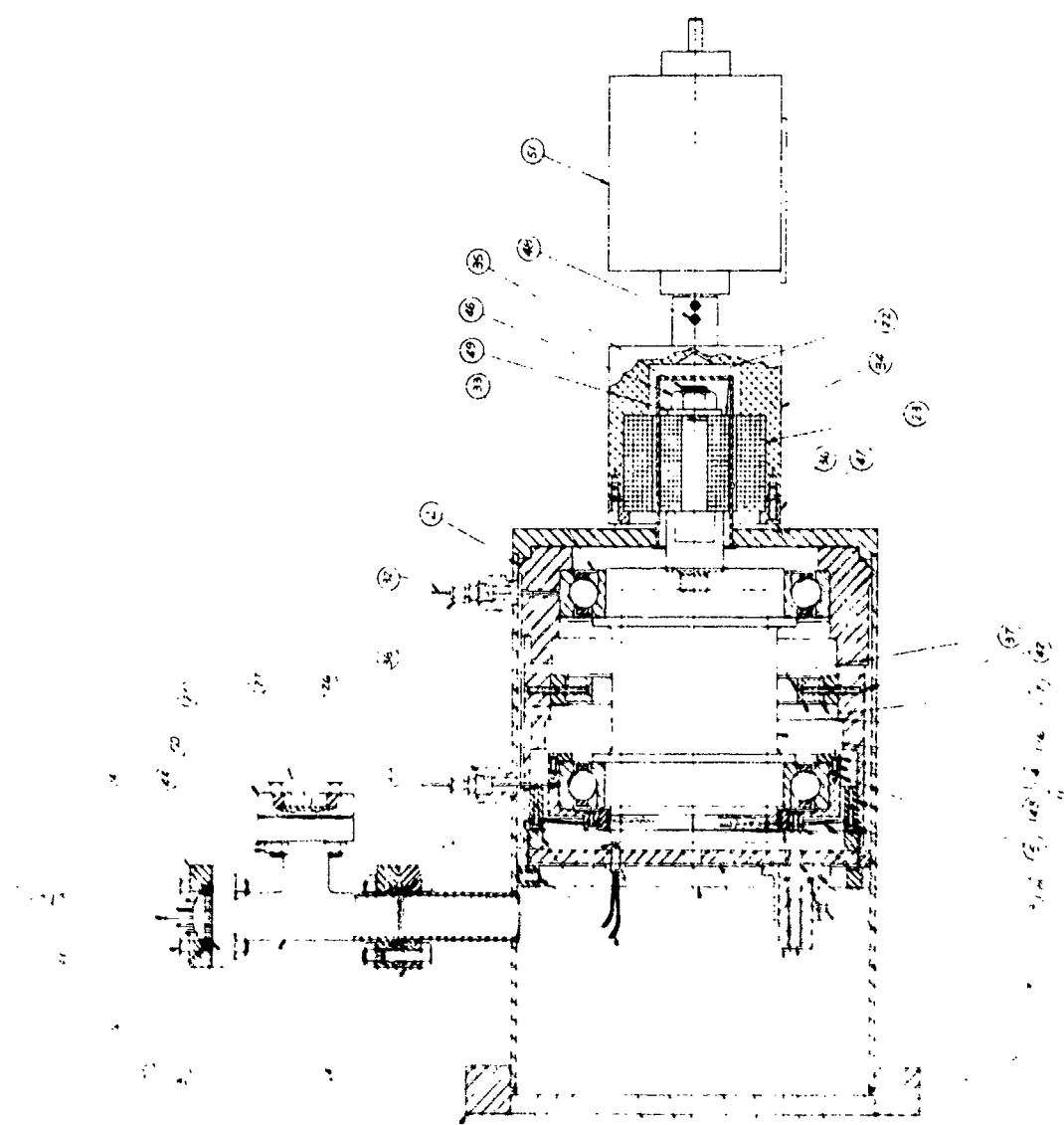


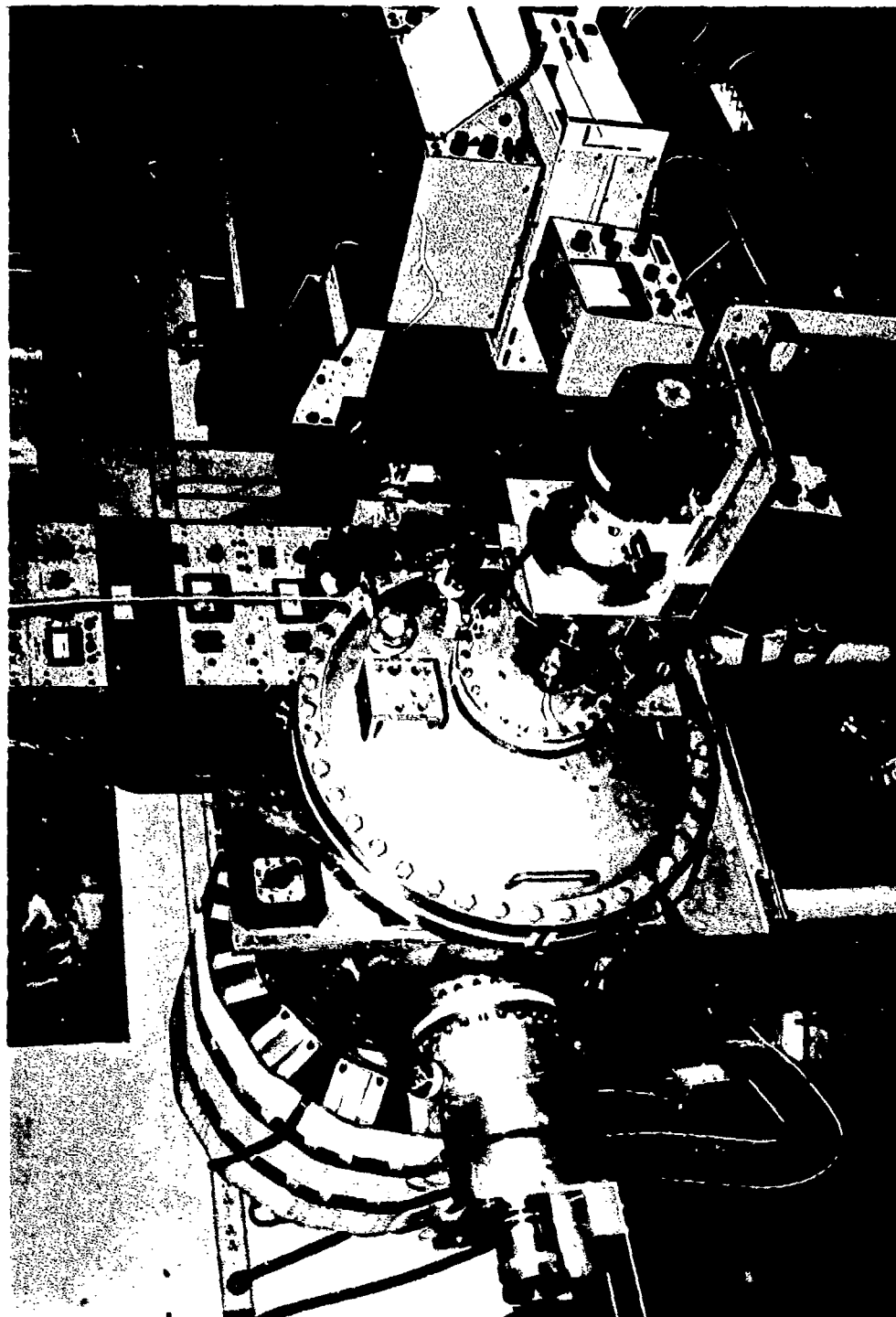
Figure 1. Bearing Test Rig

TABLE 1. BEARING TEST RIG PARTS LIST

Identifying No.	Description	No. Req'd
1	Bearing rig chamber	1
2	Inner housing	1
3	1-in. O.D. vacuum tee	1
4	Drive shaft	1
5	Bearing cartridge	1
6	Bearing locknut	1
7	Diaphragm	1
8	Diaphragm mounting ring	1
9	Diaphragm retainer ring, outer	1
10	Bearing preload ring	1
11	Bearing retainer ring	1
12	Diaphragm retainer ring, inner	1
13	Mounting rod, LVDT core	1
14	LVDT core, Hewlet-Packard 585T-050-BM	1
15	Retainer plate	1
16	Oil reservoir (90° segments)	4
17	Oil reservoir mounting ring	1
18	Assembly retainer ring	1
19	Housing, LVDT	1
20	LVDT winding, Hewlet-Packard 585DT-050-BM	1
21	6-32 x 1/2 slotted cap screw	3
22	Magnet, inner	1
23	Magnet, outer	1
24	Vacuum flange	6
25	Vacuum flange insert	4
26	Vacuum flange insert, modified	2
27	Vacuum feed through, lubricant	1
28	Vacuum feed through, electrical	1
29	Terminal header, Latronics No. 97.1735	1
30	Copper gasket, 1-in.	3
31	Magnetic pickup, Electro Products No. 3080	1
32	Thermocouple, 1/16 sheath	2
33	Test bearing	2
34	Magnet cartridge	1
35	Input shaft	1
36	Magnet lock ring	1
37	6-32 x 5/8 flat head screw	4
38	Thermocouple compression fitting, Omega SSLK-116	2
39	Adapter, thermocouple compression fitting	2
40	1/4-20 x 1/2 socket head cap screw	3

TABLE 1. BEARING TEST RIG PARTS LIST (Cont'd)

Identifying No.	Description	No. Req'd.
41	1/4-20 x 1-1/4 hexagon head cap screw	12
42	6-32 x 3/4 flat head screw	4
43	6-32 x 3/8 flat head screw	36
44	1/4-20 hexagon nut	12
45	10-32 hexagon nut	1
46	9/16-18 hexagon nut	1
47	8-32 x 3/4 flat head screw	6
48	10-32 x 3/8 socket head set screw	2
49	9/16 flat washer	1
50	1/4 lock washer	12
51	DC drive motor, Bodine No. 280	1
52	Ferromagnetic pin	1



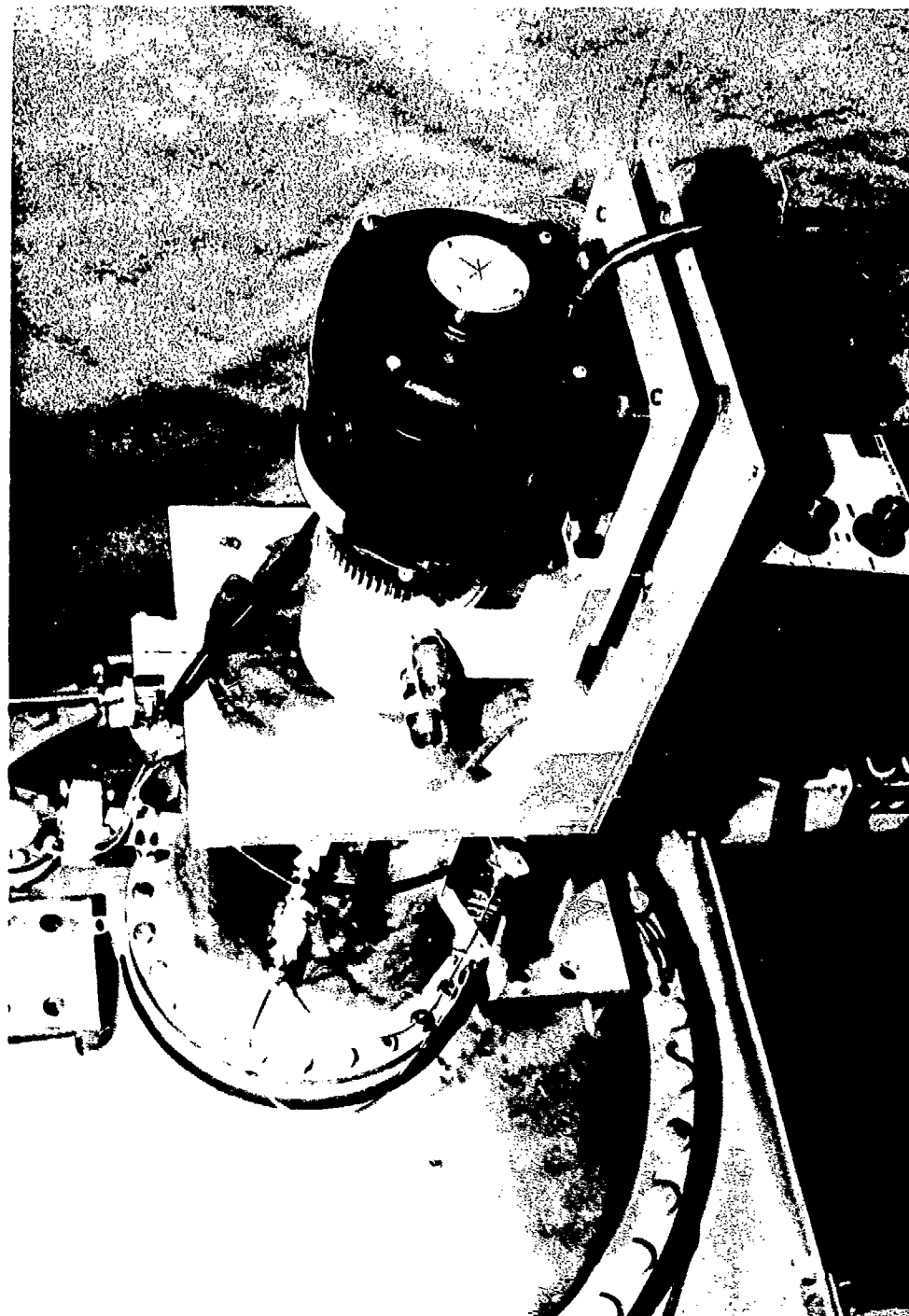


Figure 3. Closeup of Test Rig Attached to Vacuum Chamber

SECTION III

TASK I — DEVELOPMENT OF AN EXPERIMENTAL TECHNIQUE FOR FILM THICKNESS MEASUREMENT IN SLOW-SPEED LIGHTLY- LOADED ELASTOHYDRODYNAMIC CONTACTS

1. General

Section IV, Part I of this report discussed briefly the various techniques available to measure the oil film thickness in an EHD conjunction. The bearing race displacement technique, which was the one chosen to be developed in this program, was considered in detail, showing the derivation of an equation relating the total axial displacement of a dual bearing arrangement to the EHD film thicknesses at the ball-race conjunctions. Because of several assumptions that were made in the derivation of this equation, it was deemed necessary to conduct certain experiments in Task I, in order to ascertain the validity of determining the oil film thicknesses by the displacement measurement. Some of these experiments were conducted with the SwRI optical EHD tester, which was also described in Section IV, Part I of this report.

As noted in Part I of this report, the optical measurements showed that the central-region film thickness of SwRI Oil B in pure rolling was, under comparable operating conditions, considerably greater than the central-region film thicknesses of the other six oils in pure sliding. In all seven instances, the oil was supplied to the ball-disk conjunctions by means of jets in a "flooded" fashion. It was thought that this difference in central-region film thickness behavior might be due to the difference in thermal effects occurring in the conjunction inlet caused by pure sliding as against pure rolling. Accordingly, it was decided during this reporting period to obtain additional film thickness measurements for the oils in question under pure rolling conditions, and to compare these results with the previous results obtained in pure sliding. Moreover, it was reasoned that if a thermal effect should be observed in the central-region film thickness behavior, then a similar effect would likewise be found in the behavior of the minimum film thickness at the side lobes in the conjunction. Therefore, the analysis was also extended to the minimum film thickness behavior.

In the prior work performed at SwRI, (2) a straight mineral oil, designated as SwRI Oil B, was employed in EHD film thickness and friction measurements in pure rolling. The film thickness was determined by the optical interference technique, with a steel ball placed between two contrarotating glass disks. The ball diameter was varied three times: 1.91 cm (0.75 in.), 2.54 cm (1.00 in.), and 3.81 cm (1.50 in.). The load was also varied three times: 13.3 N (3.0 lb), 22.2 N (5.0 lb), and 33.4 N (7.5 lb). The sum velocity was varied five times, from 25.4 to 127 cm/sec (10 to 50 ips). The oil temperature at the conjunction inlet was approximately 27 C (80 F), and was measured and accounted for in the EHD calculations.

It was found in this work that the central-region and minimum film thicknesses obtained for the three ball sizes, three loads, and five sum velocities could be linearly correlated by appropriate dimensionless parameters. These correlations are presented in Figures 4 and 5, and the appropriate dimensionless equations are given below.

For the central-region film thickness:

$$H_c = 1.05 \Sigma_c \quad (1)$$

where $H_c = \frac{h_c}{R} \quad (2)$

$$\Sigma_c = \frac{(G U_t)^{0.74}}{(W')^{0.074}} \quad (3)$$

For the minimum film thickness:

$$H_m = 0.75 \Sigma_m \quad (4)$$

where $H_m = \frac{h_m}{R} \quad (5)$

$$\Sigma_m = \frac{G^{0.70} U_t^{0.77}}{(W')^{0.14}} \quad (6)$$

The various symbols employed in the above equations, and throughout this report, are

H_c = dimensionless central-region film thickness, defined by Eq. (2)

H_m = dimensionless minimum film thickness, defined by Eq. (5)

Σ_c = dimensionless material-velocity-load parameter for central-region film thickness correlation for circular conjunctions, defined by Eq. (3).

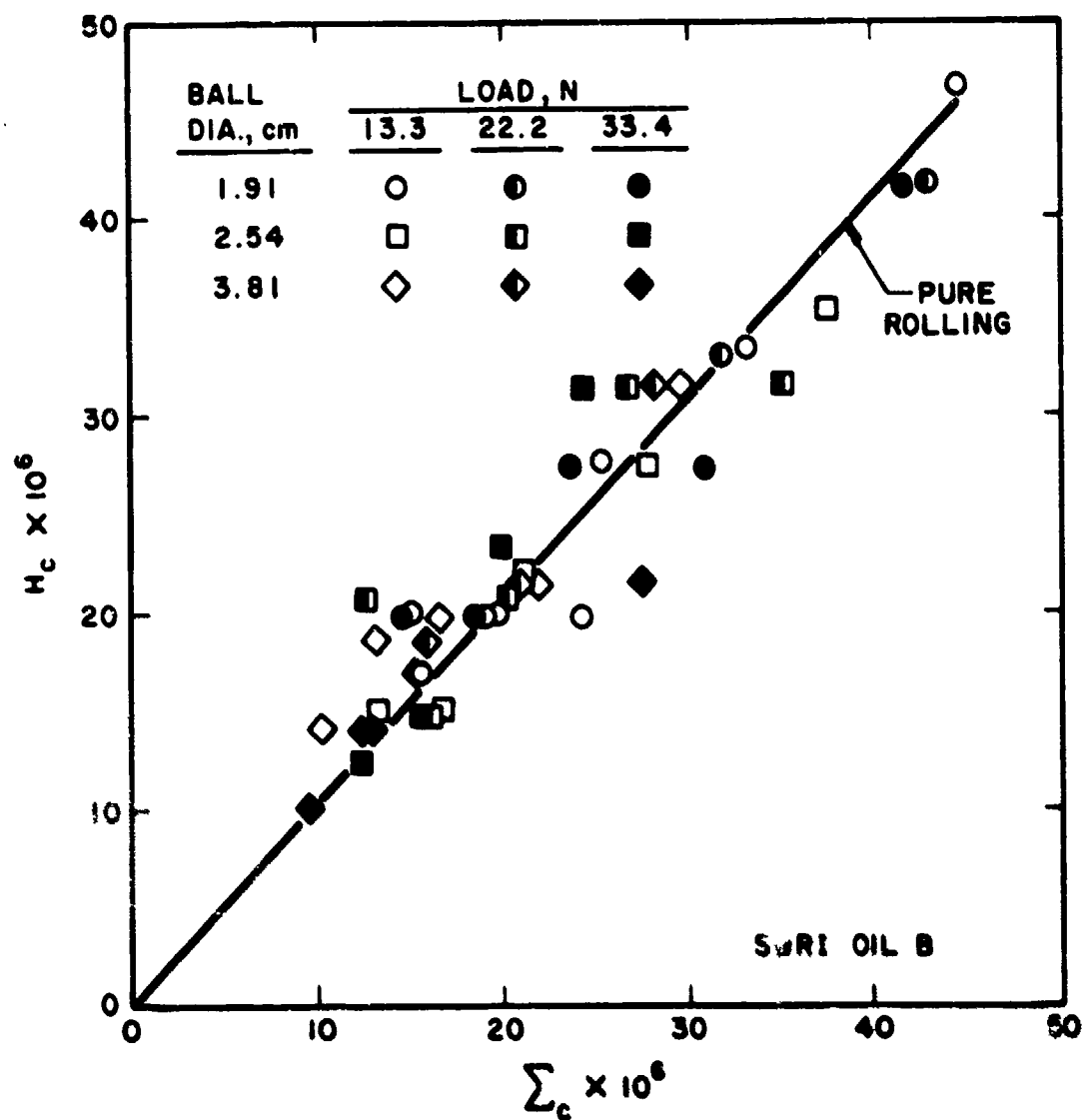


Figure 4. Dimensionless Central-Region Oil Film Thickness for SwRI Oil B in Pure Rolling

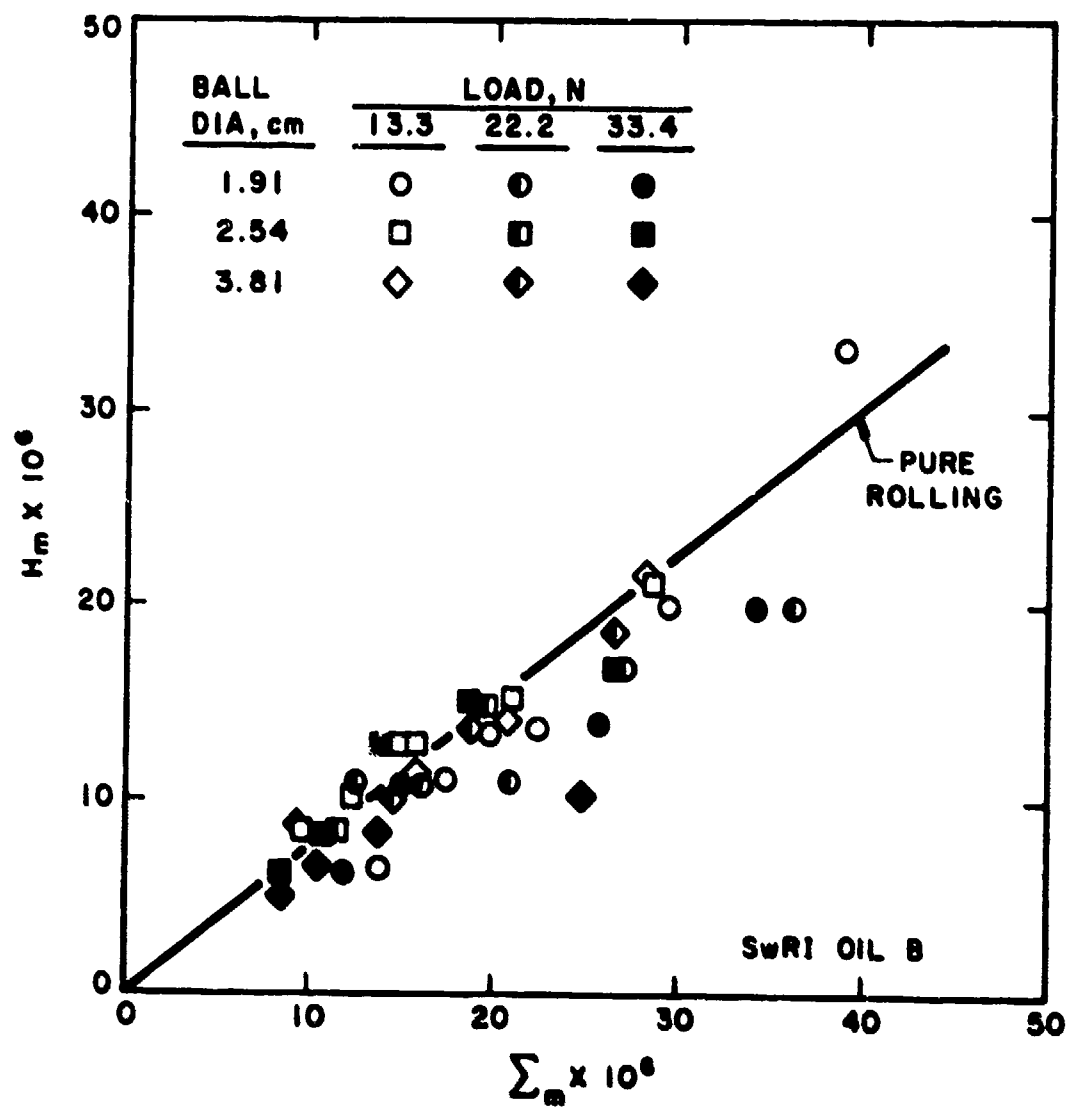


Figure 5. Dimensionless Minimum Oil Film Thickness for SwRI Oil B in Pure Rolling

Σ_m = dimensionless material-velocity-load parameter for minimum film thickness correlation for circular conjunctions, defined by Eq. (6)

h_c = central-region lubricant film thickness

h_m = minimum lubricant film thickness

R = equivalent radius of curvature = $(1/R_1 + 1/R_2)^{-1}$

R_1 = radius of curvature of body 1

R_2 = radius of curvature of body 2

G = dimensionless materials parameter = $\alpha_0 E^*$

α_0 = pressure-viscosity coefficient of lubricant at conjunction inlet temperature and near-atmospheric pressure

E^* = equivalent elastic modulus

$$= 2 \left[\frac{1 - \nu_1^2}{E_1} + \frac{1 - \nu_2^2}{E_2} \right]^{-1}$$

ν_1 = Poisson's ratio of body 1

ν_2 = Poisson's ratio of body 2

E_1 = elastic modulus of body 1

E_2 = elastic modulus of body 2

U_t = dimensionless sum velocity = $\frac{\mu_0 V_t}{E R}$

μ_0 = absolute viscosity of lubricant at conjunction inlet temperature and near-atmospheric pressure

V_t = sum velocity = $V_1 + V_2$

V_1 = surface velocity of body 1

V_2 = surface velocity of body 2

W^* = dimensionless load = $\frac{P}{E R^2}$

P = load

It is interesting to note that Eq. (1) is the same in form as a correlating equation obtained by Archard and Cowking,⁽³⁾ whose numerical constant in the equation was 0.84 instead of 1.05 as determined here. Moreover, Eq. (4) is identical in every respect to a correlating equation obtained by Westlake and Cameron.⁽⁴⁾

Figures 4 and 5 for SwRI Oil B and the two cited references employing other oils show that the relationships between H_c and Σ_c and between H_m and Σ_m in pure rolling are essentially linear up to values of Σ_c and Σ_m of about 45×10^{-6} . The implication is that, with values of Σ_c or Σ_m up to about 45×10^{-6} , any viscous heating effect in the conjunction inlet region⁽⁵⁾ was probably quite small if the motion is pure rolling. It was noted in Part I of this report that the dimensionless central-region film thicknesses, H_c , of the six different test oils in pure sliding, when plotted against the dimensionless material-velocity-load parameter, Σ_c , were less than the H_c of SwRI Oil B in pure rolling. Accordingly, it appeared that the difference noted might have been due to some unusual thermal effect associated with the sliding motion. In an effort to resolve this question, additional tests in pure rolling were conducted on some of the test oils during the current reporting period. A discussion of these results, together with the previous results, will now be presented.

2. Optical EHD Film Thickness Results

The central-region film thickness results, obtained in both pure rolling and pure sliding, are summarized for four different formulations of Apiezon C oil in Figure 6, for Apiezon A (+ antioxidant + lead naphthenate) oil in Figure 7, and for Nye 860-2 (+ antioxidant + lead naphthenate) oil in Figure 8. For purposes of comparison, the pure rolling data for SwRI Oil B are shown in these figures as dash lines up to a Σ_c value of 45×10^{-6} , but with the data points omitted for the sake of clarity.

The data in each figure are for two loads of 17.70 N (3.98 lb) and 59.78 N (13.44 lb) and one ball size of 2.54 cm (1 in.). The conjunction inlet temperature for the pure sliding tests ranged between 26.7 and 37.8 C (80 and 100 F), whereas for the pure rolling tests it ranged between 26.7 and 28.9 C (80 and 84 F). The pure sliding data are taken from Part I of this report. The pure rolling data were obtained during this reporting period.

Referring to Figure 6, the pure sliding data were obtained for four different formulations of Apiezon C of very similar viscosity characteristics, and their central-region film thickness behaviors were also similar. Therefore, pure rolling tests were made on only one of these formulations, BBRC 36233, assuming that the other three formulations would behave similarly in pure rolling. It is seen that, considering the experimental scatter, the pure rolling data for BBRC 36233 appear to lie somewhere between the pure rolling data for SwRI Oil B and the pure sliding data for the

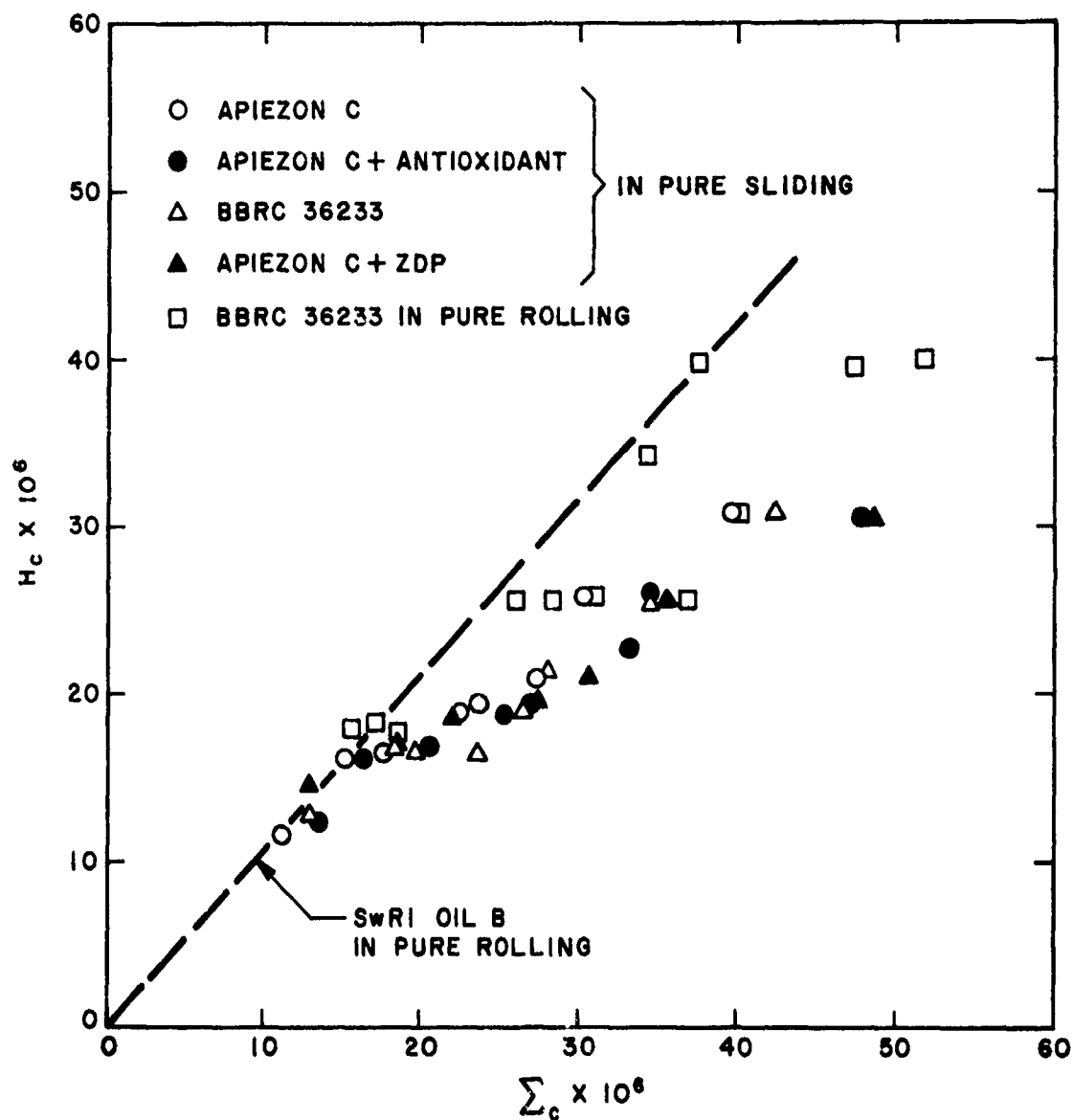


Figure 6. Dimensionless Central-Region Oil Film Thickness for Four Formulations of Apiezon C

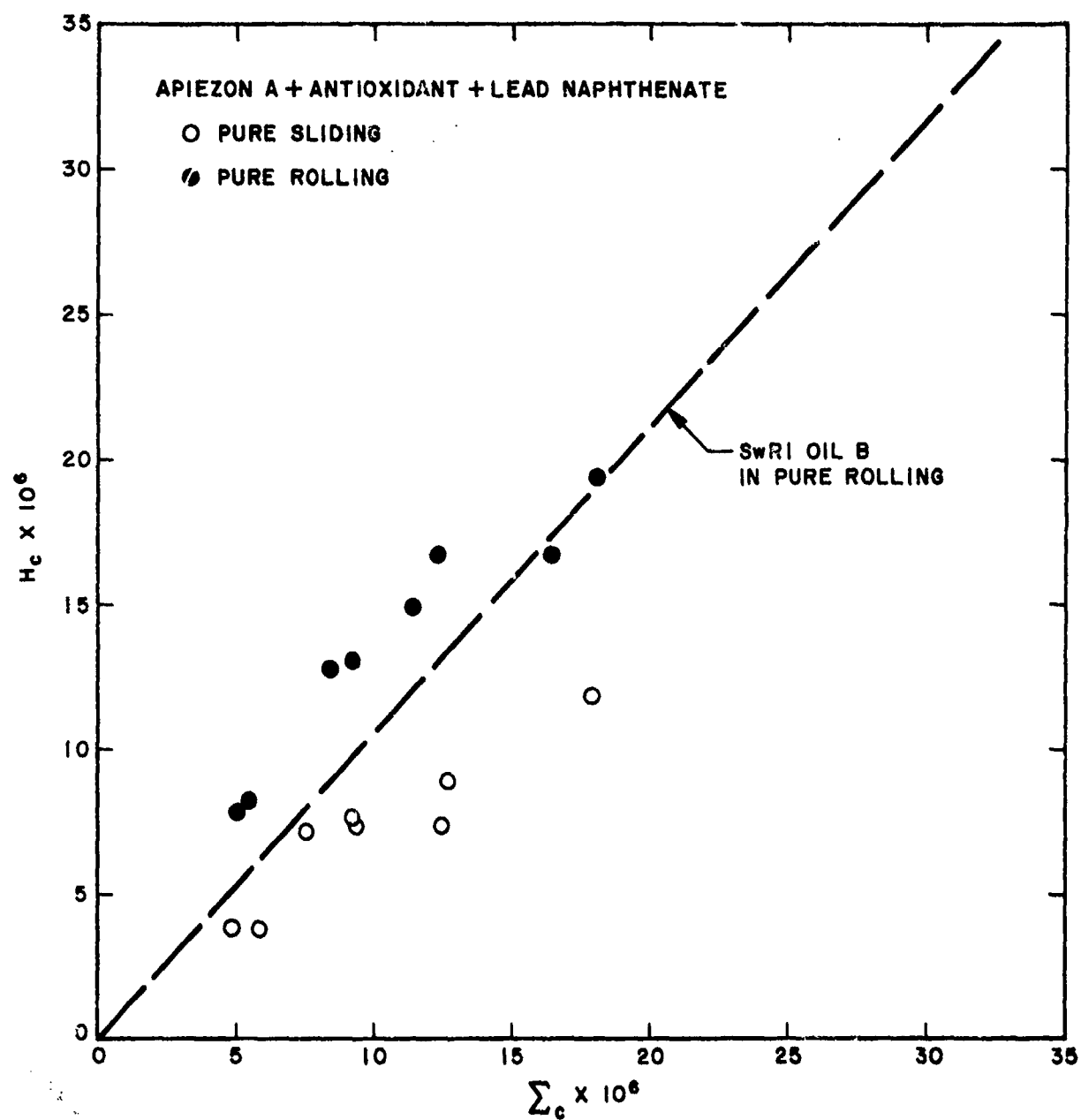


Figure 7. Dimensionless Central-Region
Oil Film Thickness for Apiezon A

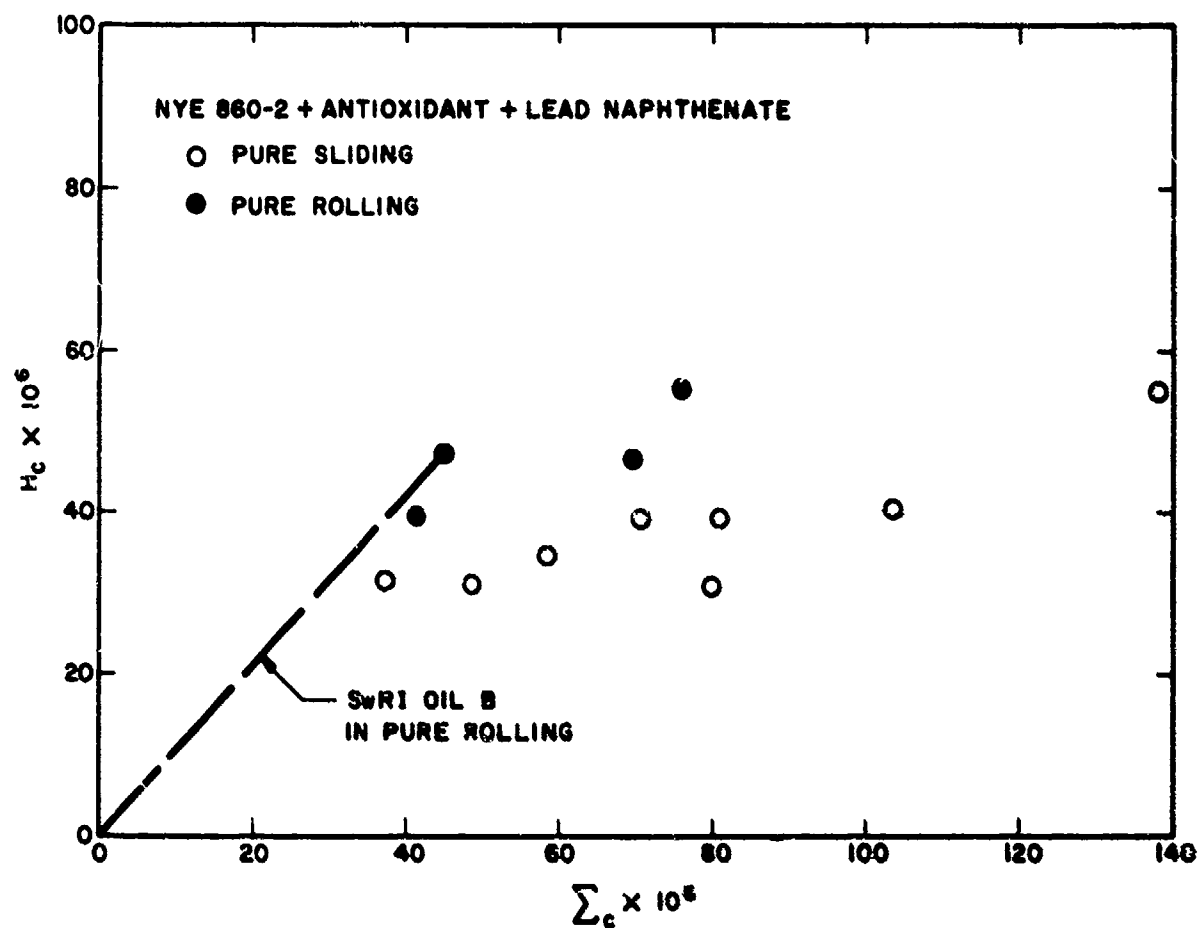


Figure 8. Dimensionless Central-Region Oil Film Thickness for NYE 860-2

Apiezon C formulations.

Figure 7 presents the pure rolling and pure sliding data for Apiezon A, which oil is less viscous than Apiezon C. Note that the pure rolling data for this oil appear to lie somewhat higher than the pure rolling data for SwRI Oil B.

Figure 8 shows the results for Nye 860-2, an oil more viscous than Apiezon C. It is seen that at values of Σ_c less than 45×10^{-6} , the pure rolling data for Nye 860-2 agree quite well with the pure rolling data for SwRI Oil B. However, at higher values of Σ_c , the linear H_c vs. Σ_c relationship begins to break down, due possibly to the increased viscous heating effect in the inlet region.

It must be recognized that experimental errors are inevitable in this type of measurement. Therefore, it is useful to compare all of the results together, in an effort to see how the data behave as a whole. This is done in Figure 9, which combines the data presented in the preceding figures by omitting the data points for the sake of clarity. In this figure, the long dashed line is the best-fit line for SwRI Oil B taken from Figure 4. The irregularly shaped boxes show the scatter range of data for the six test oils presented in Figures 6 through 8, with the solid boxes denoting the pure rolling data and the dashed boxes denoting the pure sliding data. Figure 9 suggests that the H_c versus Σ_c relationship is, in general, not linear in either the pure rolling or the pure sliding case, but can best be approximated by curves with progressively decreasing slopes as Σ_c is increased. This general trend is entirely reasonable, because the viscous shear and thus heating effect in the inlet region is expected to become progressively more severe with increasing Σ_c . As to the difference in the magnitudes of H_c between pure rolling and pure sliding, it is apparent that the velocity profile across the inlet film is skewed in the sliding case but symmetrical in the rolling case, so that the viscous shear effect is more pronounced in sliding and the friction coefficient is higher in sliding than in rolling. In other words, the character and thus magnitude of the viscous heating processes are different.

The general levelling trend of H_c at very high values of Σ_c , in both pure rolling and pure sliding, is not believed to be the result of inlet "starvation" in these tests. All these tests were performed with the oil supplied by jets to the conjunction inlet in a flooded fashion, and thus starvation was not likely. However, inlet starvation could be important in actual bearings. With the DMA bearings in which the oil is applied to the balls and races as relatively thin films, rather than by copious jets, starvation is far more likely.

During the current reporting period, all previously obtained and recently obtained results were analyzed to yield the minimum oil film thickness occurring at the side lobes in the conjunction. The corresponding H_m versus Σ_m data for pure rolling and pure sliding are presented in Figure 10 for four different formulations of Apiezon C, in Figure 11 for Apiezon A, and in

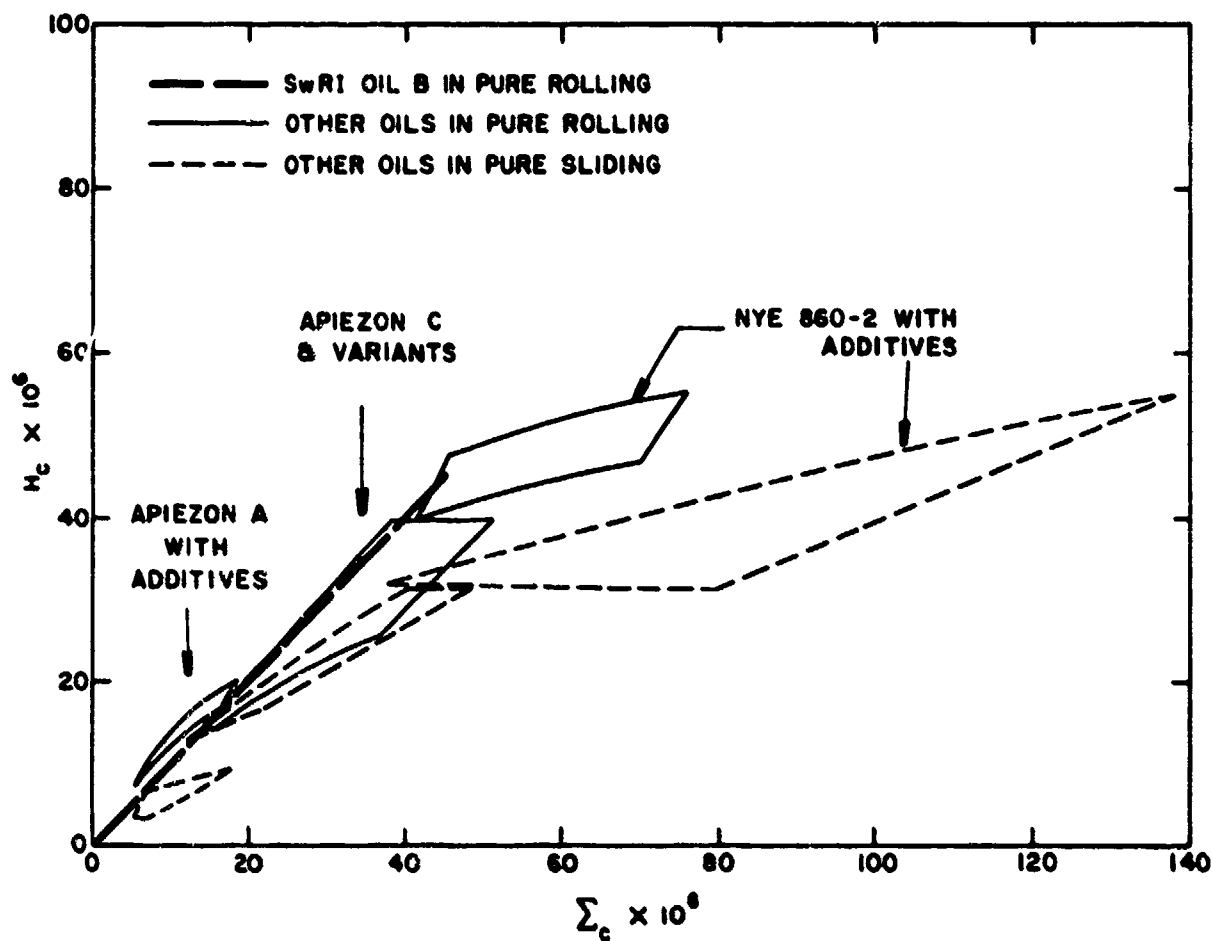


Figure 9. Dimensionless Central-Region Oil Film Thickness for Seven Oils

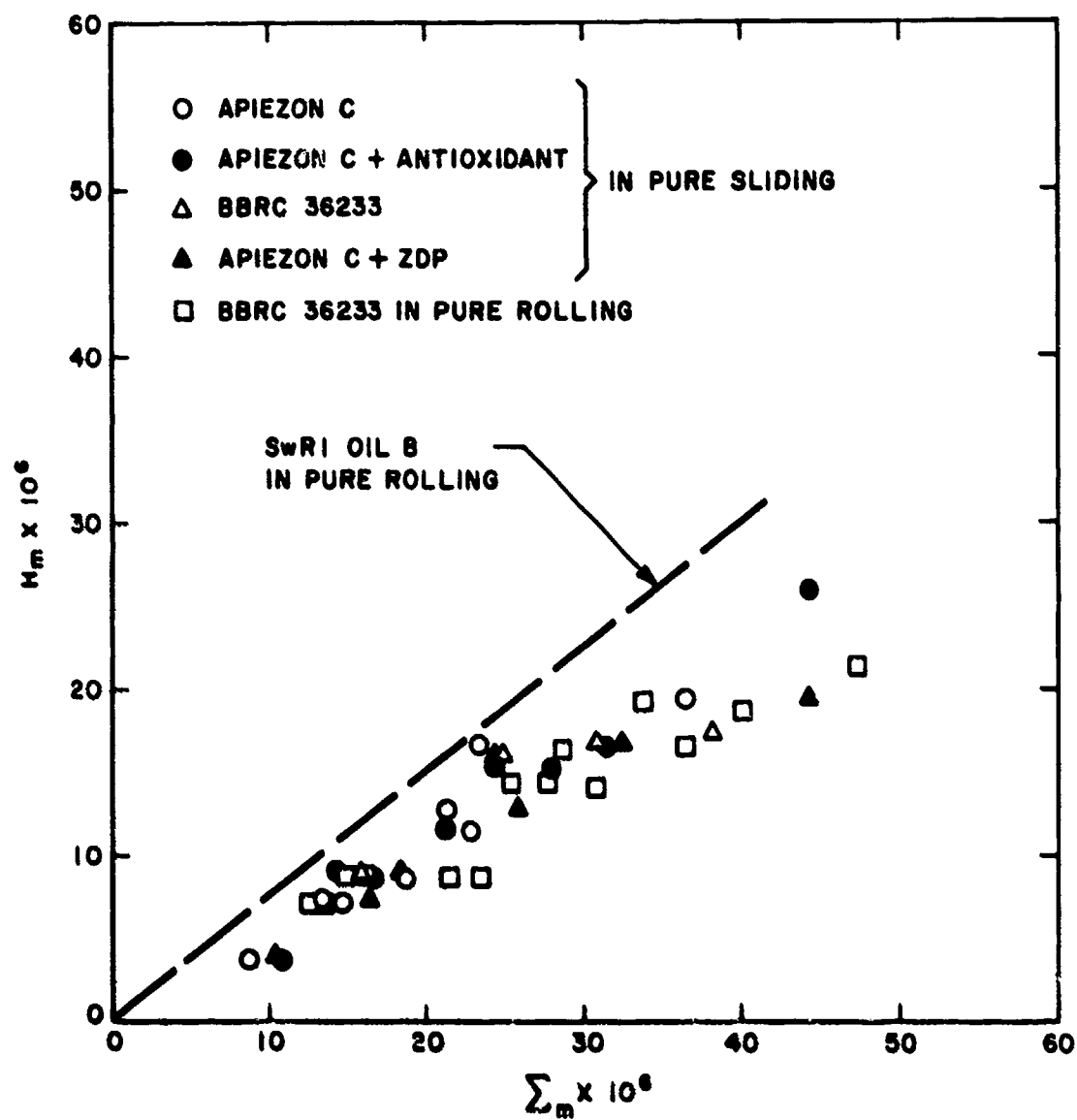


Figure 10. Dimensionless Minimum Oil Film Thickness for Four Formulations of Apiezon C

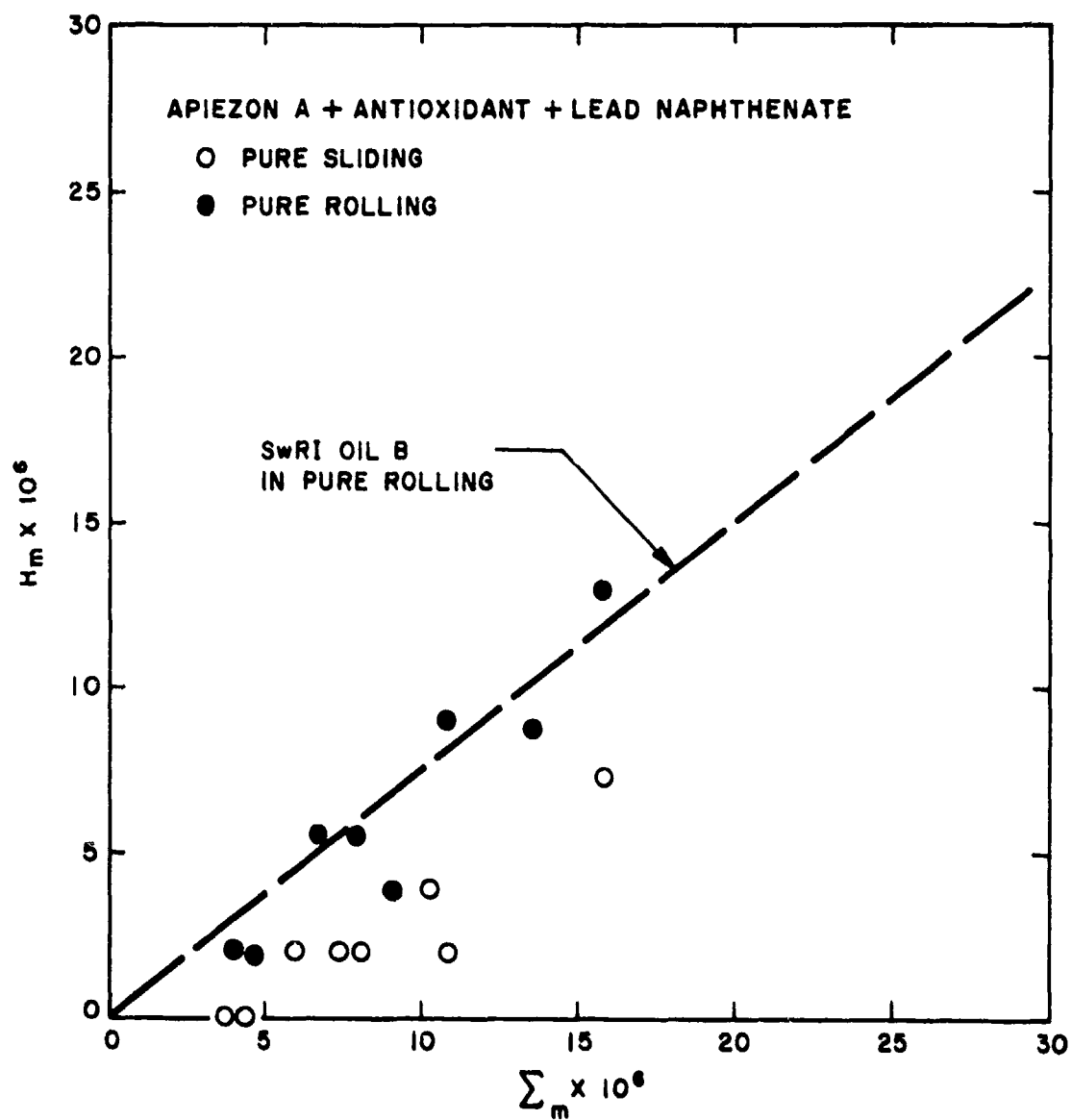


Figure 11. Dimensionless Minimum Oil Film Thickness for Apiezon A

Figure 12 for Nye 860-2, along with the pure rolling data for SwRI Oil B. The combined results for the seven oils are given in Figure 13. It is seen that these results are very similar in trends to the H_c versus Σ_c results presented in Figures 6 through 9, and the trends can basically be explained in a similar manner.

In conclusion, the linear H_c versus Σ_c and linear H_m versus Σ_m relationships, as represented by Eq. (1) and Eq. (4), respectively, incorporating the numerical correlating constants as given previously or as recommended by other investigators, appear to be approximations depending upon the range of the dimensionless material-velocity-load parameters, Σ_c and Σ_m , covered and also other details of the experiments (such as the possibility of inlet starvation, etc.). Where a flooded inlet can be assured, as in the case of these experiments, the H_c versus Σ_c and H_m versus Σ_m relationships appear to be nonlinear with progressively decreasing slopes as Σ_c or Σ_m is increased. The nonlinear trend appears to be largely dictated by thermal effects, and apparently little influenced by the oil composition as long as the operation is in the full elastohydrodynamic regime.

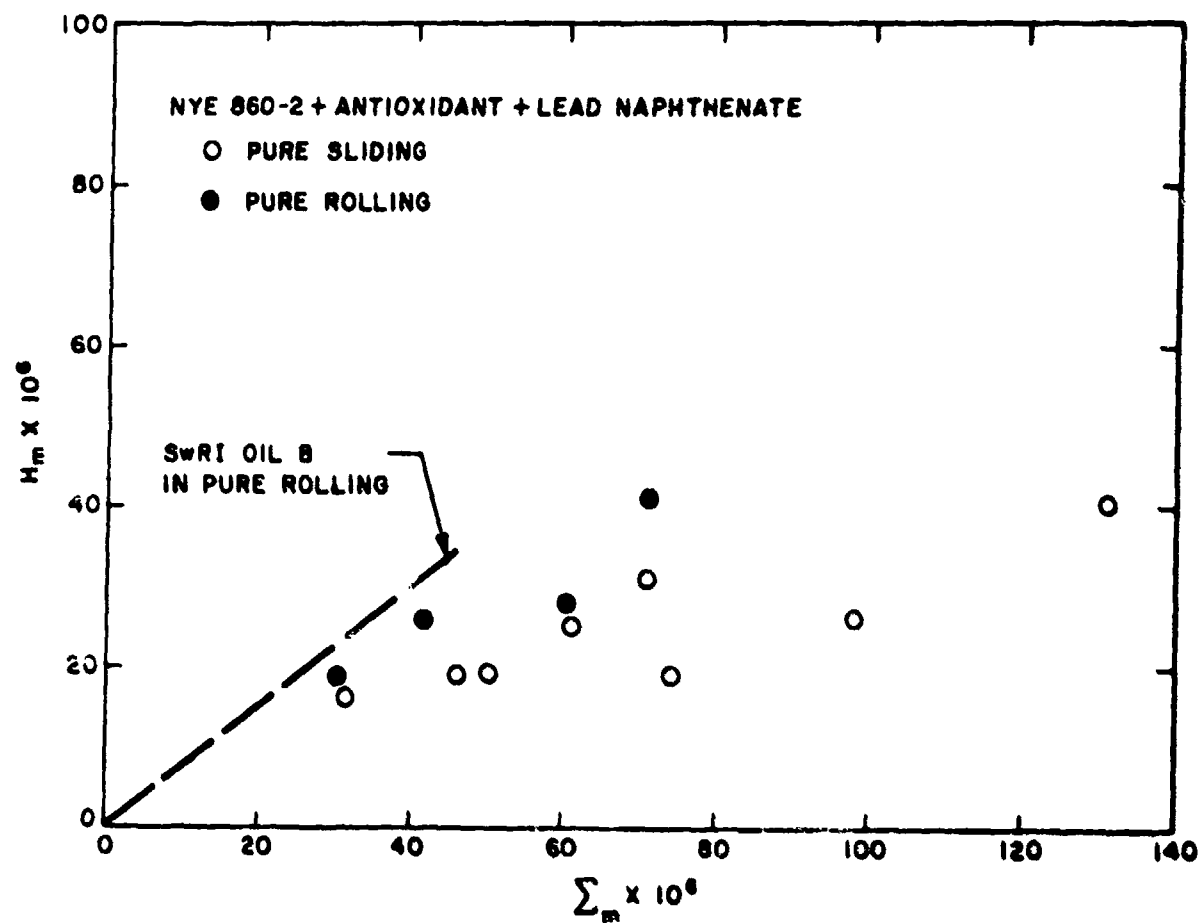


Figure 12. Dimensionless Minimum Oil Film Thickness for NYE 860-2

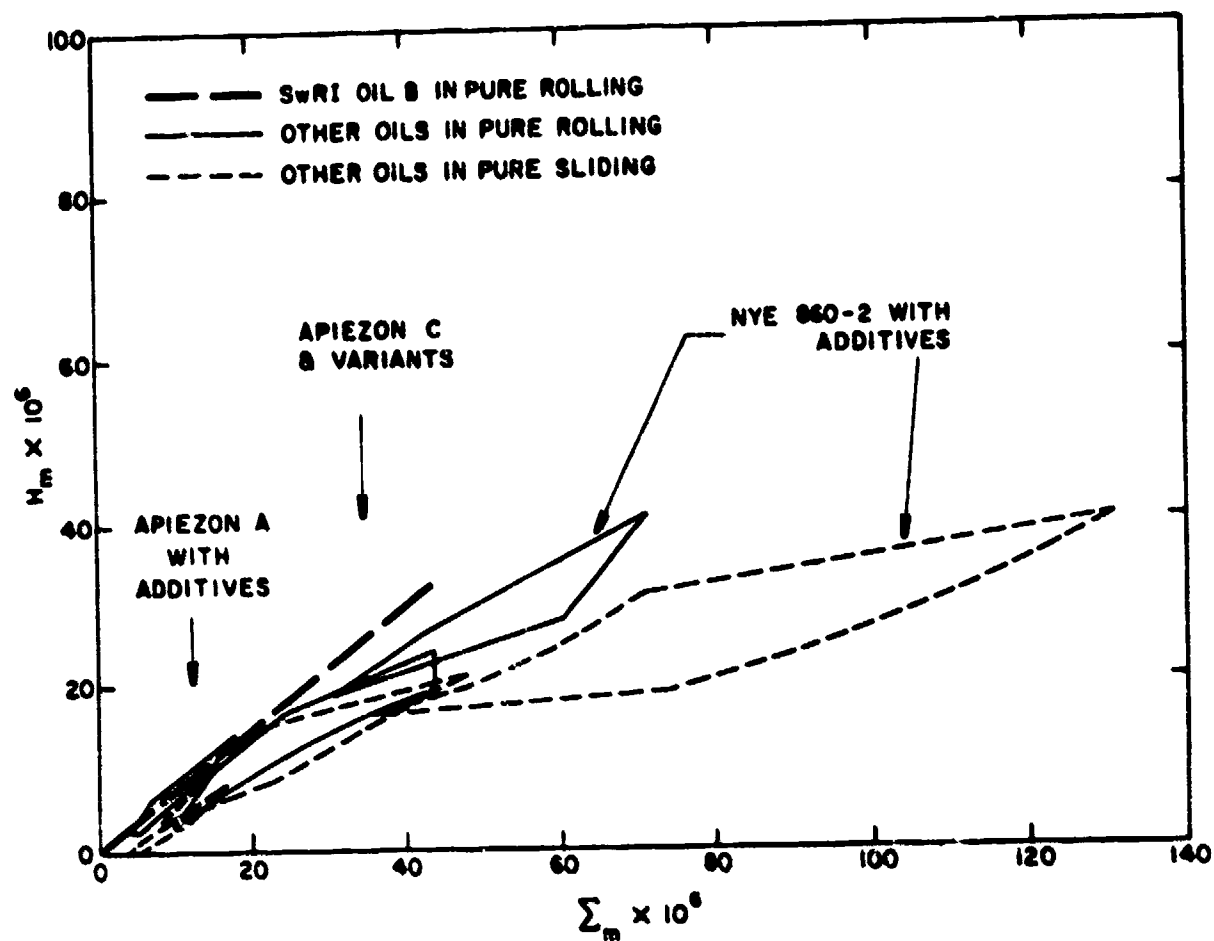


Figure 13. Dimensionless Minimum Oil Film Thickness for Seven Oils

SECTION IV

TASK II — EXPERIMENTAL MEASUREMENTS OF FILM THICKNESS IN TYPICAL DESPIN MECHANICAL ASSEMBLY BEARINGS OPERATING IN A SIMULATED SPACE ENVIRONMENT

1. General

The purpose of this task, as stated in Section V, Part I of this report, is to make quantitative measurements of oil film thicknesses in the EHD conjunctions of typical DMA bearings operating in a simulated space (vacuum) environment. As previously outlined, the measurements consider the following properties and operational variables, and their influence on the formation of an EHD oil film:

- a. oil viscosity
- b. additive effects
- c. degree of oil supply to the inlet region
- d. ball-race surface roughness
- e. temperature
- f. load
- g. speed

It was stated in Part I of this report that there would be no major variations in temperature for these Task II tests, with the room temperature being controlled at normal room conditions which would be approximately 25 C (77 F). For the purpose of obtaining additional information from the Task II experiments, the test procedure was modified to include axial displacement measurements of the bearing outer race at three different conditions (pre-pumpdown, initial after pumpdown, and 24 hours after pumpdown), instead of the original initial after pumpdown condition only. For the prepumpdown and initial after pumpdown results, measurements were made immediately after putting the test bearings into motion. Therefore, the bearings and oils were at the controlled room temperature. For the 24 hour after pumpdown results, the test bearings were allowed to seek an equilibrium temperature for normal operation of the bearings running at 100 rpm. Thus, it was possible to observe the effect of temperature, over a moderate range, on the formation of an EHD film. In other words, the bearings ran continuously at 100 rpm between the initial after pumpdown and the 24-hour after pumpdown measurements, reaching equilibrium temperatures for the appropriate test conditions.

The bearing test chamber, vacuum chamber, and associated instrumentation that were employed in this task have been described in detail in Section II, Part I, and Section II, Part II of this report and will not be repeated here.

The modified test procedure for each test in Task II was as follows: The bearings were installed in the test chamber with the proper axial preload applied to the bearings. For tests where lubricant reservoirs were employed, the reservoirs were also installed in the test chamber at this time. After the test chamber was attached to the vacuum system, but prior to pumpdown, the LVDT system was zeroed with the drive shaft not rotating. Then measurements of race displacement of the outer race of the floating bearing (forward) were rapidly made under steady operating conditions at a base speed and four speed levels of 50, 100, 150, and 200 rpm. The base speed selected was the slowest that could be attained that would maintain a steady bearing speed. This base speed created a baseline race displacement trace from which the displacements at the four other speed levels could be measured; this was necessary because of runouts in the bearings. All bearings, regardless of the precision incorporated in fabrication, will exhibit some wobble or axial runout. Typical of the axial runout measurements that have been determined in this experimental program are 50×10^{-4} to 125×10^{-4} mm (200 to 500 μ in.) for two bearings axially preloaded against each other and running at speeds up to 200 rpm. These runouts are easily detected and measured with the LVDT system and are normally displayed graphically as a sine wave or some variation thereof. When the pair of bearings, installed in the test rig and properly instrumented, are rotated very slowly, this sine wave will be generated and recorded using the LVDT and associated instrumentation. Then if the driving speed of the bearings is increased, the runout wave will be displaced from its initial position by an amount depending upon the oil film thicknesses generated in the two bearings. The base speeds for Task II tests performed varied over a range of 7 to 37 rpm. Bearing torque and temperatures were also measured at the four speed levels. It was found that the bearing temperatures did not change measurably when obtaining data if they were collected rapidly, starting with the base speed and proceeding through the four speed levels in the order of increasing speed. Also, it was found that more meaningful EHD film thickness measurements were obtained by following this increasing-speed procedure. Duplicate measurements were made for each of the four speed levels relative to a new base speed measurement. After the prepumpdown results were obtained, the bearing test rig was stopped and the test chamber was pumped down until a stable pressure was achieved. Then repeat measurements of race displacement under vacuum conditions were performed according to the same procedure as outlined above for the prepumpdown measurements. At the conclusion of these initial after pumpdown measurements, the bearing test rig was left running at a constant speed of 100 rpm for 24 hours. At the end of the 24-hour period, repeat measurements of race displacement, bearing torque, and bearing temperatures were made

exactly according to the procedure employed for obtaining the prepumpdown and initial after pumpdown results. Again, duplicate measurements were obtained. This procedure was repeated for the two axial load levels. From these measurements, the film thicknesses were determined using a computer program which solves the race displacement versus oil film thickness relationship. Development of this computer program and presentation of the computed results will be presented later.

Based on experiments discussed in Section IV, Part I of this report, it is concluded that the effects of thermal expansion are probably negligible for the speed range examined in the present program. Precautions were taken, however, when the film thickness measurements were made in Task II, to minimize any error that could be caused by thermal expansion effects. This was done by obtaining the displacement measurements as rapidly as possible following a speed change thus allowing a minimum amount of time for any thermal expansion to occur. In addition, a new zero reading to account for any instrument drift was determined immediately prior to making displacement measurements.

2. Development of Computer Program to Analyze Test Results

In Part I of this report, an equation was developed to relate the measured axial displacement of the outer race of the bearing located in the diaphragm mounting ring to the EHD film thicknesses between the balls and races in the bearings. The equation as developed in Part I is

$$\Delta L_y = 2 \left\{ 0.025 \left[0.43837 - \sin \left[\arccos \left(\frac{0.02247}{0.025 - 2 h_c} \right) \right] \right] + 2 h_c \sin \left[\arccos \left(\frac{0.02247}{0.025 - 2 h_c} \right) \right] \right\} \quad (7)$$

where ΔL_y is the total axial displacement of the outer race of the bearing in the diaphragm mount as measured by the LVDT shown in Figure 1. This total displacement is the result of the development of EHD films at the inner and outer ball-race conjunctions in two bearings.

It was assumed in the derivation of Eq. (7) that the same film thickness existed at both the inner and outer ball-race contacts in both bearings. Two oversimplifications are involved in that assumption. First, in either bearing, the EHD film thickness at a ball-outer race contact will differ from that at a ball-inner race contact because of geometry effects. From theory and

experiment, it is well known that due to better conformity of the ball and outer race, the film thickness will be thicker there than at the ball-inner race contact. For the bearings employed in the present work this difference amounts to about 10 percent. Second, due to different heat transfer paths, the operating temperatures of the two bearings in the test rig can be different, and this affects the viscosity of the oil and consequently the EHD film thickness. Depending upon the magnitude of this temperature difference, the EHD film thickness in one bearing can differ from the EHD film thickness at the corresponding location in the other bearing by as much as 20 percent. When the combined effects of geometry and temperature difference are considered, it is felt desirable to account for them when calculating the EHD film thicknesses in the two bearings from the displacement measurements. To do this requires a system of equations rather than the simple Eq. (7). Briefly, the procedure involves first solving an equation similar to Eq. (7) for the EHD film thickness at the ball-inner race contacts of the aft bearing. Then, using the known empirical relationships for the effects of geometry and viscosity on the EHD film thickness, the film thickness at the ball-outer race contacts of the aft bearing and the film thickness at the ball-inner race and ball-outer race contacts of the forward bearing can be calculated.

Further complicating the task of accounting for the effects of contact geometry within a bearing, and temperature difference between bearings, is the fact that, according to theory, a difference in contact geometry will have different effects on the minimum EHD film thickness and the central-region EHD film thickness. The same is true of the effect of viscosity. Consequently, in order to account for the geometry and viscosity effects on the EHD film thicknesses in the bearings, one must assume that it is either the minimum or the central-region EHD film thickness that is responsible for the displacement ΔL_y being measured. Unfortunately, as was discussed in Part I of this report, it is not possible to determine from the results of Task I whether it is the minimum or central-region EHD film thickness that is responsible for the displacement. Therefore, in the reduction of the displacement data from Tasks II and III, the film thicknesses in the bearings were calculated in two ways, first by using a system of equations developed by assuming that ΔL_y is due to the central-region EHD film thickness, and next by using a system of equations developed by assuming that ΔL_y is due to the minimum EHD film thickness.

Since the development of the two systems of equations for calculating the EHD film thicknesses from the bearing displacement data is rather detailed and lengthy, this is included in Appendix I. As shown in Appendix I, in order to avoid confusing the theoretical values of EHD film thicknesses, calculated using the theoretical equations of Grubin (6) and Dowson (7), with the experimentally-determined values of the EHD film thicknesses obtained from the race displacement measurements, different symbols are used. In accordance with the standard symbols used earlier, h_c , h_m , H_c , and H_m are the symbols reserved for the theoretical central-region, minimum, dimensionless central-region, and dimensionless minimum EHD film thicknesses respectively. For

the film thicknesses determined from the race displacement measurement, the symbols h , h' , H , and H' are used to denote the minimum, central-region, dimensionless minimum and dimensionless central-region EHD film thicknesses respectively. Throughout the report, comparisons of the EHD film thicknesses calculated from the measured bearing displacement data in these two ways are compared with the theoretical equations of Grubin for H_c and Dowson for H_m .

3. Experimental Test Results

As discussed above, a computer program was developed to compute the four different conjunction film thicknesses for the DMA bearings tested in Task II. A listing for the Task II data reduction program is given in Appendix II, while a sample printout of the Task II data is shown in Appendix III.

The best available expression for the central-region EHD film thickness in a flooded isothermal rectangular conjunction is due to Grubin⁽⁶⁾ and is given by

$$H_c = 1.18 \Sigma_G \quad (8)$$

where Σ_G = Grubin's dimensionless material-velocity-load parameter for rectangular conjunctions

$$= \frac{G^{0.73} U_t^{0.73}}{W^{0.09}}$$

$$W = \text{dimensionless load} = \frac{w}{\frac{\mu}{E} R}$$

w = load per unit width

and the other symbols are defined after Eq. (6).

While the central-region EHD film thickness is important to the present study, the minimum EHD film thickness is also extremely important. As is now well known, the oil film thickness profile in a rectangular conjunction is very nearly flat throughout, modified principally by a constriction in the exit region. This constriction, which is straight across the flow path for a rectangular conjunction, and almost straight for a high aspect ratio elliptic conjunction, results in a minimum oil film thickness within the conjunction, so that if surface-to-surface contact is to occur, it is apt to occur here first. Thus, the importance of predicting the minimum EHD film thickness in a bearing is evident.

Based upon theoretical analyses and considerable experimental data, Dowson⁽⁷⁾ recently proposed the following equation for computing the

minimum oil film thickness in a flooded isothermal rectangular conjunction:

$$H_m = 1.63 \Sigma_D \quad (9)$$

where Σ_D = Dowson's dimensionless material-velocity-load parameter for rectangular conjunctions

$$= \frac{G^{0.54} U_t^{0.70}}{W^{0.13}}$$

and the other symbols are given after Eq. (6) and Eq. (8).

Equation (9) is believed to be the best expression available for calculating the minimum film thickness for the rectangular or high aspect ratio elliptic conjunction with flooded, isothermal flow.

When the film thickness equations for rectangular conjunctions are used to calculate the film thickness in elliptic conjunctions, an equivalent load per unit width ⁽⁸⁾ is used. For a bearing with elliptic conjunctions, as in this study, the dimensionless load per ball is given by

$$W_e = \frac{w_e}{\frac{\pi}{E} R} \quad (10)$$

where w_e = equivalent unit load per ball = $\frac{3P}{4a}$

P = normal load per ball

a = semiwidth of major axis of contact ellipse at ball-raceway contact

and \bar{E} and R are as previously defined. Therefore, the W_e in Eq. (10) replaces W in both Eqs. (8) and (9) for angular contact bearings.

The above equations were presented and discussed in detail in Section II, Part I of this report but were repeated here because they were used extensively in analyzing the Task II data. As noted, all of the plotted Task II experimental data that are presented in the following graphs are compared with these equations. Also, Eqs. (8) and (9) were used to calculate H_c and H_m at the base speed. These calculated values were then added to the film thicknesses determined from ΔL_y to obtain H and H' plotted in the following graphs.

Since the four different conjunction films for each test condition were calculated from a single displacement measurement, ΔL_y , they all followed similar patterns, although, the magnitudes of each would vary a few percent. The variance between inner and outer race film thickness are the result of a geometrical difference in the ball-race contacts, whereas the difference between aft- and forward-bearing contact film thickness values are

a result of temperature differences between the two bearings.

Figure 14 shows typical film thickness values, calculated from the race displacement measurements, for the inner and outer contacts of the forward and aft bearings. The data were obtained prior to pumpdown for bearings treated with BBRC 36233. The dimensionless film thicknesses H and H' are plotted against the dimensionless parameters Σ_D and Σ_G respectively, which were defined and discussed earlier in this section of the report. As can be seen in the figure, the film thicknesses at all four locations display the same trends. Although there are slight load effects shown by the data at the larger dimensionless parameter values, a single straight line drawn through the experimental data for either H or H' would represent all the data very well. Of course, 24-hr after pumpdown results would display variance between the aft and forward bearings due to temperature differences, but as will be seen later these effects would be well correlated by the dimensionless parameters. Normally, the prepumpdown and initial after pumpdown results would not show an appreciable temperature difference between the aft and forward bearings, while the 24-hr after pumpdown results would exhibit a 1 to 4C (2 to 7F) temperature spread. This was not the case for tests using Nye 860-2 with antioxidant and lead naphthenate. Of all the oils tested, this one has the highest viscosity. The torque capability of the driving magnetic coupling was not great enough to turn the bearings lubricated with this oil at normal room temperature. Therefore, heat lamps directed at the bearing rig chamber were employed to raise the temperature enough to allow thinning of the lubricant until some test data could be obtained. Even then, it was not possible to turn the bearings at the higher speed levels.

Since as indicated in Figure 14 the experimental film thickness data for the four different conjunction locations behave similarly, the data for all will not be presented. The aft bearing outer race contact data were arbitrarily selected for further analysis and comparison, and all of the Task II plotted data shown in the following graphs will be values for those contacts. For purposes of generality, all of the film thickness data are presented in dimensionless form. However, the dimensional value of film thickness may be obtained by multiplying the dimensionless film thickness H or H' by the equivalent radius at the ball-outer race contacts, R_O , which is 8.84352 mm (0.34817 in.).

A summary of all bearing tests for Task II is presented in Table II. As seen in the table, a total of four test series were run and each series was designed to isolate the effects of an oil property or design variable. For each test within a series, the operating variables were load and speed. Two load levels were used, the minimum of 222-N (50-lb) axial load, and the maximum of 890-N (200-lb) axial load as prescribed in the Statement of Work. Only two load levels were selected because of the extremely weak dependence of the oil film thickness on load, as was shown in the EHD film thickness equations. Because the oil film thickness is more sensitive to the conjunction sum velocity,

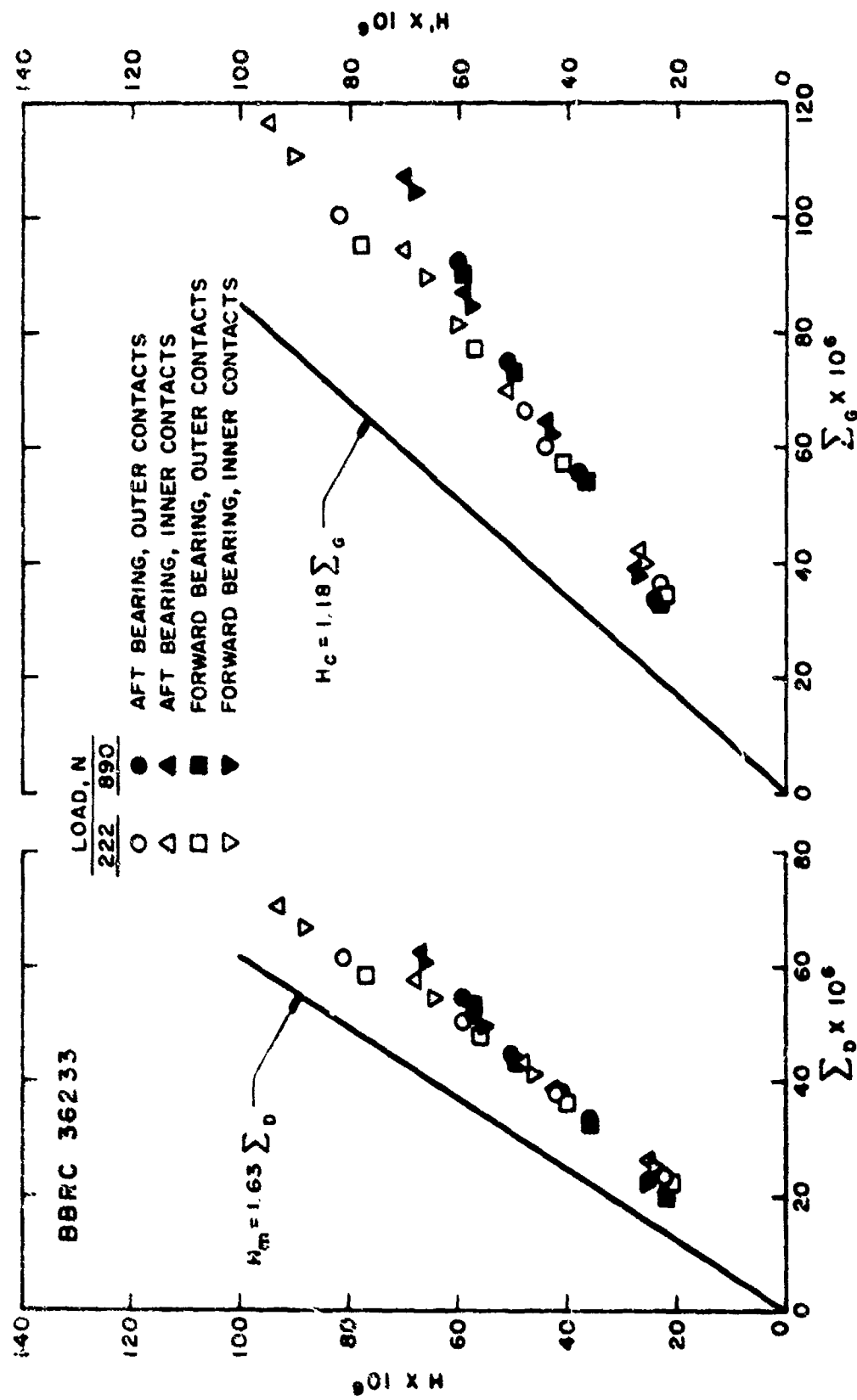


Figure 14. Dimensionless Prepumpdown Oil Film Thicknesses for Standard Bearings Having Thick Initial Film of BBRC 36233

TABLE 2. SUMMARY OF TASK II TESTS

Test Series	Variable Studied	Viscosity at 25 C (77 F), $\text{m}^2/\text{s} \times 10^6$	Additive Package	Initial Oil Film Thickness	Ball-Race Surface Roughness	Common Tests
I	Oil Viscosity	54	BBRC standard	Thick	MRC standard	x
		225	BBRC standard	Thick	MRC standard	
		1000	BBRC standard	Thick	MRC standard	
II	Additives	225	1.5% antioxidant	Thick	MRC standard	x
		225	BBRC standard	Thick	MRC standard	
		225	2.5% ZDP	Thick	MRC standard	
III	Initial Thickness of Applied Oil Film	225	BBRC standard	Thick	MRC standard	x
		225	BBRC standard	Thin	MRC standard	
IV	Ball-Race Surface Roughness	225	BBRC standard	Thick	MRC standard	x
		225	BBRC standard	Thick	Roughness doubled	
		225	BBRC standard	Thin	MRC standard	
		225	BBRC standard	Thin	Roughness doubled	

TEST CONDITIONS:

Pressure = equilibrium vapor pressure of test oil
 Temperature ≈ 25 C (77 F)
 Load = 222, 890 N (50, 200 lb) (2 load levels)
 Speed = 50, 100, 150, 200 rpm (4 speed levels)

OIL BASE STOCK DESCRIPTION:

High viscosity oil = Nye 860-2
 Intermediate-viscosity oil = Apiezon C
 Low viscosity oil = Apiezon A

ADDITIVE PACKAGE:

BBRC standard = 1.5% antioxidant + 5% Lead naphthenate

four levels of bearing speed above the base speed were used for each test within a series, 50, 100, 150, and 200 rpm, except for the high viscosity oil where the torque capability of the driving magnetic coupling was not sufficient to achieve the higher speeds.

As seen in the table, for all tests the environmental pressure in the bearing test chamber was to be the equilibrium vapor pressure of the test oil. It was found that the vapor pressure for formulations of Apiezon C, as calculated from the vapor pressure equation and constants given in Section II, Part I of this report, could not be achieved even with extended pumping time. On the other hand, it was not difficult to obtain the vapor pressure for Apiezon A as predicted by this same equation. This suggests that there might be an error in the constants in the equation for Apiezon C. As stated in Section II, Part I, the constants have not been determined for the Nyc 860-2 oil, although limited weight-loss data obtained from evaporation cell measurements at BBRC indicate that its vapor pressure may not be greatly different from that of Apiezon C. Also, as seen in the table, for all tests the room temperature would be held approximately constant at about 25C (77F). Bearing temperatures that varied moderately from 25C (77F), especially in the 24-hr after pumpdown tests, were handled satisfactorily by the EHD film thickness equations showing no consistent disagreement with the other data.

Also as seen in Table II, two initial oil film thickness coatings on the bearings were investigated. These are designated in the table simply as "thick" and "thin". For the "thick" initial oil film tests, oil impregnated reservoirs were installed in the test chambers. For the "thin" initial oil film tests, no reservoirs were used.

Each test series shown in Table II along with plotted data representing that test series will be discussed separately in the following paragraphs. Highlights of these data will be pointed out and conclusions will be drawn later based on these test results.

Test Series I. In this test series the effect of oil viscosity on the oil film thicknesses formed in the EHD conjunctions of the bearings was studied. Three separate tests were conducted, one with each of three test oils of different viscosities, a low-, medium-, and a high-viscosity oil as shown in Table II. Each oil contained the same BBRC standard additive package, which is 1.5 percent antioxidant and 5 percent lead naphthenate. The initial oil film thickness was "thick film" which was about 30×10^{-4} to 40×10^{-4} mm. The bearings had the standard surface finish on the raceways, hereinafter referred to simply as "MRC standard." As discussed earlier in this section of the report, only part of the high-viscosity oil tests were achieved because of the excessive torque required to drive the bearings, especially at the higher speeds and at normal room temperatures.

Looking at Figures 15, 16, and 17, it is clear that the measured dimensionless film thicknesses increase with increasing viscosities when plotted against either Dowson's or Grubin's dimensionless parameters. Whereas Grubin's Eq. (8) predicts a slope of 1.18 as shown by the solid curve drawn on the righthand graphs in each figure, a best-fit line drawn through the low-viscosity oil, a formulation of Apiezon A, would exhibit a slope that would be considerably less, having a value of approximately 0.63. Likewise, as seen in Figure 16, the medium-viscosity oil, a formulation of Apiezon C (BBRC 36233), would exhibit a slope of approximately 0.73 and as seen in Figure 17, the high-viscosity oil, a formulation of Nye 860-2, would have a slope approximately the same as predicted by Grubin. Going to the lefthand graphs shown in Figures 15, 16, and 17, and comparing the measured dimensionless film thicknesses, H , to Dowson's Eq. (9), it is seen that the same trend is exhibited. These experimental results show that both the low-viscosity (Apiezon A) and medium-viscosity oil (BBRC 36233) have a slope less than predicted by Dowson. On the other hand, the data for these two oils agree better with Dowson's equation than Grubin's central-region film thickness equation. The experimental results for the high-viscosity oil (Nye 860-2) appear to have a slope slightly higher than predicted by Dowson, but agree very well with Grubin. Post-test examination of bearings show that these three oils, as employed in these tests, appear to provide film thicknesses adequate to place operation in the full EHD regime. But the plotted data indicate that only the high-viscosity oil, Nye 860-2 with antioxidant and lead naphthenate, is operating in the flooded conjunction regime, therefore agreeing with the theoretical equations. Although the low-viscosity and medium-viscosity oils seem to have adequate oil film thicknesses to prevent asperity contact, there does appear to be limited lubricant starvation causing films less than predicted by either Dowson or Grubin. Although the high-viscosity oil does agree very well with the theoretical flooded isothermal flow equations, large torques are required to drive bearings supplied with this oil making it undesirable as a DMA bearing lubricant.

In general the viscosity effects for these three oils do not appear to be completely correlated by Grubin's or Dowson's parameters. Using measured ΔL_y values for calculating film thicknesses H , and H' which are then compared to both relationships appear to show better correlation between the minimum film thickness equation and the measured values, H . Of course these were short duration tests and do not predict what might happen under extended vacuum conditions.

Test Series II. This series was conducted to determine the effect of additives on the oil film thicknesses in the EHD conjunctions of the bearing. For these tests the intermediate-viscosity oil was used and the first test as shown in Table II was conducted using this oil without the antiwear additive, but the antioxidant additive was retained. Note that the second test in this series was common to Series I, where the same oil with the additive package was used, thus only two tests were required in Series II. The third test shown

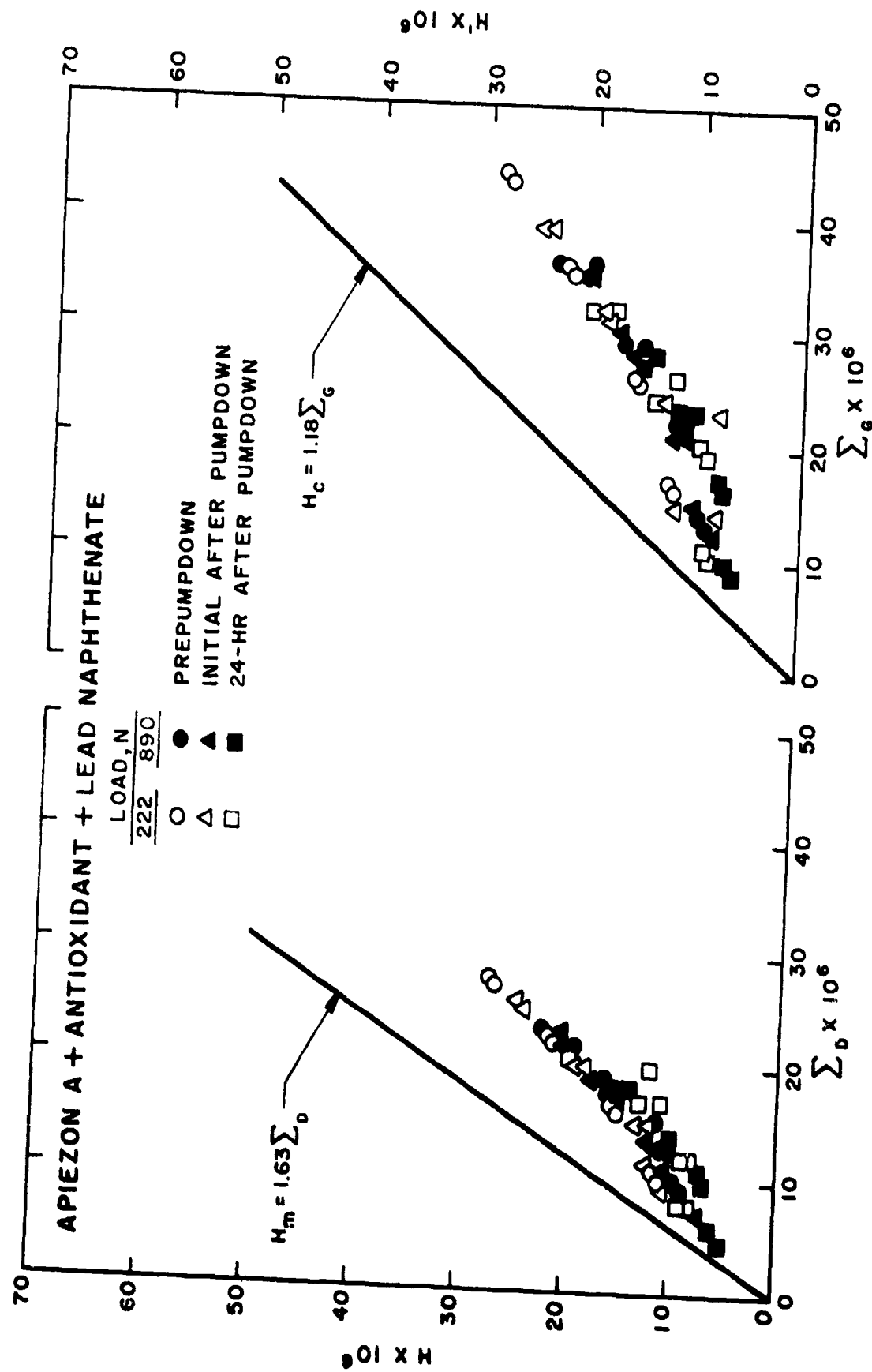


Figure 15. Dimensionless Oil Film Thicknesses for Standard Bearings Having Thick Initial Film of Low-Viscosity Oil

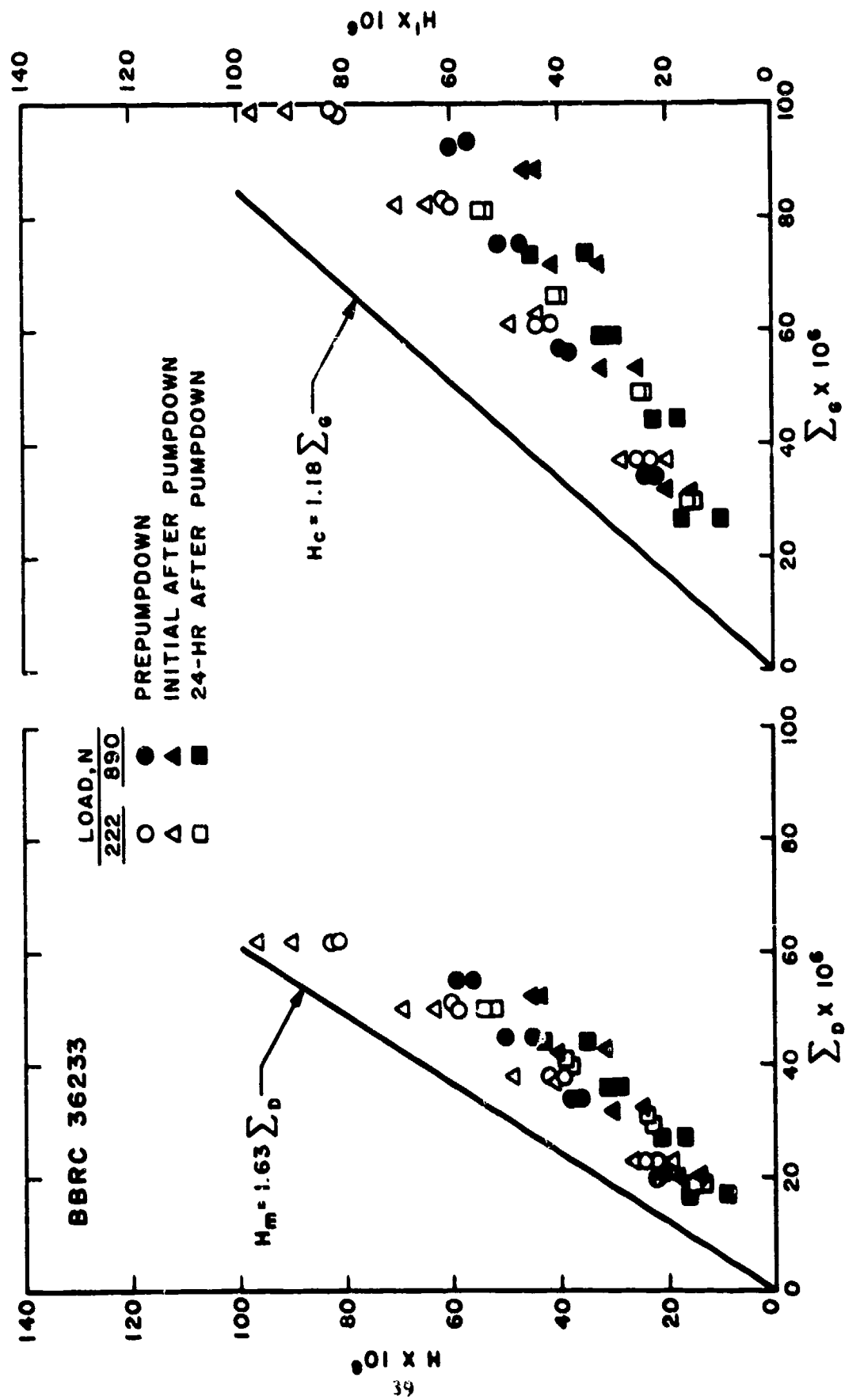


Figure 16. Dimensionless Oil Film Thicknesses for Standard Bearings Having Thick Initial Film of Intermediate-Viscosity Oil

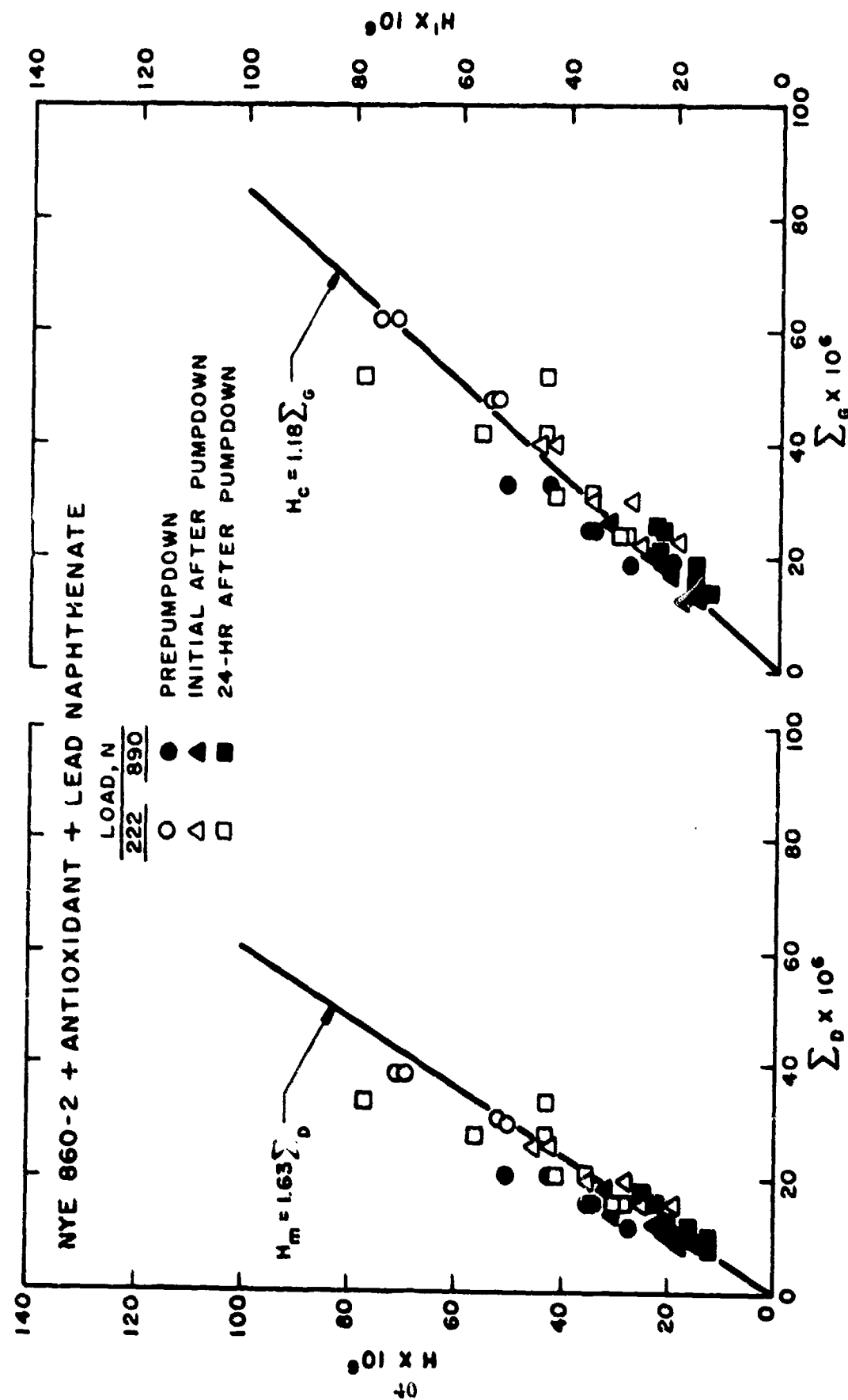


Figure 17. Dimensionless Oil Film Thicknesses for Standard Bearings Having Thick Initial Film of High-Viscosity Oil

in the table for Series II was conducted with the intermediate-viscosity oil, but with ZDP as the antiwear additive. As in Series I, the initial oil film thickness was the "thick film." The MRC standard bearings were employed for the tests in Series II.

Figures 16, 18, and 19 show a comparison of the experimentally-determined film thicknesses H and H' for each of these additives as compared to the Dowson Eq. (9) and the Grubin Eq. (8), respectively. In comparing these results it is seen that there appear to be load effects for the Apiezon C with ZDP. The low-load data clearly have larger dimensionless film thicknesses than the high-load data. On the other hand, this is not readily apparent for the Apiezon C with antioxidant or the BBRC 36233 (Apiezon C with antioxidant and lead naphthenate). If the best-fit line is drawn through each of these different formulations of Apiezon C, ignoring any load effects, the Apiezon C with ZDP would exhibit a slightly higher slope than Apiezon C with antioxidant, although not enough to be of major significance. In comparing these plots of data it appears that BBRC 36233 exhibits slightly thinner film thicknesses than the two other Apiezon oils with different additives, although the difference does not appear to be of major significance and may not be greater than the experimental error involved. Therefore, the effects of these additives on the formation of an EHD film, appear to be negligible for the particular test conditions employed in these tests.

Test Series III. In this test series the effect of the initial oil film thickness was studied. For both tests, the intermediate-viscosity oil with 1.5 percent antioxidant and 5 percent lead naphthenate (BBRC 36233) was used. Note in Table II that the first test is common to Series I, where the same initial oil film thickness with the same oil and standard test bearings were used, so that only one additional test was required in Series III. In the second test shown in the table for Series III, the initial oil film thickness was "thin film," which was about 1×10^{-4} mm, a less favorable condition for the development of full EHD oil films in the ball-raceway conjunctions. For this test, the MRC standard bearings were also used.

Figure 20 shows the dimensionless film thicknesses, H and H' plotted versus Dowson's and Grubin's parameters, respectively for "thin film" bearings. As illustrated in the figure, there is clearly a load effect as shown by the data points for this test condition which is similar to, but, more clearly distinguishable than the one discussed above for Apiezon C with ZDP and having a thick initial oil film. The first conclusion, based on these data, is these "thin film" bearings did not have a sufficient amount of lubricant to maintain the EHD film thicknesses at the higher loads. On the other hand, there appeared to be a sufficient amount of lubricant to provide both central-region and minimum film thicknesses near those predicted by both Grubin's and Dowson's equations at the low load level. In comparing these data with the results shown in Figure 16 for the same lubricant but with a thick initial oil film, it is seen that the high-load results

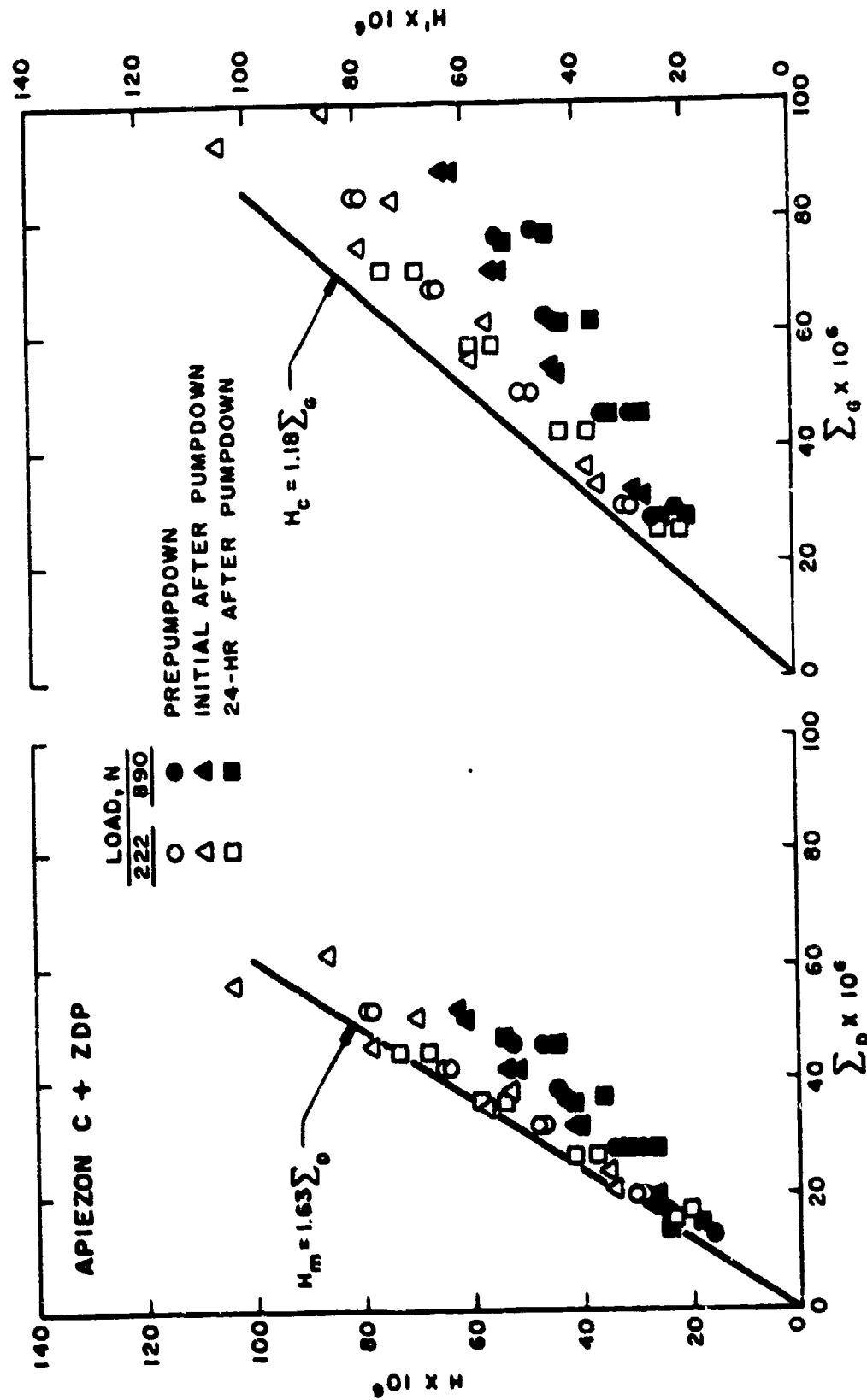


Figure 18. Dimensionless Oil Film Thicknesses for Standard Bearings Having Thick Initial Film of Intermediate-Viscosity Oil Containing Antiwear Additive ZDP

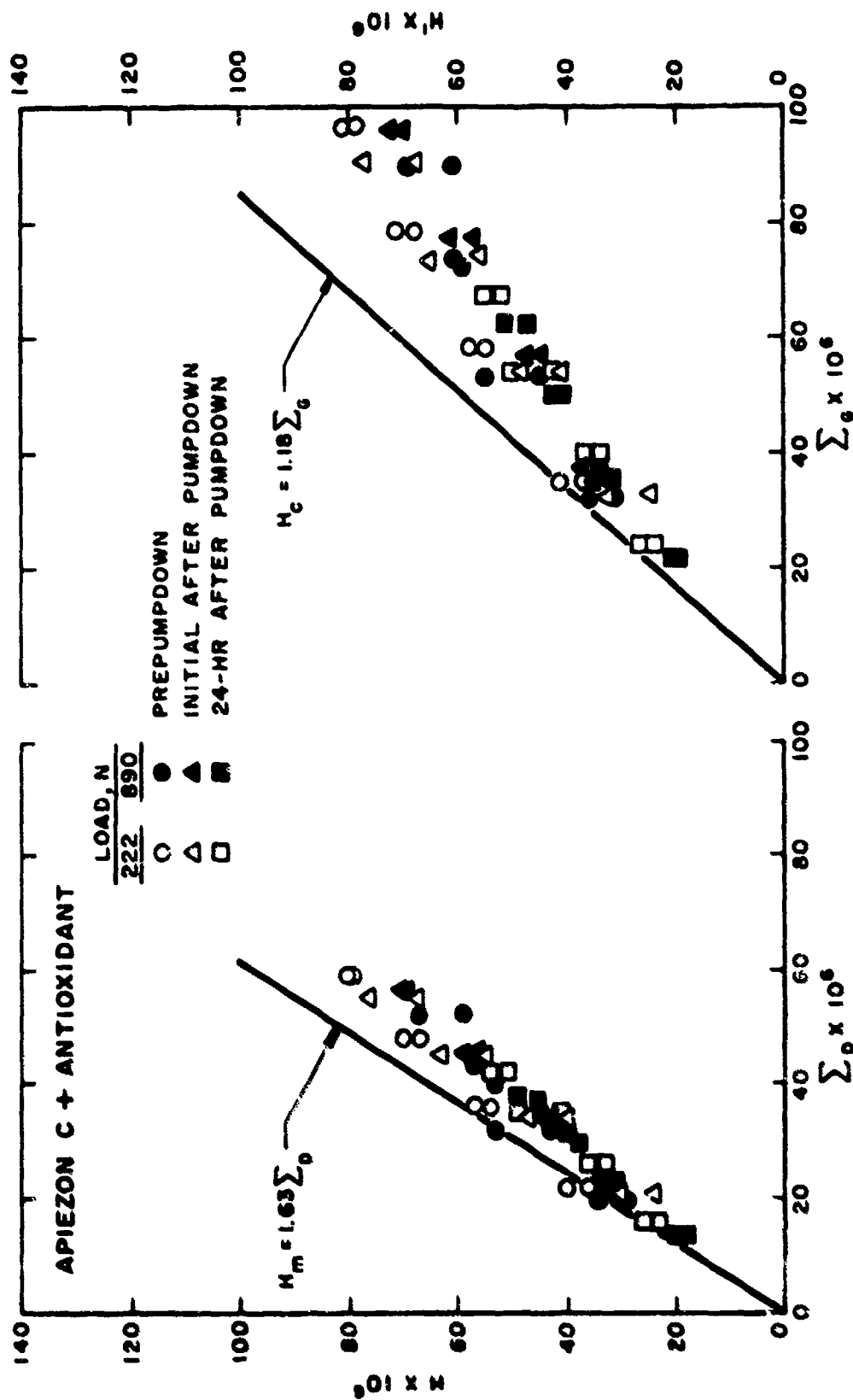


Figure 19. Dimensionless Oil Film Thicknesses for Standard Bearings Having Thick Initial Film of Intermediate-Viscosity Oil Containing No Antiwear Additive

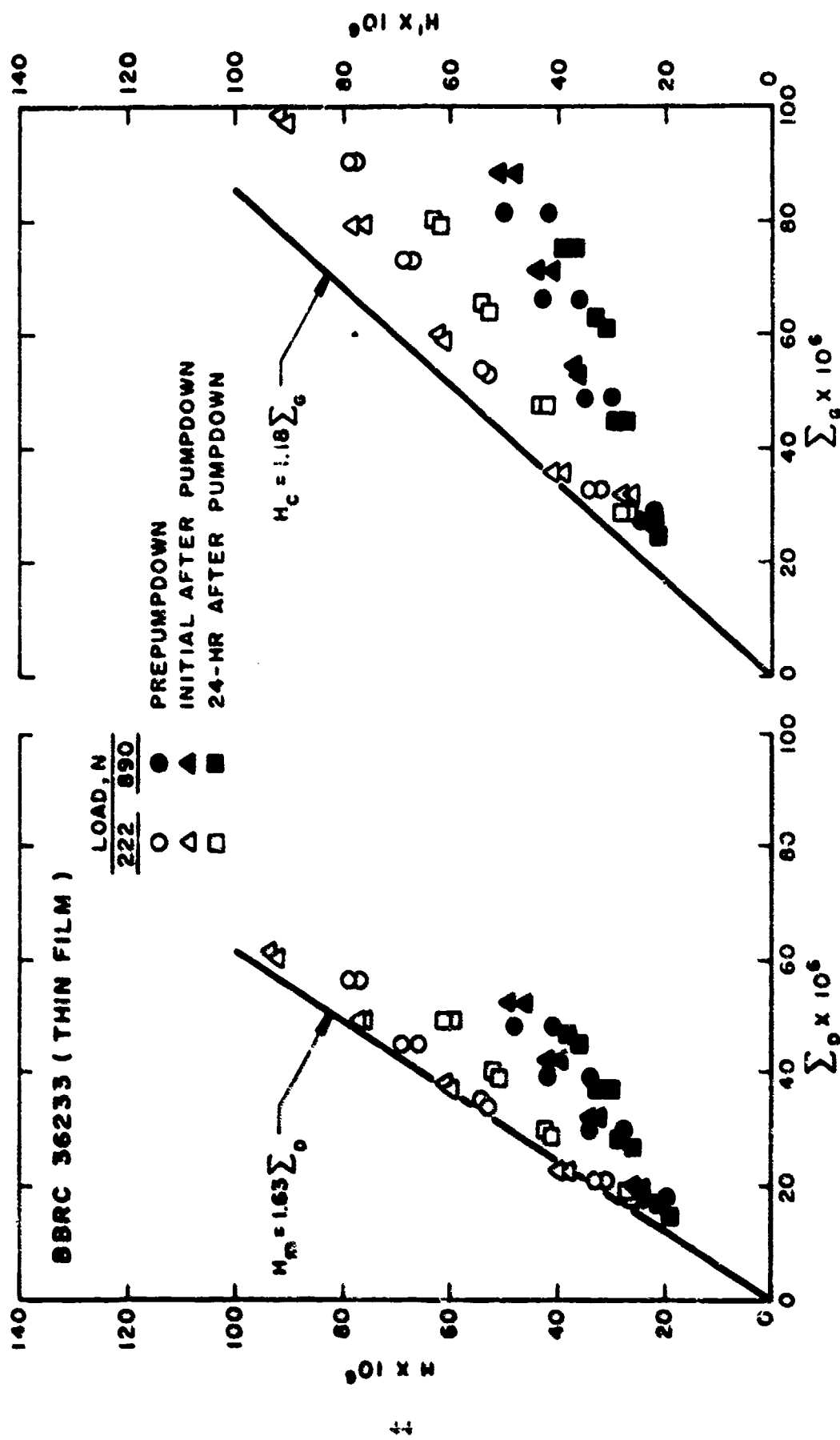


Figure 20. Dimensionless Oil Film Thicknesses for Standard Bearings Having Thin Initial Film of Intermediate-Viscosity Oil

for the "thin film" bearings (Fig. 20) agree very well with both the low-load and high-load results for the "thick film" bearings (Fig. 16). This suggests that possibly the low-load results for the "thin film" bearings are in error because of a testing load deficiency. Even if this is the case, both the "thick film" and "thin film" bearings appear to have film thicknesses sufficient to prevent asperity contact between the balls and races, but neither is performing in a flooded conjunction regime which should give experimental results in agreement with Dowson's and Grubin's equations. Again, these were short duration tests and the results might change considerably under extended operating conditions.

Test Series IV. This test series was conducted to determine the effect of ball-race surface roughness on the oil film thicknesses in the EHD conjunctions in the bearing. This was done using the intermediate-viscosity oil with the additive package of 1.5 percent antioxidant and 5 percent lead naphthenate for all tests in the series. Tests were conducted with both "thick" and "thin" initial oil film thicknesses on the bearings, as shown in Table II. The data supplied by MRC and presented in Section II, Part II of this report showed the surface roughness of the rough bearing races to be $0.204 \mu\text{m}$ ($8 \mu\text{in.}$) which is twice that shown for the standard bearings.

Figure 21 is for "thick" initial oil film with the BBRC 36233 additive package and rough ball-race surface roughness. Comparing this with Test Series I data for standard bearings lubricated with BBRC 36233 and shown in Figure 16 shows very good agreement and suggests that both the standard and rough bearings continue to operate with essentially the same film thicknesses. In fact the best-fit line drawn through both the H and H' data on both these figures would show the rough bearings to have slightly thicker film thicknesses. Again, the best correlation appears to be between the measured data and Dowson's minimum film thickness equation.

The last two tests shown in Table II are for "thin" initial oil film with one test having been conducted with standard MRC bearings and discussed above under Test Series III. The previous data showed questionable load effects. The last of these tests was for bearings having the roughness doubled and a "thin" initial oil film and the results are shown in Figure 22. These data do not show the extreme load effect that is shown in Figure 20 except possibly the low-load, prepumpdown data. This observation further suggests that the low-load data shown in Figures 18 (discussed earlier) and 20 may be in error due to insufficient loading. Disregarding the low-load results shown in Figure 20, the measured film thickness data for both the "thin" initial oil film tests agree very well. Because the measured data is significantly less than either Dowson's or Grubin's predicted values it is probable that oil starvation in these "thin film" tests was present. On the other hand, even though a flooded conjunction apparently was not maintained, operation of the bearings appeared to be satisfactory with a minimum of asperity contact between the balls and races.

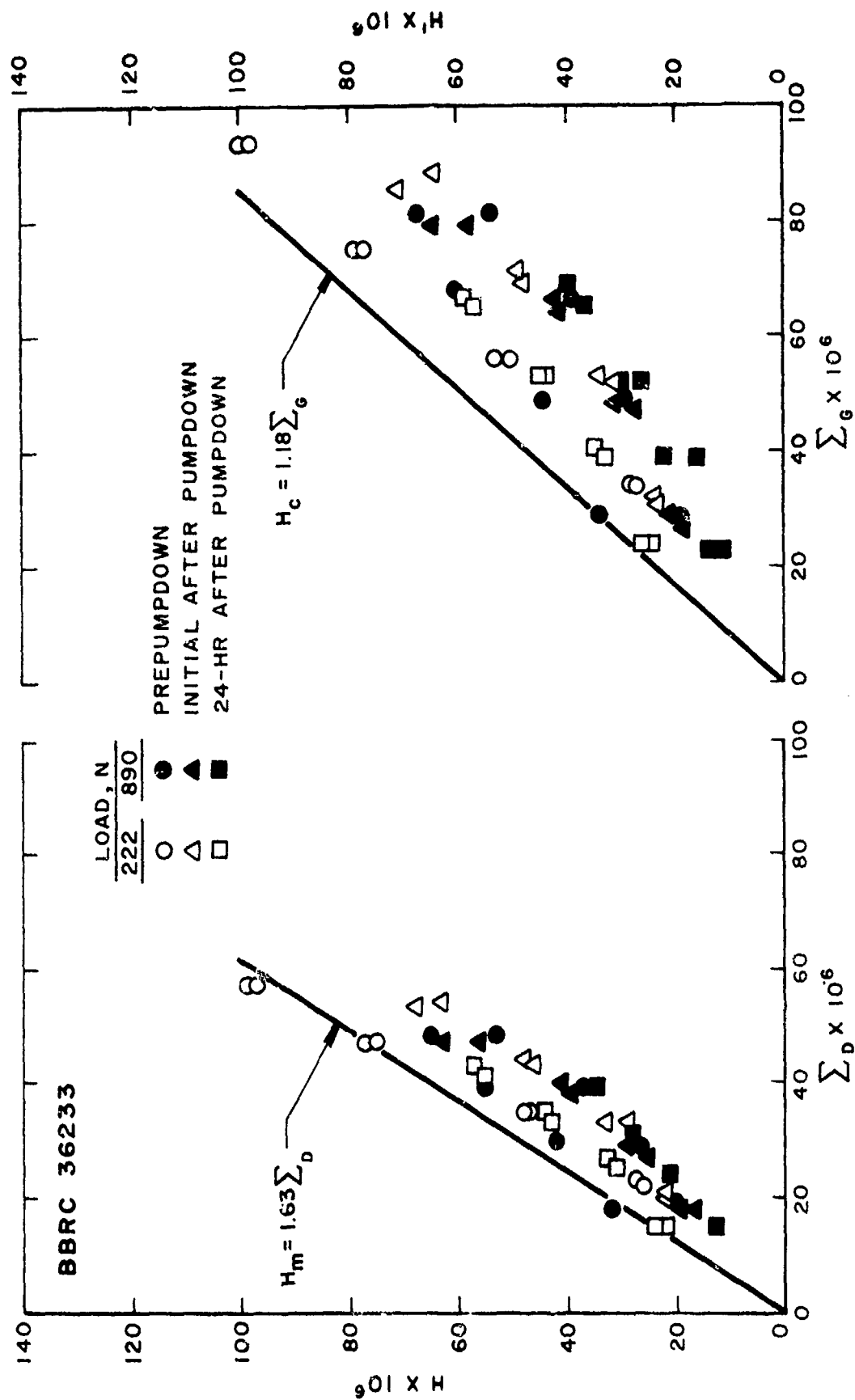


Figure 21. Dimensionless Oil Film Thicknesses for Rough Bearings
Having Thick Initial Film of Intermediate-Viscosity Oil

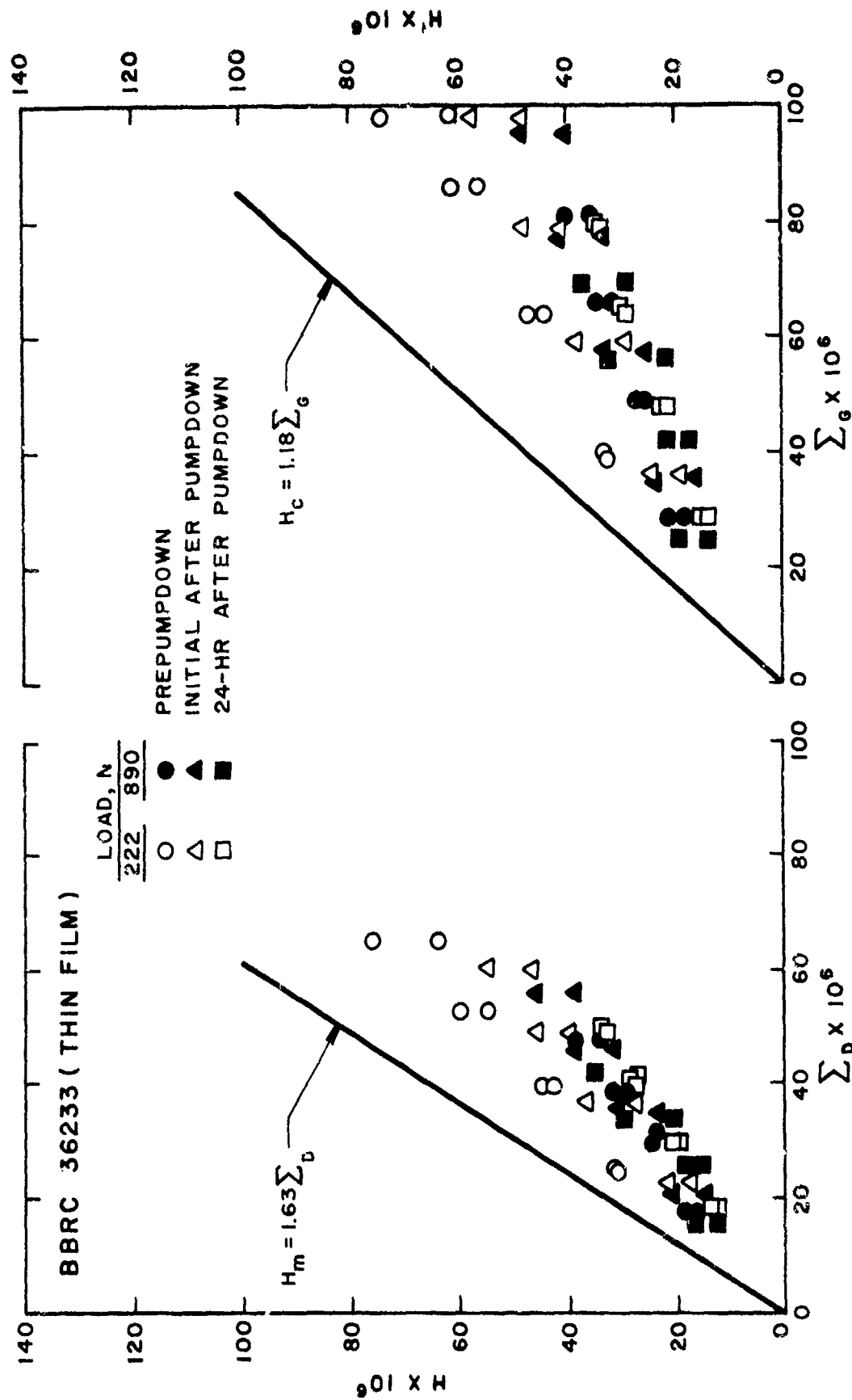


Figure 22. Dimensionless Oil Film Thicknesses for Rough Bearings Having Thin Initial Film of Intermediate-Viscosity Oil

Even though there are some discrepancies in these Task II data they do correlate well with both Dowson's and Grubin's dimensionless parameters giving much confidence in the race displacement measuring technique. Based on all of these Task II data it can be concluded that in general the film thicknesses H and H' calculated from ΔL_y measurements agreed better with Dowson's proposed minimum film thickness equation although in the case of the high-viscosity oil there appeared to be better correlation with Grubin's central-region film thickness equation. In reality it appears that the low-viscosity and medium-viscosity oils, whether the bearing be standard or rough and the initial oil film be "thick" or "thin", were operating in a slightly starved condition, but not severe enough to prevent proper operation or to cause wear or rubbing between the balls and races.

SECTION V

TASK III — ANALYSIS OF INFLUENCE OF LUBRICANT FILM THICKNESS ON BEARING LIFE EXPECTANCY IN A SIMULATED SPACE ENVIRONMENT

1. General

The purpose of this task is to provide a foundation for the development of accelerated tests, which can be used to predict bearing failure due to the loss or inadequate thickness of the EHD oil films.

As has been mentioned earlier in Part I of this report, in order to attain long bearing lives of the order of 10 to 15 years in space, it will be necessary to achieve intact EHD films in the ball-race conjunctions. This is because without full EHD films present, there will be surface contact, hence rubbing wear will occur.

Based on the test results obtained in Task II it appears that using the bearing race displacement technique for EHD film thickness measurement is valid and both Dowson's and Grubin's parameters correlate the data very well. In general, the calculated film thicknesses, using ΔL_y measurements agree better with Dowson's Eq. (9). Both the low-viscosity and medium-viscosity oils, when applied to ABEC-7 bearings, had film thicknesses less than predicted by Dowson or Grubin indicating less than flooded conditions in the ball-race conjunctions. Also the "thin" initial oil film tests operating without reservoirs and using BBRC 36233 (medium viscosity) appeared to have oil film thicknesses very nearly the same as tests using "thick" initial oil films. Of course conclusions cannot be made for these same tests when extended for long durations under vacuum conditions. This task will attempt to provide some of this information.

It is believed that as far as failures due to loss or inadequate EHD film thickness are concerned, the most realistic way to conduct accelerated tests is through control of the Λ ratio. Accordingly, the Task III test program was designed to provide basic data on bearing failure due to the loss or inadequacy of the EHD film thickness, which it is believed will serve as a foundation for the development of accelerated tests.

Task III consisted of three long-duration bearing life tests run simultaneously. Each test was conducted in a test chamber identical to the one used in Task II, with two test bearings loaded against each other with a 890-N (200-lb) axial load. Bearing speed for all three tests was maintained constant at 100 rpm. Torque was monitored in all tests by the method described in Section II, Part I of this report.

The three separate test chambers were connected to the 1.2 m³/s (1200 l/sec) vacuum pump, previously described in detail in Section II, Part I, and the bearing chamber pressure was approximately the equilibrium vapor pressure of the oil. Each chamber was provided with an LVDT identical to that used in Task II for measurement of the bearing film thicknesses.

A summary of these three tests is presented in Table III. As shown in the table, these tests were conducted at three different levels of Λ ratio designated simply as low, medium, and high, since at the time the tests were designed it was not known what the actual values would be. The three Λ levels would be obtained by varying the oil viscosity and the composite surface roughness of the ball-race combination. The low Λ value would be obtained using the Apiezon A oil with the rough bearings, the medium Λ value would be obtained using the same oil but in combination with the standard roughness bearing, and the high Λ value would be obtained using BBRC 36233 oil with the rough bearings. The Apiezon A oil would contain the standard additive package used in BBRC 36233. The degree of oil supply would be an initial thick film. Lubricant-impregnated reservoirs would also be installed in the bearing test chamber. Using values of 0.102 μm (4 $\mu\text{in.}$) and 0.204 μm (8 $\mu\text{in.}$), as supplied by MRC and given in Section II, Part II of this report, for the standard and rough bearing race surface finishes in the transverse direction (across grinding marks), respectively, and a ball surface finish of 0.025 μm (1 $\mu\text{in.}$), and employing the expression for composite surface roughness, δ_c , given in Section III, Part I, values of approximately 0.10 μm (4 $\mu\text{in.}$) and 0.18 μm (7 $\mu\text{in.}$) are obtained for δ_c . This assumes the bearing race surface finish in the direction of the grinding marks is one-half that in the transverse direction. Then using experimental values of film thicknesses as calculated from ΔL_y for the two tests using Apiezon A with antioxidant and lead naphthenate, and one test using BBRC 36233 and employing the following equation:

$$\Lambda_m = \frac{h}{\delta_c} \quad (11)$$

where Λ_m = dimensionless minimum oil film thickness ratio

h = oil film thickness calculated using Eq. (38), Appendix I

δ_c = composite surface roughness of two bearing surfaces

values of 0.71, 1.25, and 1.43 are obtained for Λ_m for the low viscosity oil and rough bearings, low viscosity oil and standard bearings, and medium viscosity oil and rough bearings, respectively, as shown in Table III. The film thickness values used in calculating the above Λ_m values were approximate average values that were obtained at the end of the long-duration tests and will be presented in the next subsection of this report under experimental results.

TABLE 3. SUMMARY OF TASK III TESTS

<u>Test No.</u>	<u>Variable Studied</u>	<u>Viscosity at 25 C (77 F), m²/s x 10⁶</u>	<u>Initial Film Thickness</u>	<u>Ball-Race Surface Roughness</u>
1	Low Λ	54	Thick	Roughness doubled
2	Medium Λ	54	Thick	MRC standard
3	High Λ	225	Thick	Roughness doubled

TEST CONDITIONS:

Pressure = equilibrium vapor pressure of test oil
 Temperature \approx 25 C (77 F)
 Load = 890 N (200 lb)
 Speed = 100 rpm

OIL DESCRIPTION:

Medium viscosity oil = BBRC 36233
 Low viscosity oil = Apiezon A + 1.5% Antioxidant + 5% Lead
 naphthenate

2. Presentation of Experimental Results from Long-Duration Bearing Tests

The computer program that was developed and discussed in Section IV, Part II of this report was modified to accommodate these Task III measurements. A listing of the modified computer program is shown in Appendix IV and the tables of computed data for the long-duration bearing tests are presented in Appendix V.

Figures 23, 24, and 25 show the measured variables for the three long-duration Task III tests as a function of time. The film thickness data points are values that were calculated from the measured displacements, ΔL_y . For these Task III tests the aft bearing-inner race contact data were plotted rather than the aft bearing-outer race contact data that were selected for plotting in the Task II tests. This was done because these inner race contact data are printed out in the Task III tables (Appendix V) whereas only the equations containing the geometric constant are given in these tables for computing the outer contact film thickness values. Again as explained in Section IV, Part II, the four different conjunction films for each test condition at any particular time are calculated from a single displacement measurement, ΔL_y . The solid lines shown on the plots of H' and H versus time in Figures 23, 24, and 25 are the values that would be obtained using Grubin's Eq. (8) and Dowson's Eq. (9) for calculating central-region and minimum dimensionless film thicknesses, respectively, at the measured bearing temperatures. When comparing the data calculated from measured ΔL_y values with these empirical values from the equations, it is seen that the actual film thicknesses in the bearings, for the different Λ_m ratios, are in general less than both the empirical minimum and central-region values predicted by the equations. This agrees with the Task II data presented in the previous section of this report and again suggests less than flooded lubrication in the ball-race conjunctions. It is worthy to note that the low Λ_m test (low viscosity oil with rough bearings) displayed very small film thicknesses throughout much of the first few hundred hours of testing, but they increased until agreeing very well with Dowson's minimum film thickness equation for the last portion of the test. On the other hand, the medium and high Λ_m tests displayed film thicknesses that increased to values close to those predicted by Dowson early during testing and remained fairly constant throughout the remainder of the tests. It is also of interest to note that at several times the measured values behaved as would be predicted when there were bearing temperature increases or decreases. For example, note the increase in measured and calculated film thickness in Figure 25 at about 1200 hours. Some of the bearing temperature changes were caused by changes in the laboratory temperature because of air conditioning failure. Some of the temperature changes were also caused by the test rig speed changing, but several of the bearing temperature changes cannot be explained.

Vacuum in the chamber seemed to behave as would be expected, with

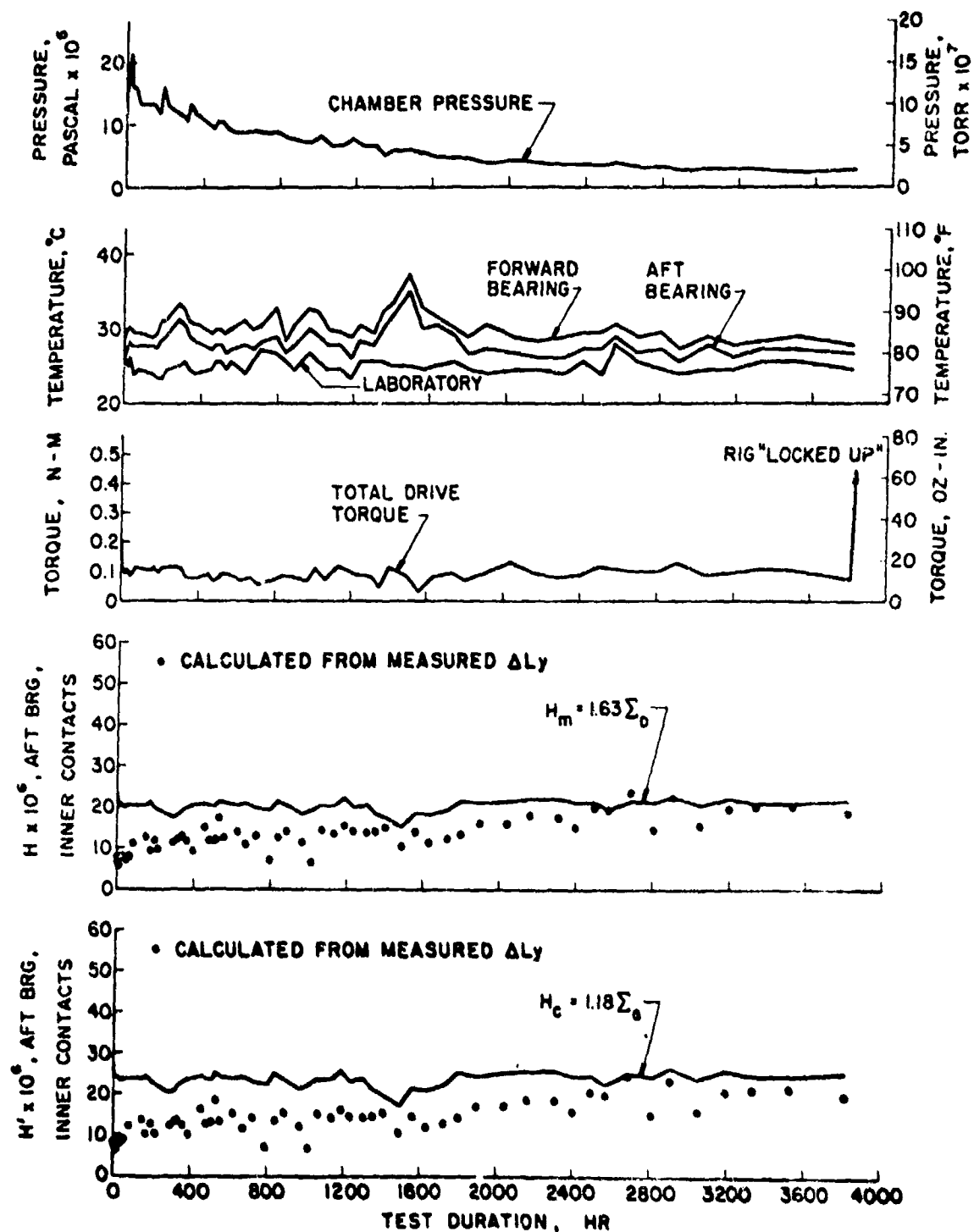


Figure 23. Measured Variables for Endurance Test Using DMA Bearings Lubricated with Thick Initial Oil Film of Apiezon A and Having Low Λ_m

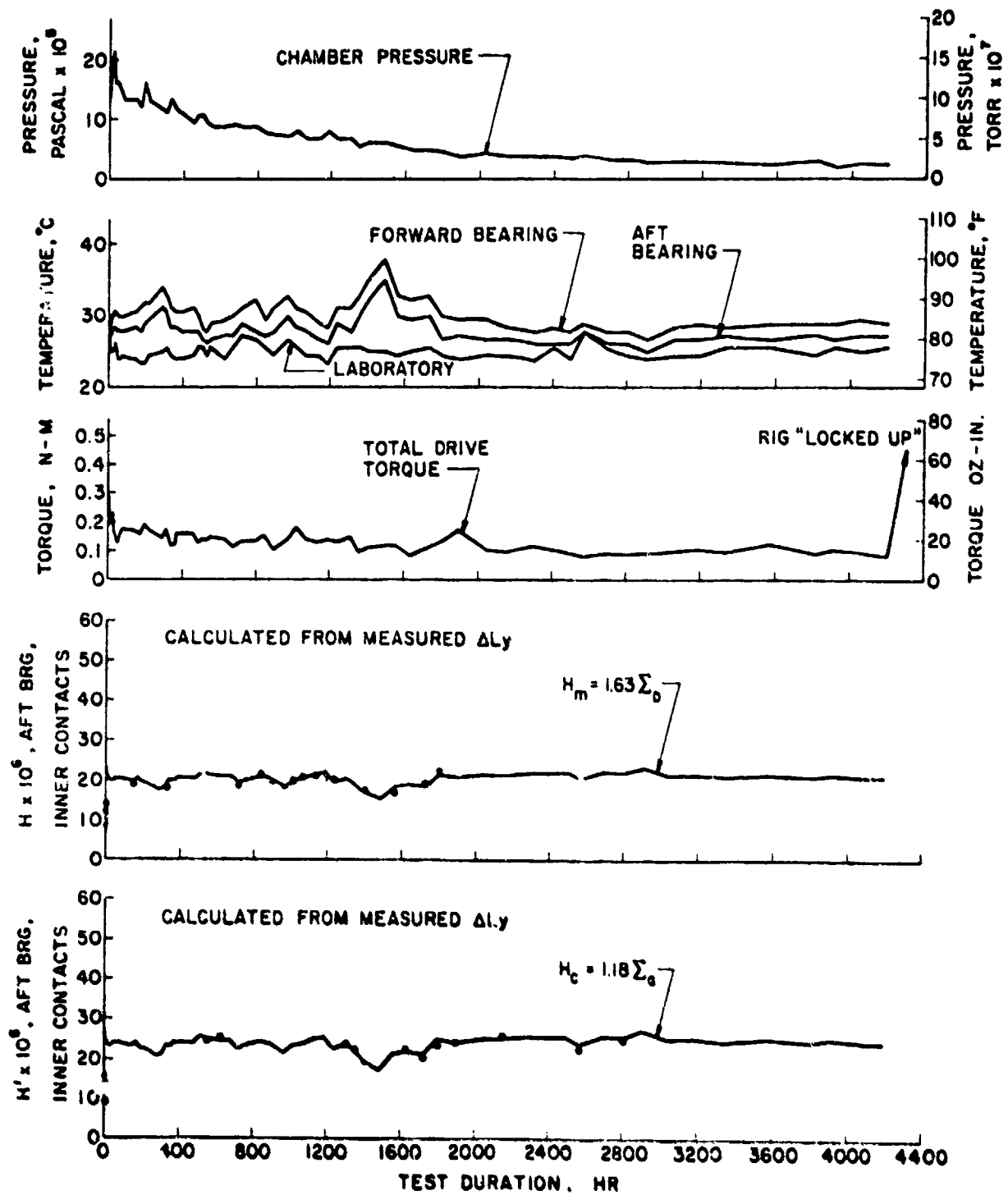


Figure 24. Measured Variables for Endurance Test Using DMA Bearings Lubricated with Thick Initial Oil Film of Apiezon A and Having Medium Δ_m

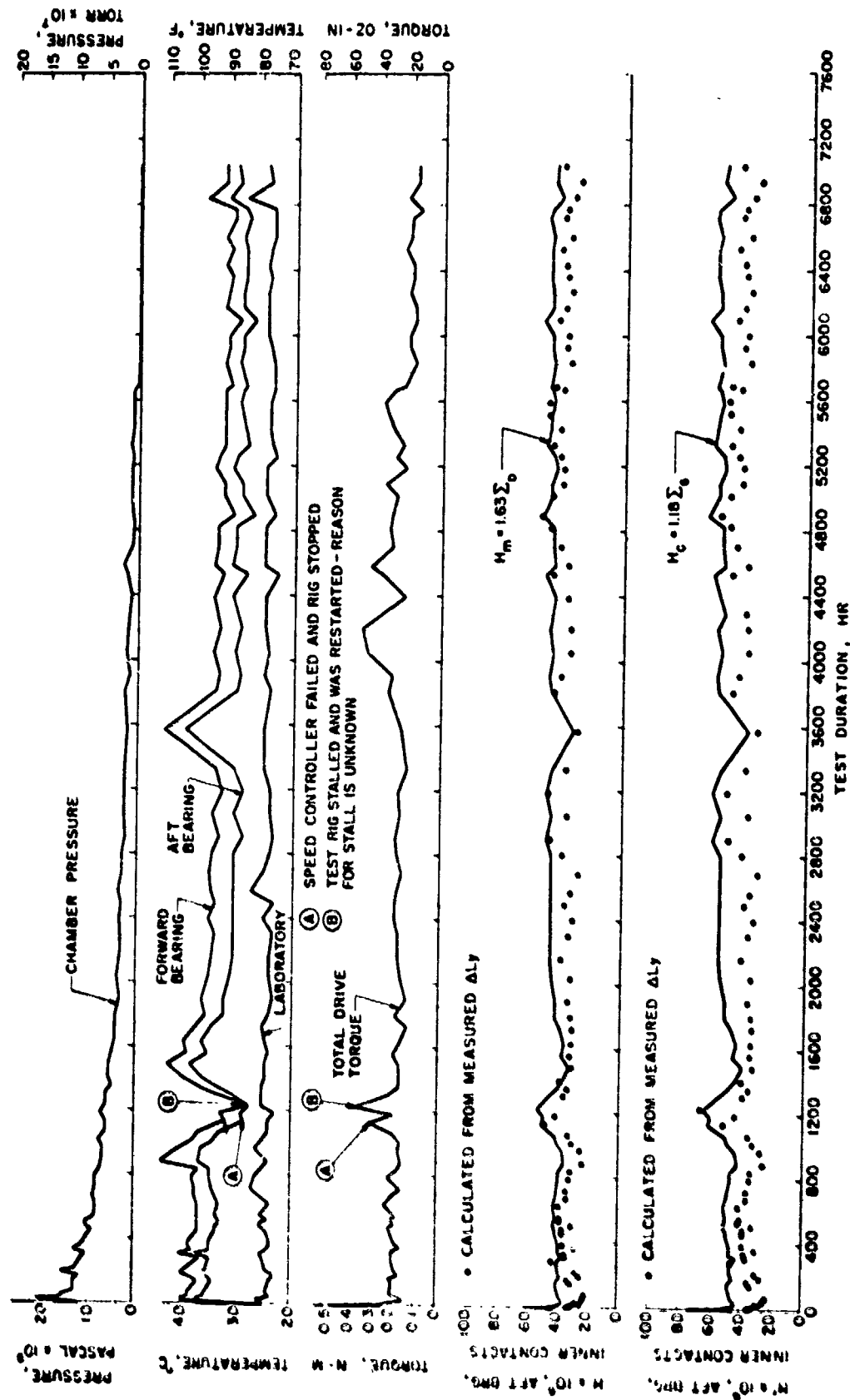


Figure 25. Measured Variables for Endurance Test Using DMA Bearings Lubricated with Thick Initial Oil Film of BBRC 36233 and Having High Δm

the pressure first increasing when the test rigs were initially put into motion and then continuing a gradual decreasing trend until the end of the program. The measured torque in the test bearings appeared to behave normally with some periodic fluctuations that can probably be attributed to the cage rubbing against the outer race in the test bearings. This will be discussed in more detail later in the report. The Test No. 1 and Test No. 2 bearings, both tests using formulations of Apiezon A oil, "locked up" within 500 hours of each other; Test No. 1 ran 3836 hours and Test No. 2 ran 4294 hours. What may be of significance is that both of these tests did employ the low-viscosity Apiezon A and did fail after similar test durations even though the Λ_m of one was 1.76 times the other and both were less than 2.0. For both tests, it appears that the oil may have been wiped from the cages at the ball-cage conjunctions and was not replenished by the oil impregnated cages or reservoirs, thus causing dry rubbing wear and eventual "lock up." This will be discussed in more detail later in the report. Upon "lock up" the bearings in these test rigs could not be freed by turning the outer magnets either backward or forward. The maximum torque capability of the driving magnetic couplings was approximately 0.63 N-m (90 oz-in.), therefore, a large amount of torque could not be applied until disassembly of the bearing rigs. It should be noted that the bearings in Test No. 2 started making an unusual noise after approximately 3336 hours of operation. Nothing unusual was observed in the measured data at this time. The noise sounded similar to moving parts rubbing against each other and continued until the end of the test. One ΔL_y measurement, taken at 3816 hours, for this Test No. 2 was obviously too great, as is shown in Figure 24.

Removal and Inspection of Two Failed Task III Bearing Rig Assemblies.

Approximately 1350 hours after the bearings in Test No. 2 "locked up" and 1850 hours after the bearings in Test No. 1 "locked up", at the request of the AFML project engineers, the following procedure was undertaken.

- a. Leave the bearing assembly with the BBRC 36233 oil running throughout the removal of the two other bearing assemblies from vacuum system.
- b. Using nitrogen, bring the chamber pressure to slightly above atmospheric, and maintain a small positive pressure differential as the bearing assemblies are removed, to prevent room air from entering the vacuum chamber.
- c. Cover the end of each bearing assembly with aluminum foil as it is removed from the vacuum chamber.
- d. After each bearing assembly is removed from the vacuum chamber, attach a cover plate to the port.
- e. When both bearing assemblies have been removed and the cover plates are in place, put the system under vacuum again.

- f. Select one of the bearing assemblies, and carefully extract the inner housing from the outer bearing rig chamber.
- g. With the inner housing fixed, and using a suitable torque wrench, apply torque to the nut holding the magnets on the shaft. Be sure that the torque is applied in the direction that the bearings rotated in the test. Gradually increase the torque until the slightest motion is observed and record this break-away torque.
- h. Remove the load in steps of 222 N (50 lb), and after each load change repeat step g above.
- i. When all the load has been removed, reapply the 890 N (200 lb) load and see if the bearing is locked up again.
- j. Carefully dismantle the bearing assembly and remove the bearings. Use gloves and laminar flow hood during the disassembly. When the bearings are removed, wrap them in aluminum foil for temporary storage.
- k. Under the laminar flow hood and using gloves, dismantle each bearing.
- l. Weigh the retainers and reservoirs and record these weights.
- m. Inspect the balls and races of each bearing for wear tracks, etc., and record findings.
- n. Inspect the retainers for wear and record findings.
- o. If the bearing components have to be cleaned for any reason during the inspection process, use heptane, save it, and send it to AFML.
- p. After the inspections are complete, reassemble each bearing, wrap in aluminum foil, label and store.
- q. Repeat steps f through p for the other bearing assembly.

The rig from Test No. 1 was selected first for the above procedure. Upon removing the inner housing from the bearing rig chamber (step f) it was evident that the cage was pushed against the inner land of the outer race of the aft bearing on one side while displaying a gap at the opposite side. This is illustrated in the photograph shown in Figure 26. Also observed was an ample amount of oil in and around the bearing. The oil appeared to be darker than when first installed in the test rig at the beginning of the test.

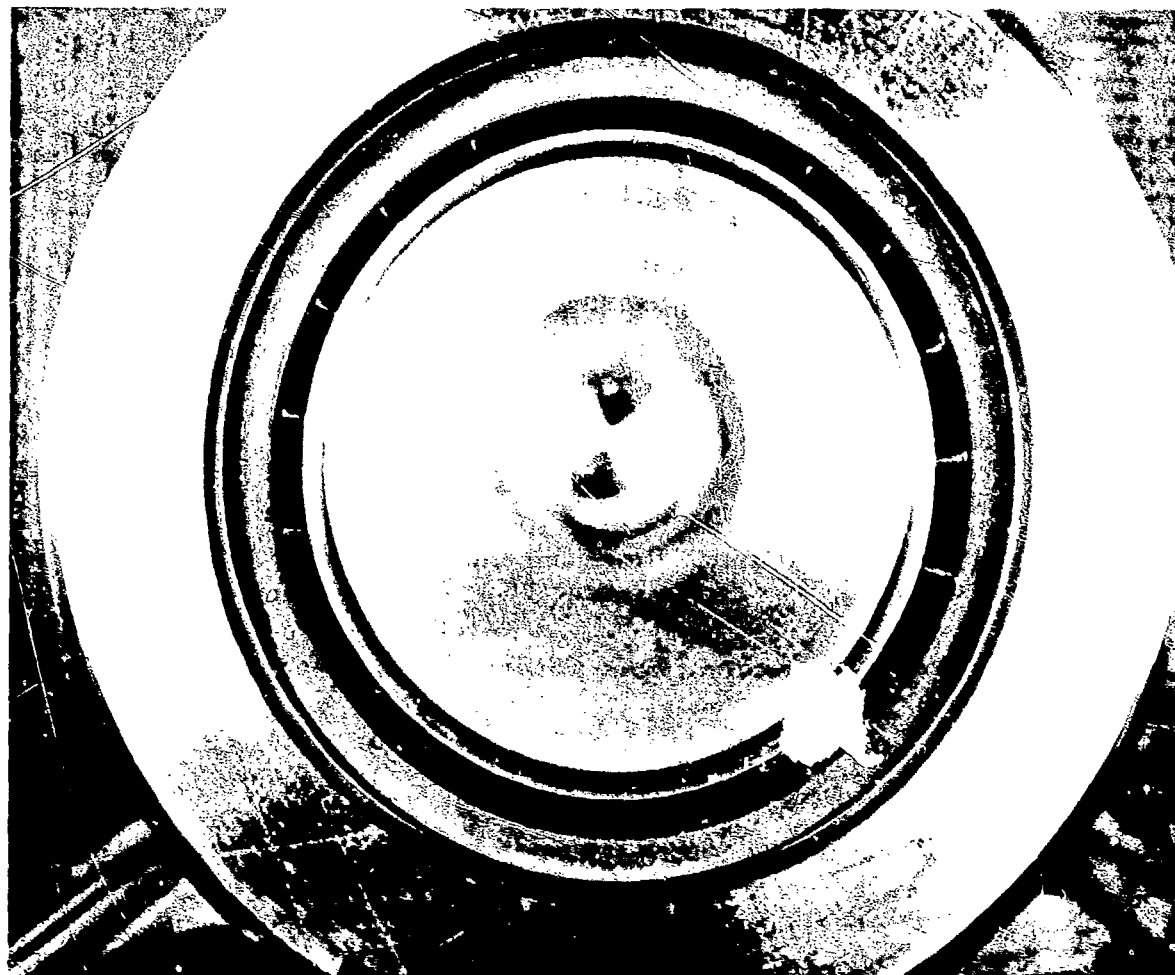


**Figure 26. View of Wedged Cage After
Endurance Test "Lock Up"**

Torque measurements were made as outlined in step g above and the results were as follows:

1. Initial full load breakaway (step g) = 0.70 N-m (99.7 oz-in.)
2. Second 667 N (150-lb) load torque measurement (step h) = 0.43 N-m (61.0 oz-in.)

The bearing became relatively free at this time, therefore, it was reloaded to 890-N (200-lb) axial load and similar torque measurements were taken giving an average value of 0.071 N-m (10.0 oz-in.). Again the axial load was reduced to 667 N (150 lb) and repeat measurements of torque gave an average value of 0.018 N-m (2.6 oz-in.). At this time the bearings appeared to be completely free and the cage had moved away from the inner land of the outer race seeking a more concentric position. At this time the axial load of 890 N (200 lb) was reapplied and the inner housing placed back in the bearing rig chamber. Instrumentation was again installed and the rig was attached to the Task II vacuum system. Bearing displacement and torque measurements were made both in air prior to pumpdown and after evacuation of the test chamber. These appeared to be somewhat higher than normal, but, the bearings would operate. There was an unusual noise (chatter) in the bearings above approximately 60 rpm. After running approximately 24 hours the test was stopped because the rig was found stalled, but the bearings were not "locked up." The cause of the stall is not known. The rig was completely disassembled. Photographs and observations were made during disassembly and these will be discussed later.

At this time the rig from Test No. 2 was disassembled. Again, when the inner housing of the rig was removed from the bearing rig chamber (step f above) it was noted that the cage was pushed against the inner land of the outer race of the aft bearing on one side while displaying a gap at the opposite side. A small pool of oil was present at the bottom of the inner housing in front of the loading diaphragm. Oil could also be seen around the ball-inner race contacts. Prior to proceeding through the disassembly procedure given above for determining "breakaway" torque of the bearings it was decided to attempt to push the bearing cage to a central position. Since the cage was securely wedged between the outer race and the balls, it required gradually moving the cage to a more central position by prying with a screwdriver between the cage and inner race at several locations. This was carefully done, and once the cage moved away from the inner land of the outer race the bearing movement became free and easy. Average torque required to rotate the bearings after this "freeing" maneuver was 0.082 N-m (11.6 oz-in.) which indicated extremely free bearings in the rig. It should be noted that in both cases of "locked up" bearing rigs, it appeared that the aft bearings had stalled because of wedging between the cages and the outer races. At this time the Test No. 2 rig was completely disassembled. Photographs and observations of both the failed ("locked up") bearings will be presented and discussed at this time.

Highlights of Task III Failed Bearings. Figures 27 and 28 show a close-up view of the ball track on the outer and inner races of the forward bearing in Test No. 2. As seen in these photographs there was an appreciable amount of dark debris collected on both sides of the ball track. The three other bearings employed in these two tests showed somewhat less of this debris. Close inspection of the outer land surface of the phenolic cages for the four test bearings showed that the bearing having the most debris on the inner and outer races also had the most rubbing wear on the phenolic cage. In other words, the amount of rubbing wear on the outer land or surface of the cage appeared to be directly related to the amount of dark debris deposited along the ball tracks on the bearing races. This material was easily removed from the race surfaces by wiping with a clean cloth or paper tissue. Figure 29 illustrates a flake of debris deposited in the ball pocket of the Test No. 2 forward bearing. All four of the bearings used in these two tests displayed some of these shiny flakes of debris in the ball pockets, although, they appeared to be larger in the two bearings used in Test No. 2. Also shown in Figure 29 are the darkened wear tracks on the outer land surface near the ball pockets of the phenolic cage. Seemingly, these wear tracks were deeper and more noticeable near the ball pockets that contained flakes of wear debris. Apparently these flakes are composed of wear material that has been removed from the cages.

Post-test inspection of the ball surfaces revealed a film of oil remaining intact with no visible wear track, pitting, or flaking. After wiping the debris from the race surfaces, they were found to be bright and shiny showing no evidence of pitting or extreme wear.

Figure 30 shows four of the oil-impregnated reservoirs that were removed from one of the rigs used in Task III tests. These reservoirs appeared very much as they did when installed in the test rigs. They were very brittle and extreme care had to be exercised to keep from breaking small pieces from the reservoirs during assembly or disassembly. Before and after weight measurement showed that the average oil weight loss for these reservoirs was only 1.4 and 2.2 percent during these two failed Task III tests.

Based on the test results and observations obtained during Task III, it can be concluded that the bearing lubricated with Apiezon A and having a low and medium Λ_m did not fail because of insufficient EHD lubrication at the ball-race conjunctions. Instead it appeared that the failures were caused by torque increases that were due to wedging of the cages between the balls and outer races. This indicates either a poor design of the bearing cages or poor lubrication between the cage and the balls and between the cage and the outer race lands of the bearing. Inspection of the failed bearings led to the conclusion that the contacting surfaces between the balls and cages would become "dried out" because of poor cage lubricant feed. Once this happened, wear of the cage in the ball pockets would be initiated and continue

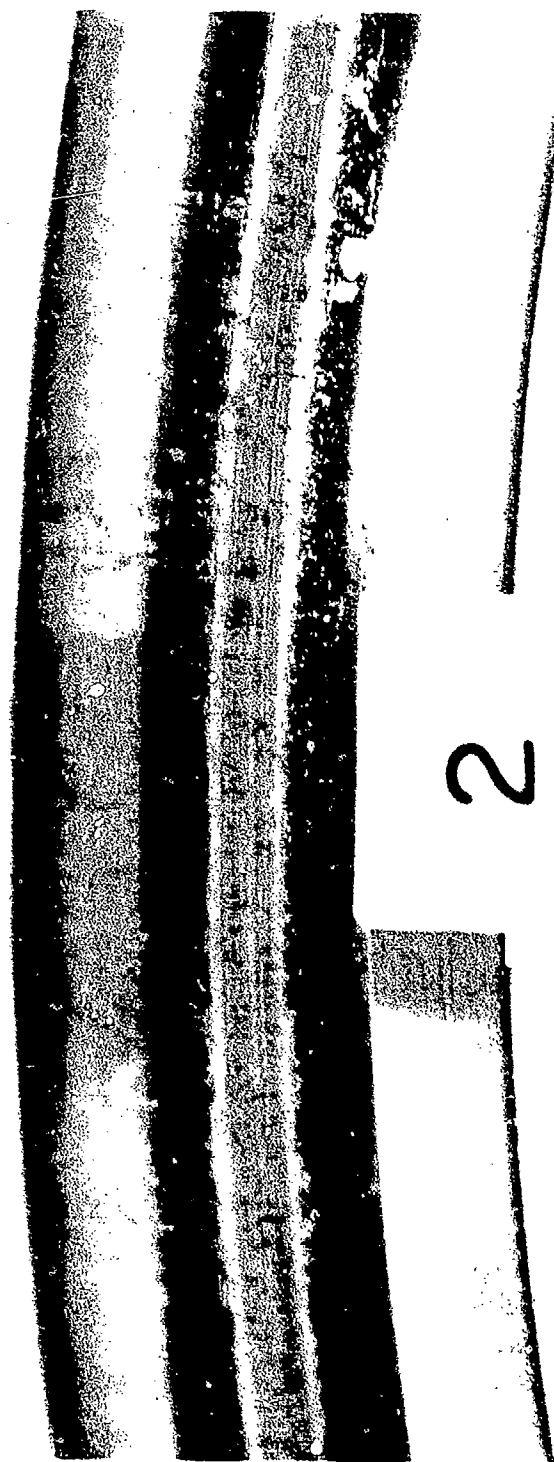


Figure 27. Ball Track in Outer Race of Forward Bearing



2

Figure 28. Ball Track in Inner Race of Forward Bearing

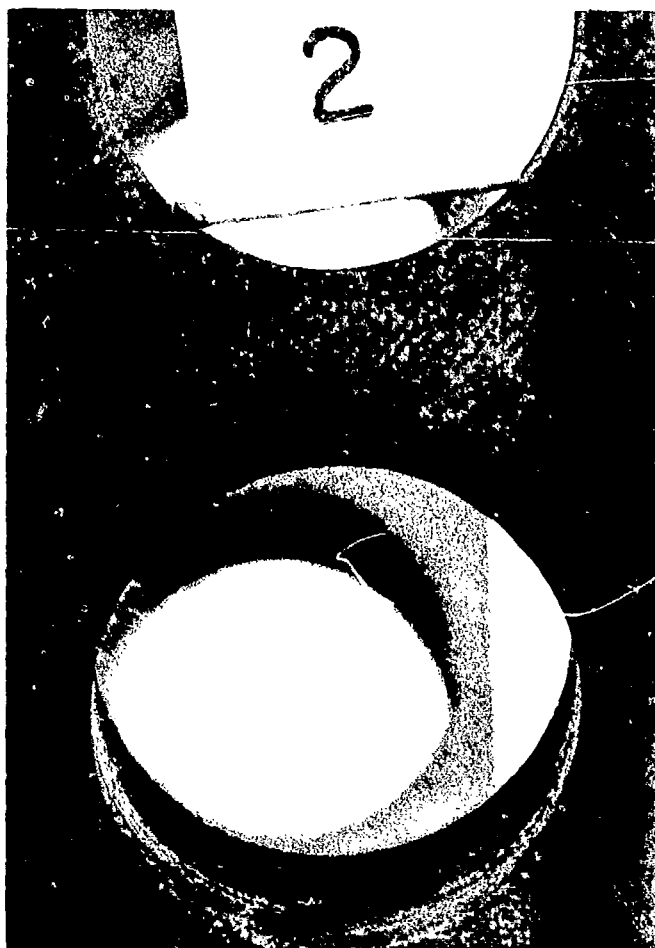


Figure 29. Flake of Debris Deposited in Ball Pocket
of Forward Bearing Cage

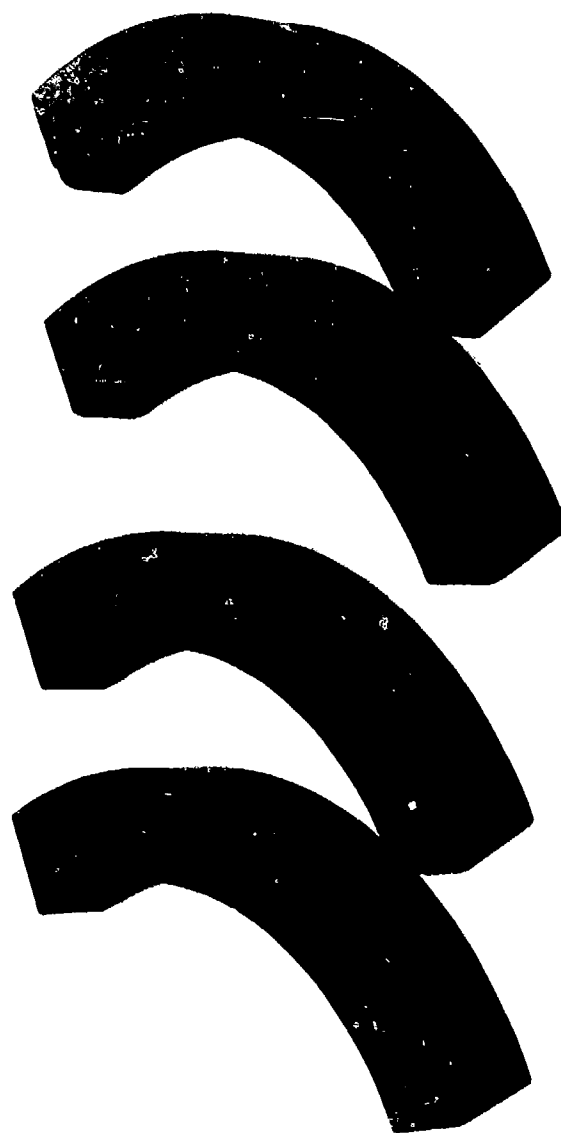


Figure 30. Four Oil-Impregnated Reservoirs as
Removed from Test Rig

to propagate as is shown in Figure 29. Simultaneously, due to increased friction between the balls and cage, the cage would be pushed against the lands of the outer race of the bearing with additional forces. Due to these larger forces and additional wear the bearings would soon reach the point where "lock up" occurred because of insufficient driving torque.

SECTION VI

CONCLUSIONS AND RECOMMENDATIONS

1. Conclusions

Task I. From the results of the optical interference measurements of the EHD film thicknesses for the various oils employed in this study, it is concluded that the special test oils formulated for vacuum use behave in general in the same manner as do ordinary straight mineral oils. This was shown in Section III in Figures 9 and 13. The results shown in these figures emphasize the fact that when optically-measured EHD film thickness data for different oils are compared, the data should be obtained under identical operating conditions. That is, due to thermal effects in the conjunction inlet region, EHD film thickness data obtained under pure sliding conditions should not be compared with those obtained in pure rolling, except at very low values of the dimensionless correlating parameters Σ_c and Σ_m . As Σ_c and Σ_m increase, the difference between the EHD film thickness for pure rolling and pure sliding becomes greater.

From these optical measurements it is also concluded that even for flooded conjunction inlet conditions, the linear relationships between H_c versus Σ_c and H_m versus Σ_m , as proposed by the correlating equation of Archard(3) and Cameron,(4) break down as Σ_c and Σ_m are increased. It is believed that the nonlinear trend is due to thermal effects, and apparently not influenced by the oil composition as long as operation is in the full EHD regime.

Task II. From the EHD film thickness measurements made for the DMA bearings using the race displacement technique, a number of conclusions may be drawn. Taking any individual figure among Figures 14 through 22, it is concluded that the dimensionless parameters Σ_D and Σ_G correlate the EHD film thicknesses calculated from the measured race displacement reasonably well. For any given oil there is a unique and approximately linear relationship between H and Σ_D or H' and Σ_G regardless of the individual values of load and speed, and regardless of the individual values of viscosity which occur due to moderate temperature differences resulting from internal heat generation in the bearings. However, as indicated by the data presented in Figures 15, 16, and 17, there is apparently some effect which is not accounted for by the parameters Σ_D and Σ_G . These three figures show that for three oils of considerably different viscosity grades, the slope of the curves of H versus Σ_D and H' versus Σ_G increase progressively with an increase in the viscosity grade of the oil. For the most viscous oil, the Nye 860-2, the measured film thickness data are in excellent agreement with the theoretical equations of Grubin and Dowson for flooded isothermal conditions. For the two other oils, the BBRC 36233 and

Apiezon A with additives, the measured EHD film thicknesses are less than predicted by the theoretical equations. While this disagreement could be attributed to thermal effects caused by viscous heating in the conjunction inlets, as noted in the results of the optical EHD film thickness measurements from Task I, this is not believed likely. If viscous heating was responsible, then the effects would be expected to be present in all three cases. Moreover, these effects should be greater for the case of the most viscous oil but, as noted above, an opposite trend is observed. It is believed that a more plausible explanation is that oil starvation is responsible for the lack of agreement with the theoretical equations. This starvation effect could be due to the balls pushing the oil out of the running track, but what is probably more likely is that the retainer is actually wiping some of the oil from the balls. Apparently, this wiping action is more severe for the least viscous oil.

Also from the results obtained in Task II, it is concluded that there is no significant effect of additives or ball-race composite surface roughness on the development of EHD films within the bearings.

Finally, by comparing Figures 16, 20, 21, and 22, it is also concluded that the EHD film thicknesses which develop within the bearing are not significantly affected by the thickness of the initial oil film coating applied to the bearings, at least for the range of initial film thickness coatings investigated in this study. The thinnest initial oil film coating used was approximately $0.1 \mu\text{m}$ ($4 \mu\text{in.}$). For initial oil film coatings thinner than this, even more severe starvation effects may be expected.

Task III. From the post-test examinations of the bearings from the two long-duration tests where the bearings failed, it is concluded that the failure was due to a lubrication problem at the interfaces between the retainer and the other bearing components and not due to inadequate EHD film thicknesses at the ball-race contacts. It is further concluded that this problem is associated with lubricant feed from the retainer to the balls and to the interfaces where the retainer rubs on the lands of the bearing. Considering the fabrication technique used for the cotton-phenolic retainer material, it is evident that it is possible for lubricant feed to occur from the retainer to the balls. However, it does not appear possible for lubricant feed to occur from the phenolic to the lands of the bearing. This is because the layers of cotton material in the phenolic are parallel to the bearing lands, and lubricant feed cannot occur in a direction perpendicular to these layers. The bearings used in the present study have outer-land-riding cages. Thus the rubbing which occurs between the retainer and the outer lands of the bearing cause a torque on the retainer which opposes the driving torque. Since there cannot be lubricant feed from the retainer to the retainer-bearing land interface, the lubrication of that interface must largely depend upon the initial oil coating on the two surfaces. If this coating is depleted, then it is possible for excessive resisting torques to develop thus requiring a greater

force between the balls and the retainer. This can accelerate the retainer wear at the ball pockets and can cause a glazing of the retainer at the ball pockets thus impeding lubricant feed at the ball-retainer interfaces. It is believed that this retainer problem can be alleviated by the use of a ball-piloted retainer. In that case, all locations where the retainer contacts the other bearing components are capable of receiving lubricant feed from the retainer.

From the measurements of the EHD film thicknesses in the bearing using the race displacement technique, the Λ_m ratio for the tests where Apiezon A with additives was employed was as low as 0.71. Yet examination of the bearing races and balls indicated that little, if any, rubbing wear occurred. It is thus concluded that lubrication was very nearly in the full EHD regime for these tests. Consequently, it has not been possible to determine the effect of Λ_m on the bearing-lubricant system life. However, it has been established from these tests that for periods of about 4000 hours, satisfactory operation from an EHD film standpoint can be attained at Λ_m values of the order of unity or slightly less.

2. Recommendations

In view of the apparent starvation effects observed in the Task II and Task III work, as exemplified by the measured EHD film thicknesses in the bearings being less than the theoretically predicted values, several further studies are recommended. First, it is believed important to study and define the effectiveness of oil feed from retainers. It is recommended that several different retainer materials be investigated, including the contemporary phenolic material, and also several more advanced materials which might provide improved lubricant feed characteristics.

It is also recommended that the effect of retainer/bearing processing variations be studied further. To define more completely the effects of initial oil film thickness on the development of adequate EHD film thicknesses within the bearing, it is recommended that several processing conditions be used that will result in initial oil film thickness coatings less than the thinnest initial coating of $0.1 \mu\text{m}$ ($4 \mu\text{in.}$) employed in this study. The objective would be to define the thickness of the coating below which severe oil starvation would occur.

Because the Task II and Task III tests involved only moderate changes in bearing temperature, it is also recommended that the effect of temperature variation on the development and maintenance of adequate EHD films be studied more completely. This can be done by cycling the environmental temperature of the bearing test chambers to produce the same temperature environment as is experienced by DMA bearings in actual space service.

Finally, it is recommended that further long-term testing be done to

define the influence of the Λ_m ratio on bearing-lubricant performance and life expectancy. This should be done using rougher bearing races than were employed in the present study to produce Λ_m values low enough to place operation in the boundary lubrication regime. The bearing retainer design should be changed to ball-piloted retainers so that bearing seizure due to the retainers can be avoided. It is also recommended that the effects of antiwear additive concentration be included in these long-term studies. This is because when lubrication is in the boundary lubrication regime, with asperity interactions occurring, the antiwear additive plays an important role in determining the wear rate due to rubbing of the bearing components. The potential of the Λ_m level and additive concentration as accelerating factors for bearing-lubricant life-expectancy tests can thus be established.

APPENDIX A

DEVELOPMENT OF FILM THICKNESS — BEARING RACE DISPLACEMENT EQUATIONS USED IN COMPUTER PROGRAMS

1. General

Before the race displacement technique can be used to make measurements of the oil film thickness in an angular contact bearing, a relationship between the EHD films which develop in the ball-race conjunctions and the axial displacement of the movable bearing race must be determined. For this purpose, an analogy can be drawn between the axial race displacement due to a slight change in ball diameter, and that due to the development of EHD films in the ball-race conjunctions.

Consider now the sketch in Figure 31, which is a cross section taken through the center of a ball in an angular contact bearing. The upper race in the sketch is considered to be the rotating inner race, and the lower one is the outer race which is elastically restrained in the axial direction. Let the initial ball size and outer race position be represented by the solid lines. Consider now that the ball is replaced by one of a slightly larger size, indicated by the broken lines, with no other changes in the bearing being made. The inner race is held stationary axially, thus the outer race must move to the new position, shown by the broken lines, to accommodate the larger ball. The axial distance that the outer race moves is ΔS , which is also the distance moved by the center of the outer race curvature, i. e., from C_1 to C'_1 . The initial contact angle, β_0 , will decrease slightly to β'_0 , while the initial contact points on the inner and outer races will change from A and B to A' and B'. If the increase in ball diameter is Δd then it may be shown⁽⁹⁾ that the axial displacement ΔS is related to the change in ball diameter by

$$\Delta S = B_0 d_0 (\sin \beta_0 - \sin \beta'_0) + \Delta d \sin \beta'_0 \quad (12)$$

where ΔS = axial displacement of outer race

B_0 = total curvature referred to original ball diameter

$$= \frac{r_0}{d_0} + \frac{r_1}{d_0} - 1$$

r_0 = radius of curvature of outer race (transverse to raceway)

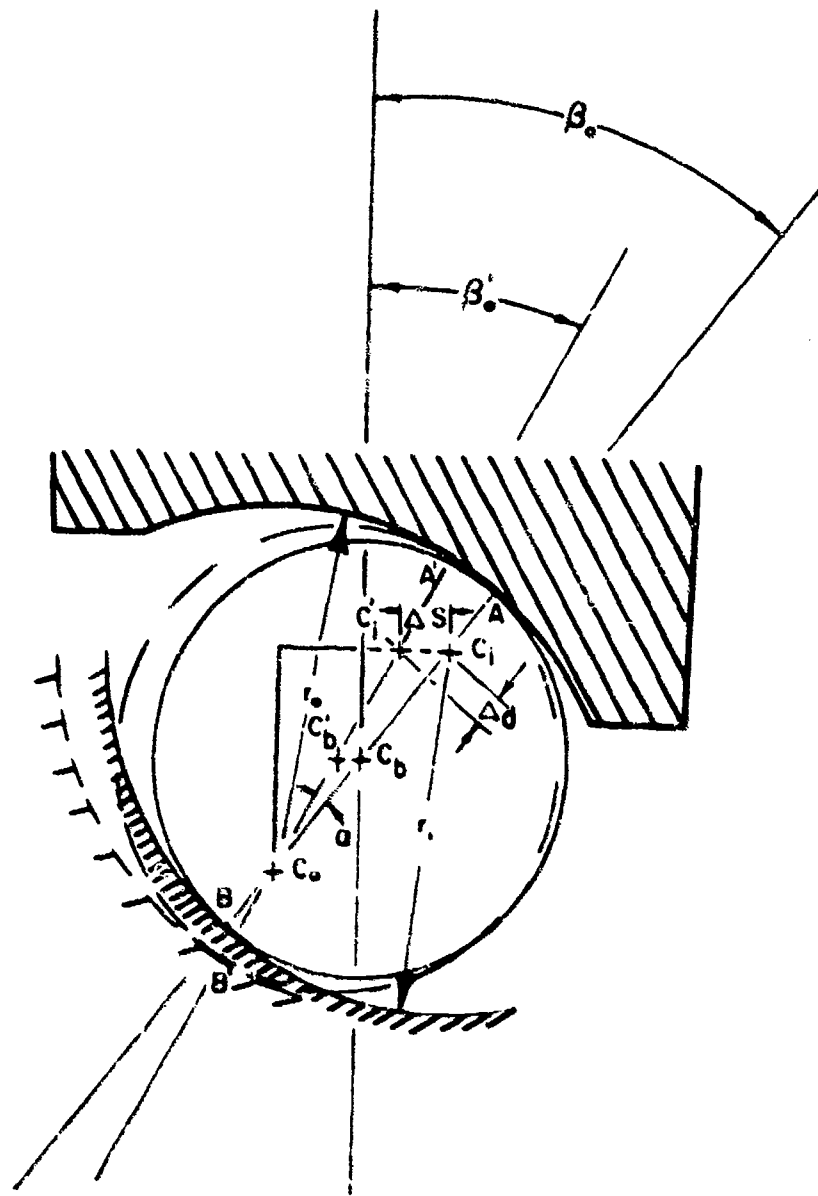


Figure 31. Schematic Drawing Showing
Axially Displaced Bearing Race

- r_i = radius of curvature of inner race (transverse to raceway)
 d_o = original ball diameter
 β_o = original contact angle
 β'_o = contact angle after race displacement
 Δd = increase in ball diameter

It may also be shown that the "new" contact angle is related to the initial contact angle by

$$\cos \beta'_o = \frac{B_o d_o \cos \beta_o}{B_o d_o - \Delta d} \quad (13)$$

2. System of Equations Relating Central-Region EHD Film Thickness to Bearing Displacement

Now imagine that instead of the outer race being displaced axially by increasing the ball diameter, it is displaced by the development of EHD films at the inner and outer ball-race conjunctions. If it is assumed that the axial displacement is due to the central-region EHD film thickness, then we may write

$$\Delta d = h'_i + h'_o \quad (14)$$

where h'_i = central-region EHD film thickness at ball-inner race contacts

h'_o = central-region EHD film thickness at ball-outer race contacts

Substituting Eqs. (13) and (14) into Eq. (12), then

$$\Delta S = B_o d_o \left[\sin \beta_o - \sin \left[\arccos \left(\frac{B_o d_o \cos \beta_o}{B_o d_o - (h'_i + h'_o)} \right) \right] \right] + (h'_i + h'_o) \sin \left[\arccos \left(\frac{B_o d_o \cos \beta_o}{B_o d_o - (h'_i + h'_o)} \right) \right] \quad (15)$$

represents the axial displacement for one bearing.

If the axial displacement ΔS is a known quantity obtained by measurement, and the bearing geometry is defined, then Eq. (15) contains two unknowns, h'_i and h'_o . Hence an equation is needed relating h'_i to h'_o .

Considering for the present only the contacts at the inner race of the bearing and applying Eq. (8) and the definitions for G and U_t

$$H'_i = \frac{h'_i}{R_i} = 1.18 \frac{(\alpha_o^* E)^{0.73} \left(\frac{\mu_o V_t}{E R_i} \right)^{0.73}}{W_{ei}^{0.09}} \quad (16)$$

Now for a given bearing operating at a given speed, load, and temperature, the variables E , α_o , μ_o , and V_t will be constant. For that situation Eq. (16) may be written

$$\frac{h'_i}{R_i} = \frac{C}{W_{ei}^{0.09} R_i^{0.73}}$$

or
$$h'_i = C \frac{R_i^{0.27}}{W_{ei}^{0.09}} \quad (17)$$

$$\text{where } C = 1.18 (\alpha_o^* E)^{0.73} \left(\frac{\mu_o V_t}{E} \right)^{0.73}$$

Applying Eq. (10) to the inner race contacts

$$W_{ei} = \frac{w_{ei}}{E R_i} = \frac{3 P}{4 a_i E R_i} \quad (18)$$

where all symbols are as previously defined, and the subscript "i" is used to denote the inner race. For the bearings used in the present program the semiwidth of the major axis of the contact ellipse at the ball-inner race contacts is given by

$$a_i = 0.16467 P^{1/3} \quad (19)$$

where a_i = mm, P = Newtons. Substituting Eq. (19) into Eq. (18)

$$W_{ei} = 4.55456 \frac{P^{2/3}}{E^* R_i}$$

or, at constant load

$$W_{ei} = C_1 \frac{4.55456}{R_i} \quad (20)$$

where $C_1 = P^{2/3} / E^*$. Now substituting Eq. (20) into Eq. (17)

$$h'_i = C \frac{R_i^{0.27}}{\left(C_1 \frac{4.55456}{R_i} \right)^{10.09}}$$

$$\text{or } h'_i = 0.87245 C_2 R_i^{0.36} \quad (21)$$

$$\text{where } C_2 = C / C_1^{0.09}$$

For the bearings used in the present study, $R_i = 7.03148$ mm (0.27683 in.). With this value substituted into Eq. (21)

$$h'_i = 1.76066 C_2 \quad (22)$$

Now the same exercise given by Eqs. (16) through (22) may be repeated for the ball-outer race contacts. The assumption is made that within a given bearing the temperature of the oil at the conjunction inlets of the ball-inner race contacts is the same as that at the ball-outer race contacts; then μ_o and α_o will be the same at all contacts within the bearing.

For the bearings used in the present study, the semiwidth of the major axis of the contact ellipse at the ball-outer race contacts is given by

$$a_o = 0.16178 P^{1/3} \quad (23)$$

where $a_o = \text{mm}$, $P = \text{Newtons}$. The equivalent radius at the ball-outer race contacts is $R_o = 8.84352 \text{ mm}$ (0.34817 in.). Following the same procedure as given by Eqs. (16) through (22) for the outer race we obtain

$$h'_o = 1.90912 C_2 \quad (24)$$

Dividing Eq. (24) by Eq. (22) and rearranging

$$h'_o = 1.08432 h'_i \quad (25)$$

In other words, due to the better conformity at the ball-outer race contacts, the central-region EHD film thickness is about 8 percent thicker there than at the ball-inner race contacts.

Substituting Eq. (25) into Eq. (15)

$$\begin{aligned} \Delta S = B_o d_o \left[\sin \beta_o - \sin \left[\arccos \left(\frac{B_o d_o \cos \beta_o}{B_o d_o - 2.08432 h'_i} \right) \right] \right] \\ + 2.08432 h'_i \sin \left[\arccos \left(\frac{B_o d_o \cos \beta_o}{B_o d_o - 2.08432 h'_i} \right) \right] \end{aligned} \quad (26)$$

The axial displacement ΔS given by Eq. (26) is for a single bearing. Since there are two bearings in each of the test rigs used in Task II and Task III, the total axial displacement, ΔL_y , measured by the LVDT system is the sum of the displacements of the forward and aft bearings. That is

$$\Delta L_y = \Delta S_{\text{aft}} + \Delta S_{\text{fwd}} \quad (27)$$

where $\Delta S_{\text{aft}} =$ contribution of aft bearing to total axial displacement

$\Delta S_{\text{fwd}} =$ contribution of forward bearing to total axial displacement

Now applying Eq. (26) to the ball-inner race contacts of both bearings and substituting into Eq. (27)

$$\begin{aligned}
\Delta L_y = & B_o d_o \left[\sin \beta_o - \sin \left[\arccos \left(\frac{B_o d_o \cos \beta_o}{B_o d_o - 2.08432 h'_i(\text{aft})} \right) \right] \right] \\
& + 2.08432 h'_i(\text{aft}) \sin \left[\arccos \left(\frac{B_o d_o \cos \beta_o}{B_o d_o - 2.08432 h'_i(\text{aft})} \right) \right] \\
& + B_o d_o \left[\sin \beta_o - \sin \left[\arccos \left(\frac{B_o d_o \cos \beta_o}{B_o d_o - 2.08432 h'_i(\text{fwd})} \right) \right] \right] \\
& + 2.08432 h'_i(\text{fwd}) \sin \left[\arccos \left(\frac{B_o d_o \cos \beta_o}{B_o d_o - 2.08432 h'_i(\text{fwd})} \right) \right] \quad (28)
\end{aligned}$$

In most cases the two bearings in a given test rig do not operate at the same temperature, and bearing temperature affects lubricant viscosity and pressure viscosity coefficient hence EHD film thickness. Thus in general $h'_i(\text{aft}) \neq h'_i(\text{fwd})$ and some analytical scheme must be employed to relate $h'_i(\text{aft})$ to $h'_i(\text{fwd})$.

Returning to Eq. (16), for the two given bearings operating at constant speed and load, the variables W_{ei} and V_t are constant. Since \bar{E} and R_i are also constant, Eq. (16) may be written

$$h'_i = C_3 (\alpha_o \mu_o)^{0.73} \quad (29)$$

$$\text{where } C_3 = 1.18 \frac{R_i^{0.27} V_t^{0.73}}{W_{ei}^{0.09}}$$

Applying Eq. (29) to the ball-inner race contacts of the forward and aft bearings

$$h'_i(\text{aft}) = C_3 (\alpha_o \mu_o)_{\text{aft}}^{0.73} \quad (30)$$

$$h'_i(\text{fwd}) = C_3 (\alpha_o \mu_o)_{\text{fwd}}^{0.73} \quad (31)$$

Dividing Eq. (31) by Eq. (30) and rearranging

$$h'_i(\text{fwd}) = \psi h'_i(\text{aft}) \quad (32)$$

$$\text{where } \psi = \left[\frac{(\alpha_o \mu_o)_{\text{fwd}}}{(\alpha_o \mu_o)_{\text{aft}}} \right]^{0.73}$$

Now Eq. (32) may be substituted into Eq. (28) to yield

$$\begin{aligned} \Delta L_y = B_o d_o & \left\{ \left[\sin \beta_o - \sin \left[\arccos \left(\frac{B_o d_o \cos \beta_o}{B_o d_o - 2.08432 h'_i(\text{aft})} \right) \right] \right] \right. \\ & + \left[\sin \beta_o - \sin \left[\arccos \left(\frac{B_o d_o \cos \beta_o}{B_o d_o - 2.08432 \psi h'_i(\text{aft})} \right) \right] \right] \\ & + 2.08432 \left\{ h'_i(\text{aft}) \sin \left[\arccos \left(\frac{B_o d_o \cos \beta_o}{B_o d_o - 2.08432 h'_i(\text{aft})} \right) \right] \right. \\ & \left. \left. + \psi h'_i(\text{aft}) \sin \left[\arccos \left(\frac{B_o d_o \cos \beta_o}{B_o d_o - 2.08432 \psi h'_i(\text{aft})} \right) \right] \right\} \right\} \quad (33) \end{aligned}$$

For each set of operating conditions, the value of the temperature correction factor ψ can be determined using the measured bearing temperatures to evaluate α_o and μ_o for the forward and aft bearings. Then with the measured value of ΔL_y , and the known geometric quantities B_o , d_o , and β_o for the bearings, Eq. (33) can be solved iteratively for $h'_i(\text{aft})$, the EHD film thickness at the ball-inner race contacts of the aft bearing. Once $h'_i(\text{aft})$ has been calculated, then $h'_i(\text{fwd})$, $h'_o(\text{aft})$, and $h'_o(\text{fwd})$ can be calculated using Eqs. (25) and (32)

3. System of Equations Relating Minimum EHD Film Thickness to Bearing Displacement

The development of the following system of equations relating minimum EHD film thickness to bearing displacement follows a line of reasoning identical to that given above for relating central-region EHD film thickness to bearing displacement. Consequently, for the sake of brevity, the development of the system equations will not be presented here in great detail. The development begins by assuming that the measured axial displacement is due to the minimum EHD film thickness, then similar to Eq. (14) we write

$$\Delta d = h_i + h_o \quad (34)$$

where h_i = minimum EHD film thickness at ball-inner race contacts

h_o = minimum EHD film thickness at ball-outer race contacts

Then an equation identical to Eq. (15) results except that h'_i and h'_o are replaced by h_i and h_o respectively.

Instead of Eq. (8) we use Eq. (9) to obtain

$$H_i = \frac{h_i}{R_i} = 1.63 \frac{(\alpha_o^* E)^{0.54} \left(\frac{\mu_o V_t}{E R_i} \right)^{0.70}}{W_{ei}^{0.13}} \quad (35)$$

From this point an identical line of reasoning yields

$$h_o = 1.10109 h_i \quad (36)$$

which may be compared with Eq. (25). That is, the minimum EHD film thickness at the ball-outer race contacts is about 10 percent thicker than at the ball-inner race contacts.

Continuing the development it is found that

$$h_i(\text{fwd}) = \zeta h_i(\text{aft}) \quad (37)$$

$$\text{where } \zeta = \left[\left(\frac{\alpha_o(\text{fwd})}{\alpha_o(\text{aft})} \right)^{0.54} \left(\frac{\mu_o(\text{fwd})}{\mu_o(\text{aft})} \right)^{0.70} \right]$$

The key equation which follows is

$$\Delta L_y = B_o d_o \sin \beta_o - \sin \left[\arccos \left(\frac{B_o d_o \cos \beta_o}{B_o d_o - 2.10109 h_i(\text{aft})} \right) \right] \\ + \left\{ \sin \beta_o - \sin \left[\arccos \left(\frac{B_o d_o \cos \beta_o}{B_o d_o - 2.10109 \zeta h_i(\text{aft})} \right) \right] \right\}$$

$$\begin{aligned}
& + 2.10109 \left\{ h_i(\text{aft}) \sin \left[\arccos \left(\frac{B_o d_o \cos \beta_o}{B_o d_o - 2.10109 h_i(\text{aft})} \right) \right] \right. \\
& \left. + \zeta h_i(\text{aft}) \sin \left[\arccos \left(\frac{B_o d_o \cos \beta_o}{B_o d_o - 2.10109 \zeta h_i(\text{aft})} \right) \right] \right\} \quad (38)
\end{aligned}$$

As described above, for each set of operating conditions, the value of the temperature correction factor ζ can be determined, and with the measured ΔL_y , Eq. (38) may be solved iteratively for $h_i(\text{aft})$. Then $h_i(\text{fwd})$, $h_o(\text{aft})$, and $h_o(\text{fwd})$ can be calculated using Eqs. (36) and (37).

APPENDIX B

LISTING FOR TASK II DATA REDUCTION PROGRAM

```

PROGRAM DROPT (INPUT,OUTPUT,TAPE$=INPUT,TAPE$=OUTPUT)
  C
  C * DATA REDUCTION FOR OIL FILM *
  C * TEMPERATURE IN DMA BEARINGS, *
  C * PROGRAMMED BY NEER CARTER, *
  C * JOHN TYLER, AND MARY CARTER *
  C * * * * * * * * * * *
  C
  DIMENSION LN(4),DELTY(4),MCAI(4),MMAI(4),MCAO(4),MMAO(4),MCFI(4),
  * MMFI(4),MCFIO(4),MMFIO(4),MCAI(4),MMAI(4),MCAO(4),
  * MMCAO(4),MCFI(4),MMFI(4),MCFIO(4),MMFIO(4),MCAIS(4),
  * MMCAIS(4),MCFIS(4),MMFIS(4),MCAOS(4),MMCAOS(4),
  * MCFOS(4),MMFOS(4),MCAIS(4),MMAIS(4),MCAOS(4),
  * MMCAOS(4),MCFIS(4),MMFIS(4),MCFOS(4),MMFOS(4),
  * TORQUE(4),TORQSI(4),
  * NOIL(8)
  C
  COMMON VIS,KX,METAL,ALPHAO,PMI,UMEGA,P,GAM,G,BEEO,RFIO,DMXAI,DMXFI,
  * DMCAO,DMMFO,MATIO,KHALL,SPACE,S,ESTAR,DELY,HATIOA,RATIOV
  C
  EXTERNAL DELTAC,DELTA
  LOGO FORMAT ( 25, 15 )
  LOGO FORMAT ( 25, 15 )
  1 CONTINUE
  2 READ (5,1000) NOIL
  IF (EOP(5)) GO TO 2
  2 READ (5,1016) NHEAR,NTMCA,NTEST
  C
  C BEARING GEOMETRY AND MATERIAL (NOTE UNITS ARE CONVERTED TO SI SYSTEM)
  C
  MALLCO=.1125E-2,S4E-2
  MACEE=.2,17E-2,S4E-2
  SEBALL/SPACE
  ESTAR=11.66E6,845E3
  PMI=.26,+.3,1415E/180
  RFIO=.276E3,2.54E-2
  QEODCO,NMI=.2,S4E-2
  READ (5,1001) FLOAD
  1001 FORMAT (F3,0)
  FLOADS=FLOAD*PMI
  PMFLOAD/180,81N(PMI)
  A1=Q,0.1066E+1(1,3)
  A2=Q,0.1067E+1(1,3)
  PSEPA=.9E8
  A1CALC=.54E-2
  A2CALC=.54E-2
  READ (5,1002) A,B,GAM,G,KX,BETA
  1002 FORMAT(3F10.5,F10.4,F10.3,F10.5)
  SPACE=1
  10 CONTINUE
  WRITE (4,1003) NTEST,NOIL,NHEAR,NTMCA,FLOADS,FLOAD
  READ (5,1004) NASEN,TEMPA,TEMPF,NPSPEED,PRESS
  1004 FORMAT (2F3,0,13,E10,3)
  PMSI=PRESS*133.3
  DEIGAS=MSF*2,+.3,1415E/180
  TEMPA$=(TEMPA-32)*5/9
  TEMPF$=(TEMPF-32)*5/9
  C
  C BASE CALCULATIONS FOR AFT BEARING
  C
  CALL FLPROP (TEMPAS,A,B,GAM,G,KX,BETA,ALPHAO,VIS)

```

```

C INNER CONTACTS
C CALL FILM (REOF,AI,OMCAL,BHMAI)
C OUTER CONTACTS
C CALL FILM (REOO,AO,OMCAO,BHMAO)
C FILM THICKNESS CALCULATIONS FOR APT BEARING
C READ (S,IONS) ((X(I),DELTA(I),TORQUE(I)),I=1,NSPEED)
C 10% FORMAT (1P5.1)
C ON 20 I=1,NSPEED
C INNER CONTACTS
C OMEGASIN(I)=2.*3.14159/60.
C CALL FILM (REOI,AI,MCFI(I),MHFI(I))
C OUTER CONTACTS
C 20 CALL FILM (REOO,AO,MCAO(I),MHMO(I))
C ALPHASALPHAO=VIS
C ALPHASALPHAO
C VISAPRIVIS
C WRASE CALCULATIONS FOR FORWARD BEARING
C OMEGASIN(I)=2.*3.14159/60.
C CALL FLPROP (TEMPF,A,B,GAM,SEYA,ALPHAO,VIS)
C INNER CONTACTS
C CALL FILM (REOI,AI,MCFI(I),MHFI(I))
C OUTER CONTACTS
C CALL FILM (REOO,AO,MCAO(I),MHMO(I))
C FILM THICKNESS CALCULATIONS FOR FORWARD BEARING
C ON 40 I=1,NSPEED
C INNER CONTACTS
C OMEGASIN(I)=2.*3.14159/60.
C CALL FILM (REOI,AI,MCFI(I),MHFI(I))
C OUTER CONTACTS
C 40 CALL FILM (REOO,AO,MCAO(I),MHMO(I))
C ALPHASALPHAO=VIS
C ALPHASALPHAO
C VISAPRIVIS
C EXPERIMENTAL FILM THICKNESSES CALCULATED FROM MEASURED BEARING

```


[illegible]


```

SUBROUTINE FLPROP (I,A,B,CAM,G,XK,BETA,ALPHA,E)
V=ALOG10(I+273.)
X=2-9*V
E=10.*((10.*X)-0.6
E=E*(CAM-G*(I-15.6))*0.001
ALPHA=X/X/I+BETA
RETURN
END

```

```

000014
000023
000025
000035
000042
000047
000050

```

```

000007 SUBROUTINE FILM (RED,A,MC,MM)
COMMON VIS,XK,BETA,ALPHA0,PHI,OMEGA,P,GAM,G,RECO,REGI,DHXA1,DHXP1,
      DHXA0,DHXP0,RATIO,RHALL,RACEF,S,FSTAR,DELT,RATIOA,RATIOV
C
C CALCULATE DIMENSIONLESS CENTRAL-REGION FILM THICKNESS
C
      X1=(1+P+S*CGS(PHI))/(2+S*(1+S*CGS(PHI)))
      X2=(VIS*2+PBALL*X1+OMEGA)/(ESTAR*REG)
      X3=X2**0.73
      X4=(ALPHA0*(STAR)
      X5=X4**0.73
      X6=3.*P/(4.*A*ESTAR*RECO)
      X7=X5**0.73
      MC=1.19*X5*X3/X7
C
C CALCULATE DIMENSIONLESS MINIMUM FILM THICKNESS
C
      X9=X2**0.70
      X0=X4**0.54
      X10=X4**0.13
      MU21=.63*X9*X8/X10
      QETHIN
      END
000057
000063
000067
000073
000077
000077

```

```

FUNCTION DELTAC (HX)
COMMON V15,XA,ETA,ALPHA0,PHI,OMEGA,P,GAM,G,REQN,REGI,DMXA1,DMXF1,
      DMXA0,DMXF0,RATIO,RHALL,RPACE,S,ELSTAR,DELTLY,RATIOA,RATIOV
      *
      V1=0.02566*COS(PHI)/(0.02566-2.08432*HX)
      V2=ACOS(V1)
      V3=SIN(V2)
      V4=SIN(PHI)-Y3
      V5=0.02566*COS(PHI)/(0.02566-2.08432*RATIO+0.73*HX)
      V6=ACOS(V5)
      V7=SIN(V6)
      V8=SIN(PHI)-Y7
      V9=0.02566*(V4+V7)
      V10=HX+V3
      V11=RATIO+0.23*HX+V2
      V12=2.08432*(V10+V11)
      XLV=Y4+V12
      DELTAC=DELTLY-XLY
      RETURN
      END

```

```

000003
000004
000005
000006
000007
000008
000009
000010
000011
000012
000013
000014
000015
000016
000017
000018
000019
000020
000021
000022
000023
000024
000025
000026
000027
000028
000029
000030
000031
000032
000033
000034
000035
000036
000037
000038
000039
000040
000041
000042
000043
000044
000045
000046
000047
000048
000049
000050
000051
000052
000053
000054
000055
000056
000057
000058
000059
000060
000061
000062
000063
000064
000065
000066
000067
000068
000069
000070
000071
000072
000073
000074
000075
000076
000077
000078
000079
000080
000081
000082
000083
000084
000085
000086
000087
000088
000089
000090
000091
000092
000093
000094
000095
000096
000097
000098
000099
000100

```

```

000003      FUNCTION DELTAM (MX)
COMMON VIS,XX,BETA,ALPHA0,PHI,OMEGA,P,GAM,G,REQQ,REQI,DHXAI,DHXFI,
      DHXAO,DHXFO,RATIO,RHALL,RRACE,S,ESTAR,DELTLY,RATIOA,RATIOV
10  V1=0.025E6*COS(PH1)/(0.025E6-2.10109*MX)
      V2=ACOS(V1)
      V3=SI4(Y2)
      V4=SI(PH1)-V3
      V5=0.025E6*COS(PH1)/(0.025E6-2.10109*RATIOA+0.54*RATIOV+0.70*MX)
      V6=ACOS(V5)
      V7=SI(Y4)
      V8=SI(PH1)-V7
      V9=0.025E6*(V4+V8)
      V10=MX+V3
      V11=41104+0.54*RATIOV+0.70*MX+V7
      V12=2.10109*(V10+V11)
      KLV=Y9+V12
      DELTAM=DELTLY-XLV
      RETURN
      END
000004
000005
000006
000007
000008
000009
000010
000011
000012
000013
000014
000015
000016
000017
000018
000019
000020
000021
000022
000023
000024
000025
000026
000027
000028
000029
000030
000031
000032
000033
000034
000035
000036
000037
000038
000039
000040
000041
000042
000043
000044
000045
000046
000047
000048
000049
000050
000051
000052
000053
000054
000055
000056
000057
000058
000059
000060
000061
000062
000063
000064
000065
000066
000067
000068
000069
000070
000071
000072
000073
000074
000075
000076
000077
000078
000079
000080
000081
000082
000083
000084
000085
000086
000087
000088
000089
000090
000091
000092
000093
000094
000095
000096
000097
000098
000099
000100

```


GO TO 200
100 EXE00
200 CONTINUE
1000
250 RETURN
END

000110
000111
000112
000113
000114
000115

APPENDIX C

SAMPLE PRINTOUT OF TASK II DATA

0.21 = 12.0
BASE SEED (8PM)

INNER CONTACTS

FILM THICKNESS (MICROINCHES)

FORWARD BEARING

94

TEST NO. 19
 OIL & GEAR TEST
 ACTING ENGINEER = STD
 INITIAL FILM THICKNESS = 1.000E-06
 LOAD(LBS) = 200
 AFT TEMPERATURE = 79.0
 F&O TEMPERATURE = 80.0
 PRESSURE(TORR) = 1.000E-06

INITIAL AFTER SHUT DOWN RESULTS

BASE SPEED(RPM) = 1000

FILM THICKNESS(MICROMETERS)

AFT BEARING									
OUTER CONTACTS					INNER CONTACTS				
BMCAO	BMCAI	BMCAJ	BMCAK	BMCAI	BMCAO	BMCAI	BMCAJ	BMCAK	BMCAI
.111	.116	.116	.116	.116	.111	.111	.111	.111	.111
FORWARD BEARING									
OUTER CONTACTS					INNER CONTACTS				
BMCAO	BMCAI	BMCAJ	BMCAK	BMCAI	BMCAO	BMCAI	BMCAJ	BMCAK	BMCAI
.111	.116	.116	.116	.116	.111	.111	.111	.111	.111
TORQUE									
BMCAO	BMCAI	BMCAJ	BMCAK	BMCAI	BMCAO	BMCAI	BMCAJ	BMCAK	BMCAI
.111	.116	.116	.116	.116	.111	.111	.111	.111	.111

FILM THICKNESS(MICROINCHES)

AFT BEARING									
OUTER CONTACTS					INNER CONTACTS				
BMCAO	BMCAI	BMCAJ	BMCAK	BMCAI	BMCAO	BMCAI	BMCAJ	BMCAK	BMCAI
.111	.116	.116	.116	.116	.111	.111	.111	.111	.111
FORWARD BEARING									
OUTER CONTACTS					INNER CONTACTS				
BMCAO	BMCAI	BMCAJ	BMCAK	BMCAI	BMCAO	BMCAI	BMCAJ	BMCAK	BMCAI
.111	.116	.116	.116	.116	.111	.111	.111	.111	.111
TORQUE									
BMCAO	BMCAI	BMCAJ	BMCAK	BMCAI	BMCAO	BMCAI	BMCAJ	BMCAK	BMCAI
.111	.116	.116	.116	.116	.111	.111	.111	.111	.111

Case 3:20-cv-00336-3578

FILM THICKNESS (MICROMETERS)

FILM THICKNESS (MICRONS)

[illegible]

APPENDIX D

LISTING OF TASK III DATA REDUCTION PROGRAM

[illegible]


```

C SOLVE FOR INCREMENT IN FILM THICKNESS FOR INNER CONTACTS OF FORWARD
C BEARING BY USING CONNECTION FOR BEARING TEMPERATURE DIFFERENCE
C
000221      DMXCFI=RTI*0.73*DMXCAI
000225      DMXCFI=RTI*0.54*DMXCAI
C
C CONVERT FILM THICKNESS INCREMENTS FROM MICROINCHES TO METERS
C
000305      CI=2.54E-2/1.0F6
000307      DMXCAI=DMXCAI*CI
000310      DMXCFI=DMXCFI*CI
000312      DMXMAI=DMXMAI*CI
000313      DMXWFI=DMXWFI*CI
C
C NONDIMENSIONALIZE FILM THICKNESS INCREMENTS
C
000314      DMXCAI=DMXCAI/RTI
000315      DMXCFI=DMXCFI/RTI
000316      DMXMAI=DMXMAI/RTI
000317      DMXWFI=DMXWFI/RTI
C
C FILM THICKNESSES IN AFT BEARING (INCREMENT PLUS BASE)
C
000320      MXCAI(I)=DMXCAI+BMCAI(I)
000323      MXMAI(I)=DMXMAI+BMMAI(I)
C
C FILM THICKNESSES IN FORWARD BEARING (INCREMENT PLUS BASE)
C
000325      MXCFI(I)=DMXCFI+HMXCFI(I)
000327      MXWFI(I)=DMXWFI+HMXWFI(I)
C
C CONVERT FILM THICKNESSES FROM DIMENSIONLESS TO MICROMETERS
C
000332      CI=RTI*1.26
000333      BMCAIS(I)=BMCAI(I)*CI
000336      HMMAIS(I)=HMMAI(I)*CI
000337      BMCFIS(I)=BMCFI(I)*CI
000341      HMXFIS(I)=HMXFI(I)*CI
000342      MXCAIS(I)=MXCAI(I)*CI
000344      HMMAIS(I)=HMMAI(I)*CI
000345      MXCFIS(I)=MXCFI(I)*CI
000347      HMXFIS(I)=HMXFI(I)*CI
000350      HMCAIS(I)=HMCAI(I)*CI
000352      HMMAIS(I)=HMMAI(I)*CI
000353      MCFIS(I)=MCFI(I)*CI
000355      HMXFIS(I)=HMXFI(I)*CI
C
C CONVERT TORQUE, LOAD, AND TEMPERATURE TO SI UNITS
C
000356      TORQSI(I)=TORQUE(I)*7.0812E-3
000360      XLOADS(I)=XLOAD
C
C CONVERT FILM THICKNESSES FROM DIMENSIONLESS TO MICROINCHES
C
000362      HI=CI*39.37
000364      BMCAI(I)=BMCAI(I)*HI
000366      HMMAI(I)=HMMAI(I)*HI
000370      BMCFI(I)=BMCFI(I)*HI

```



```

1      BMCAIS(1),MXCAIS(1),MCAIS(1),BMMAIS(1),HMAIS(1),
2      HMAIS(1),TEMPF(1),BMCFIS(1),MXCFIS(1),MCFIS(1),
3      BMMFIS(1),MXMFIS(1),MMFIS(1)
1130  FORMAT(1X,F5.0,F8.1,F7.3,F7.2,2(4X,F2.1,6F7.3))
      LINE=LINE+1
150  CONTINUE
      GO TO 1
      END
000669
000669
000669
000670
000671

```



```

SUBROUTINE FLPRUP (T,A,B,GAP,G,KK,HETA,ALPHAQ,E)
  Y=ALOG10(T*273.)
  HZA=B*Y
  Z=10.+(10.0**Y)-0.6
  TEF=(GAP-G*(T-15.6))/Z
  ALPHAQ=KK/100HETA
  RETURN
END

```

```

000010
000020
000030
000040
000050
000060
000070
000080

```



```

000000
000001      FUNCTION DELTAM (MX)
000002      COMMON VIS,RS,EFT,ALPHA0,PHI,OMEGA,P,GAM,G,REQI,OMXAI,OMXFI,
000003      MARIO,MALL,MACE,S,ESTAR,DELTLY,RATIOA,RATIOV
000004      10 V10R,DPST6COS(PHI)/(S,DPSE6-2,10104MS)
000005      V26COS(PI)
000006      V2516(V2)
000007      V2516(OMI)-V3
000008      V550,DPST6COS(PHI)/(R,DPSE6-2,10104RATIOA=0,54RATIOV=0,70MX)
000009      V56COS(V4)
000010      V2516(V4)
000011      V2516(PMI)-V7
000012      V250,DPSE6(V6+V8)
000013      V102MX=V7
000014      V12RATIOA=0,54RATIOV=0,70MX=V7
000015      V12P2,10104(V10+V11)
000016      ELV2V6V12
000017      DELTAM=DELTY-ELY
000018      RETURN
000019      END
000020
000021
000022
000023
000024
000025
000026
000027
000028
000029
000030
000031
000032
000033
000034
000035
000036
000037
000038
000039
000040
000041
000042
000043
000044
000045
000046
000047
000048
000049
000050
000051
000052
000053
000054
000055
000056
000057
000058
000059
000060
000061
000062
000063
000064
000065
000066
000067
000068
000069
000070
000071
000072
000073
000074
000075
000076
000077
000078
000079
000080
000081
000082
000083
000084
000085
000086
000087
000088
000089
000090
000091
000092
000093
000094
000095
000096
000097
000098
000099
000100

```

SUBROUTINE BISECT(X,NX,DX,EPS,IER,FCT)

PURPOSE
TO SOLVE NONLINEAR EQUATIONS

USAGE
CALL BISECT (X,NX,DX,EPS,IER,FCT)
PARAMETER FCT REQUIRES AN EXTERNAL STATEMENT.

DESCRIPTION OF PARAMETERS
X - THE STARTING VALUE OF THE SEARCH VARIABLE.
NX - THE NUMBER OF SEARCH INTERVALS.
DX - THE SEARCH INTERVAL.
EPS - THE UPPER BOUND OF RELATIVE ERROR.
IER - A RESULTING ERROR PARAMETER.
IER = 0, SUCCESSFUL SEARCH.
IER = 1, NO CHANGE OF SIGN FOUND IN SEARCH RANGE.
FCT - THE NAME OF THE EXTERNAL FUNCTION SUBPROGRAM USED.

SUBROUTINES AND FUNCTION SUBPROGRAMS REQUIRED
THE EXTERNAL FUNCTION SUBPROGRAM FCT(X) MUST BE CODED BY THE USER SO THAT FCT(X) IS AT RESOLUTION.

METHOD
A SEARCH FOR A CHANGE OF SIGN IS PERFORMED AND WHEN FOUND THE INTERVAL CONTAINING THE SOLUTION IS CONTINUALLY HALVED.

```

1000  IER=0
1010  EX=0
1020  DO 200 I=1,NX
1030  IF (X-NX) GO TO 100
1040  FCT(X)
1050  IF (FCT(X)-EPS) 250,250,100
1060  FCT(X)
1070  IF (FCT(X)-EPS) 250,250,100
1080  FCT(X)
1090  IF (FCT(X)-EPS) 250,250,100
1100  FCT(X)
1110  IF (FCT(X)-EPS) 250,250,100
1120  FCT(X)
1130  IF (FCT(X)-EPS) 250,250,100
1140  FCT(X)
1150  IF (FCT(X)-EPS) 250,250,100
1160  FCT(X)
1170  IF (FCT(X)-EPS) 250,250,100
1180  FCT(X)
1190  IF (FCT(X)-EPS) 250,250,100
1200  FCT(X)
1210  IF (FCT(X)-EPS) 250,250,100
1220  FCT(X)
1230  IF (FCT(X)-EPS) 250,250,100
1240  FCT(X)
1250  IF (FCT(X)-EPS) 250,250,100
1260  FCT(X)
1270  IF (FCT(X)-EPS) 250,250,100
1280  FCT(X)
1290  IF (FCT(X)-EPS) 250,250,100
1300  FCT(X)
1310  IF (FCT(X)-EPS) 250,250,100
1320  FCT(X)
1330  IF (FCT(X)-EPS) 250,250,100
1340  FCT(X)
1350  IF (FCT(X)-EPS) 250,250,100
1360  FCT(X)
1370  IF (FCT(X)-EPS) 250,250,100
1380  FCT(X)
1390  IF (FCT(X)-EPS) 250,250,100
1400  FCT(X)
1410  IF (FCT(X)-EPS) 250,250,100
1420  FCT(X)
1430  IF (FCT(X)-EPS) 250,250,100
1440  FCT(X)
1450  IF (FCT(X)-EPS) 250,250,100
1460  FCT(X)
1470  IF (FCT(X)-EPS) 250,250,100
1480  FCT(X)
1490  IF (FCT(X)-EPS) 250,250,100
1500  FCT(X)
1510  IF (FCT(X)-EPS) 250,250,100
1520  FCT(X)
1530  IF (FCT(X)-EPS) 250,250,100
1540  FCT(X)
1550  IF (FCT(X)-EPS) 250,250,100
1560  FCT(X)
1570  IF (FCT(X)-EPS) 250,250,100
1580  FCT(X)
1590  IF (FCT(X)-EPS) 250,250,100
1600  FCT(X)
1610  IF (FCT(X)-EPS) 250,250,100
1620  FCT(X)
1630  IF (FCT(X)-EPS) 250,250,100
1640  FCT(X)
1650  IF (FCT(X)-EPS) 250,250,100
1660  FCT(X)
1670  IF (FCT(X)-EPS) 250,250,100
1680  FCT(X)
1690  IF (FCT(X)-EPS) 250,250,100
1700  FCT(X)
1710  IF (FCT(X)-EPS) 250,250,100
1720  FCT(X)
1730  IF (FCT(X)-EPS) 250,250,100
1740  FCT(X)
1750  IF (FCT(X)-EPS) 250,250,100
1760  FCT(X)
1770  IF (FCT(X)-EPS) 250,250,100
1780  FCT(X)
1790  IF (FCT(X)-EPS) 250,250,100
1800  FCT(X)
1810  IF (FCT(X)-EPS) 250,250,100
1820  FCT(X)
1830  IF (FCT(X)-EPS) 250,250,100
1840  FCT(X)
1850  IF (FCT(X)-EPS) 250,250,100
1860  FCT(X)
1870  IF (FCT(X)-EPS) 250,250,100
1880  FCT(X)
1890  IF (FCT(X)-EPS) 250,250,100
1900  FCT(X)
1910  IF (FCT(X)-EPS) 250,250,100
1920  FCT(X)
1930  IF (FCT(X)-EPS) 250,250,100
1940  FCT(X)
1950  IF (FCT(X)-EPS) 250,250,100
1960  FCT(X)
1970  IF (FCT(X)-EPS) 250,250,100
1980  FCT(X)
1990  IF (FCT(X)-EPS) 250,250,100
2000  FCT(X)

```

411600
 411600
 411600
 411600
 411600
 411600

APPENDIX E
TASK III DATA

POLUT-1 AB 0317611TMM 8139140J # 4941 000140Z = 515900J N39.0 W096.0
2E480'1 AB 0317614TMM 8139140J 700000Z = 515900J N39.0 W096.0

END

FORWARD READING, INFER CONCEPTS

110

607011 AB 03174117W 8130440J 03W41 10000000 0 8130440J 0000 00000000
030001 AB 03174117W 8130440J 03W41 10000000 0 8130440J 031 0 10000000

1448 CO. 12813 \$1381.03 8341 2404203

1970	1971	1972	1973	1974	1975	1976	1977	1978	1979	1980	1981	1982	1983	1984	1985	1986	1987	1988	1989	1990	1991	1992	1993	1994	1995	1996	1997	1998	1999	2000	2001	2002	2003	2004	2005	2006	2007	2008	2009	2010	2011	2012	2013	2014	2015	2016	2017	2018	2019	2020	2021	2022	2023	2024	2025	2026	2027	2028	2029	2030	2031	2032	2033	2034	2035	2036	2037	2038	2039	2040	2041	2042	2043	2044	2045	2046	2047	2048	2049	2050	2051	2052	2053	2054	2055	2056	2057	2058	2059	2060	2061	2062	2063	2064	2065	2066	2067	2068	2069	2070	2071	2072	2073	2074	2075	2076	2077	2078	2079	2080	2081	2082	2083	2084	2085	2086	2087	2088	2089	2090	2091	2092	2093	2094	2095	2096	2097	2098	2099	2100	2101	2102	2103	2104	2105	2106	2107	2108	2109	2110	2111	2112	2113	2114	2115	2116	2117	2118	2119	2120	2121	2122	2123	2124	2125	2126	2127	2128	2129	2130	2131	2132	2133	2134	2135	2136	2137	2138	2139	2140	2141	2142	2143	2144	2145	2146	2147	2148	2149	2150	2151	2152	2153	2154	2155	2156	2157	2158	2159	2160	2161	2162	2163	2164	2165	2166	2167	2168	2169	2170	2171	2172	2173	2174	2175	2176	2177	2178	2179	2180	2181	2182	2183	2184	2185	2186	2187	2188	2189	2190	2191	2192	2193	2194	2195	2196	2197	2198	2199	2200	2201	2202	2203	2204	2205	2206	2207	2208	2209	2210	2211	2212	2213	2214	2215	2216	2217	2218	2219	2220	2221	2222	2223	2224	2225	2226	2227	2228	2229	2230	2231	2232	2233	2234	2235	2236	2237	2238	2239	2240	2241	2242	2243	2244	2245	2246	2247	2248	2249	2250	2251	2252	2253	2254	2255	2256	2257	2258	2259	2260	2261	2262	2263	2264	2265	2266	2267	2268	2269	2270	2271	2272	2273	2274	2275	2276	2277	2278	2279	2280	2281	2282	2283	2284	2285	2286	2287	2288	2289	2290	2291	2292	2293	2294	2295	2296	2297	2298	2299	2300	2301	2302	2303	2304	2305	2306	2307	2308	2309	2310	2311	2312	2313	2314	2315	2316	2317	2318	2319	2320	2321	2322	2323	2324	2325	2326	2327	2328	2329	2330	2331	2332	2333	2334	2335	2336	2337	2338	2339	2340	2341	2342	2343	2344	2345	2346	2347	2348	2349	2350	2351	2352	2353	2354	2355	2356	2357	2358	2359	2360	2361	2362	2363	2364	2365	2366	2367	2368	2369	2370	2371	2372	2373	2374	2375	2376	2377	2378	2379	2380	2381	2382	2383	2384	2385	2386	2387	2388	2389	2390	2391	2392	2393	2394	2395	2396	2397	2398	2399	2400	2401	2402	2403	2404	2405	2406	2407	2408	2409	2410	2411	2412	2413	2414	2415	2416	2417	2418	2419	2420	2421	2422	2423	2424	2425	2426	2427	2428	2429	2430	2431	2432	2433	2434	2435	2436	2437	2438	2439	2440	2441	2442	2443	2444	2445	2446	2447	2448	2449	2450	2451	2452	2453	2454	2455	2456	2457	2458	2459	2460	2461	2462	2463	2464	2465	2466	2467	2468	2469	2470	2471	2472	2473	2474	2475	2476	2477	2478	2479	2480	2481	2482	2483	2484	2485	2486	2487	2488	2489	2490	2491	2492	2493	2494	2495	2496	2497	2498	2499	2500	2501	2502	2503	2504	2505	2506	2507	2508	2509	2510	2511	2512	2513	2514	2515	2516	2517	2518	2519	2520	2521	2522	2523	2524	2525	2526	2527	2528	2529	2530	2531	2532	2533	2534	2535	2536	2537	2538	2539	2540	2541	2542	2543	2544	2545	2546	2547	2548	2549	2550	2551	2552	2553	2554	2555	2556	2557	2558	2559	2560	2561	2562	2563	2564	2565	2566	2567	2568	2569	2570	2571	2572	2573	2574	2575	2576	2577	2578	2579	2580	2581	2582	2583	2584	2585	2586	2587	2588	2589	2590	2591	2592	2593	2594	2595	2596	2597	2598	2599	2600	2601	2602	2603	2604	2605	2606	2607	2608	2609	2610	2611	2612	2613	2614	2615	2616	2617	2618	2619	2620	2621	2622	2623	2624	2625	2626	2627	2628	2629	2630	2631	2632	2633	2634	2635	2636	2637	2638	2639	2640	2641	2642	2643	2644	2645	2646	2647	2648	2649	2650	2651	2652	2653	2654	2655	2656	2657	2658	2659	2660	2661	2662	2663	2664	2665	2666	2667	2668	2669	2670	2671	2672	2673	2674	2675	2676	2677	2678	2679	2680	2681	2682	2683	2684	2685	2686	2687	2688	2689	2690	2691	2692	2693	2694	2695	2696	2697	2698	2699	2700	2701	2702	2703	2704	2705	2706	2707	2708	2709	2710	2711	2712	2713	2714	2715	2716	2717	2718	2719	2720	2721	2722	2723	2724	2725	2726	2727	2728	2729	2730	2731	2732	2733	2734	2735	2736	2737	2738	2739	2740	2741	2742	2743	2744	2745	2746	2747	2748	2749	2750	2751	2752	2753	2754	2755	2756	2757	2758	2759	2760	2761	2762	2763	2764	2765	2766	2767	2768	2769	2770	2771	2772	2773	2774	2775	2776	2777	2778	2779	2780	2781	2782	2783	2784	2785	2786	2787	2788	2789	2790	2791	2792	2793	2794	2795	2796	2797	2798	2799	2800	2801	2802	2803	2804	2805	2806	2807	2808	2809	2810	2811	2812	2813	2814	2815	2816	2817	2818	2819	2820	2821	2822	2823	2824	2825	2826	2827	2828	2829	2830	2831	2832	2833	2834	2835	2836	2837	2838	2839	2840	2841	2842	2843	2844	2845	2846	2847	2848	2849	2850	2851	2852	2853	2854	2855	2856	2857	2858	2859	2860	2861	2862	2863	2864	2865	2866	2867	2868	2869	2870	2871	2872	2873	2874	2875	2876	2877	2878	2879	2880	2881	2882	2883	2884	2885	2886	2887	2888	2889	2890	2891	2892	2893	2894	2895	2896	2897	2898	2899	2900	2901	2902	2903	2904	2905	2906	2907	2908	2909	2910	2911	2912	2913	2914	2915	2916	2917	2918	2919	2920	2921	2922	2923	2924	2925	2926	2927	2928	2929	2930	2931	2932	2933	2934	2935	2936	2937	2938	2939	2940	2941	2942	2943	2944	2945	2946	2947	2948	2949	2950	2951	2952	2953	2954	2955	2956	2957	2958	2959	2960	2961	2962	2963	2964	2965	2966	2967	2968	2969	2970	2971	2972	2973	2974	2975	2976	2977	2978	2979	2980	2981	2982	2983	2984	2985	2986	2987	2988	2989	2990	2991	2992	2993	2994	2995	2996	2997	2998	2999	3000	3001	3002	3003	3004	3005	3006	3007	3008	3009	3010	3011	3012	3013	3014	3015	3016	3017	3018	3019	3020	3021	3022	3023	3024	3025	3026	3027	3028	3029	3030	3031	3032	3033	3034	3035	3036	3037	3038	3039	3040	3041	3042	3043	3044	3045	3046	3047	3048	3049	3050	3051	3052	3053	3054	3055	3056	3057	3058	3059	3060	3061	3062	3063	3064	3065	3066	3067	3068	3069	3070	3071	3072	3073	3074	3075	3076	3077	3078	3079	3080	3081	3082	3083	3084	3085	3086	3087	3088	3089	3090	3091	3092	3093	3094	3095	3096	3097	3098	3099	3100	3101	3102	3103	3104	3105	3106	3107	3108	3109	3110	3111	3112	3113	3114	3115	3116	3117	3118	3119	3120	3121	3122	3123	3124	3125	3126	3127	3128	3129	3130	3131	3132	3133	3134	3135	3136	3137	3138	3139	3140	3141	3142	3143	3144	3145	3146	3147	3148	3149	3150	3151	3152	3153	3154	3155	3156	3157	3158	3159	3160	3161	3162	3163	3164	3165	3166	3167	3168	3169	3170	3171	3172	3173	3174	3175	3176	3177	3178	3179	3180	3181	3182	3183	3184	3185	3186	3187	3188	3189	3190	3191	3192	3193	3194	3195	3196	3197	3198	3199	3200	3201	3202	3203	3204	3205	3206	3207	3208	3209	3210	3211	3212	3213	3214	3215	3216	3217	3218	3219	3220	3221	3222	3223	3224	3225	3226	3227	3228	3229	3230	3231	3232	3233	3234	3235	3236	3237	3238	3239	3240	3241	3242	3243	3244	3245	3246	3247	3248	3249	3250	3251	3252	3253	3254	3255	3256	3257	3258	3259	3260	3261	3262	3263	3264	3265	3266	3267	3268	3269	3270	3271	3272	3273	3274	3275	3276	3277	3278	3279	3280	3281	3282	3283	3284	3285	3286	3287	3288	3289	3290	3291	3292	3293	3294	3295	3296	3297	3298	3299	3300	3301	3302	3303	3304	3305	3306	3307	3308	3309	3310	3311	3312	3313	3314	3315	3316	3317	3318	3319	3320	3321	3322	3323	3324	3325	3326	3327	3328	3329	3330	3331	3332	3333	3334	3335	3336	3337	3338	3339	3340	3341	3342	3343	3344	334
------	------	------	------	------	------	------	------	------	------	------	------	------	------	------	------	------	------	------	------	------	------	------	------	------	------	------	------	------	------	------	------	------	------	------	------	------	------	------	------	------	------	------	------	------	------	------	------	------	------	------	------	------	------	------	------	------	------	------	------	------	------	------	------	------	------	------	------	------	------	------	------	------	------	------	------	------	------	------	------	------	------	------	------	------	------	------	------	------	------	------	------	------	------	------	------	------	------	------	------	------	------	------	------	------	------	------	------	------	------	------	------	------	------	------	------	------	------	------	------	------	------	------	------	------	------	------	------	------	------	------	------	------	------	------	------	------	------	------	------	------	------	------	------	------	------	------	------	------	------	------	------	------	------	------	------	------	------	------	------	------	------	------	------	------	------	------	------	------	------	------	------	------	------	------	------	------	------	------	------	------	------	------	------	------	------	------	------	------	------	------	------	------	------	------	------	------	------	------	------	------	------	------	------	------	------	------	------	------	------	------	------	------	------	------	------	------	------	------	------	------	------	------	------	------	------	------	------	------	------	------	------	------	------	------	------	------	------	------	------	------	------	------	------	------	------	------	------	------	------	------	------	------	------	------	------	------	------	------	------	------	------	------	------	------	------	------	------	------	------	------	------	------	------	------	------	------	------	------	------	------	------	------	------	------	------	------	------	------	------	------	------	------	------	------	------	------	------	------	------	------	------	------	------	------	------	------	------	------	------	------	------	------	------	------	------	------	------	------	------	------	------	------	------	------	------	------	------	------	------	------	------	------	------	------	------	------	------	------	------	------	------	------	------	------	------	------	------	------	------	------	------	------	------	------	------	------	------	------	------	------	------	------	------	------	------	------	------	------	------	------	------	------	------	------	------	------	------	------	------	------	------	------	------	------	------	------	------	------	------	------	------	------	------	------	------	------	------	------	------	------	------	------	------	------	------	------	------	------	------	------	------	------	------	------	------	------	------	------	------	------	------	------	------	------	------	------	------	------	------	------	------	------	------	------	------	------	------	------	------	------	------	------	------	------	------	------	------	------	------	------	------	------	------	------	------	------	------	------	------	------	------	------	------	------	------	------	------	------	------	------	------	------	------	------	------	------	------	------	------	------	------	------	------	------	------	------	------	------	------	------	------	------	------	------	------	------	------	------	------	------	------	------	------	------	------	------	------	------	------	------	------	------	------	------	------	------	------	------	------	------	------	------	------	------	------	------	------	------	------	------	------	------	------	------	------	------	------	------	------	------	------	------	------	------	------	------	------	------	------	------	------	------	------	------	------	------	------	------	------	------	------	------	------	------	------	------	------	------	------	------	------	------	------	------	------	------	------	------	------	------	------	------	------	------	------	------	------	------	------	------	------	------	------	------	------	------	------	------	------	------	------	------	------	------	------	------	------	------	------	------	------	------	------	------	------	------	------	------	------	------	------	------	------	------	------	------	------	------	------	------	------	------	------	------	------	------	------	------	------	------	------	------	------	------	------	------	------	------	------	------	------	------	------	------	------	------	------	------	------	------	------	------	------	------	------	------	------	------	------	------	------	------	------	------	------	------	------	------	------	------	------	------	------	------	------	------	------	------	------	------	------	------	------	------	------	------	------	------	------	------	------	------	------	------	------	------	------	------	------	------	------	------	------	------	------	------	------	------	------	------	------	------	------	------	------	------	------	------	------	------	------	------	------	------	------	------	------	------	------	------	------	------	------	------	------	------	------	------	------	------	------	------	------	------	------	------	------	------	------	------	------	------	------	------	------	------	------	------	------	------	------	------	------	------	------	------	------	------	------	------	------	------	------	------	------	------	------	------	------	------	------	------	------	------	------	------	------	------	------	------	------	------	------	------	------	------	------	------	------	------	------	------	------	------	------	------	------	------	------	------	------	------	------	------	------	------	------	------	------	------	------	------	------	------	------	------	------	------	------	------	------	------	------	------	------	------	------	------	------	------	------	------	------	------	------	------	------	------	------	------	------	------	------	------	------	------	------	------	------	------	------	------	------	------	------	------	------	------	------	------	------	------	------	------	------	------	------	------	------	------	------	------	------	------	------	------	------	------	------	------	------	------	------	------	------	------	------	------	------	------	------	------	------	------	------	------	------	------	------	------	------	------	------	------	------	------	------	------	------	------	------	------	------	------	------	------	------	------	------	------	------	------	------	------	------	------	------	------	------	------	------	------	------	------	------	------	------	------	------	------	------	------	------	------	------	------	------	------	------	------	------	------	------	------	------	------	------	------	------	------	------	------	------	------	------	------	------	------	------	------	------	------	------	------	------	------	------	------	------	------	------	------	------	------	------	------	------	------	------	------	------	------	------	------	------	------	------	------	------	------	------	------	------	------	------	------	------	------	------	------	------	------	------	------	------	------	------	------	------	------	------	------	------	------	------	------	------	------	------	------	------	------	------	------	------	------	------	------	------	------	------	------	------	------	------	------	------	------	------	------	------	------	------	------	------	------	------	------	------	------	------	------	------	------	------	------	------	------	------	------	------	------	------	------	------	------	------	------	------	------	------	------	------	------	------	------	------	------	------	------	------	------	------	------	------	------	------	------	------	------	------	------	------	------	------	------	------	------	------	------	------	------	------	------	------	------	------	------	------	------	------	------	------	------	------	------	------	------	------	------	------	------	------	------	------	------	------	------	------	------	------	------	------	------	------	------	------	------	------	------	------	------	------	------	------	------	------	------	------	------	------	------	------	------	------	------	------	------	------	------	------	------	------	------	------	------	------	------	------	------	------	------	------	------	------	------	------	------	------	------	------	------	------	------	------	------	------	------	------	------	------	------	------	------	------	------	------	------	------	------	------	------	------	------	------	------	------	------	------	------	------	------	------	------	------	------	------	------	------	------	------	------	------	------	------	------	------	------	------	------	------	------	------	------	------	------	------	------	------	------	------	------	------	------	------	------	------	------	------	------	------	------	------	------	------	------	------	------	------	------	------	------	------	------	------	------	------	------	------	------	------	------	------	------	------	------	------	------	------	------	------	------	------	------	------	------	------	------	------	------	------	------	------	------	------	------	------	------	------	------	------	------	------	------	------	------	------	------	------	------	------	------	------	------	------	------	------	------	------	------	------	------	------	------	------	------	------	------	------	------	------	------	------	------	------	------	------	------	------	------	------	------	------	------	-----

001011 00 0317041700 030001 00000000 0300000000 00000000
20000001 00 0317041700 030001 00000000 0300000000 00000000

OFF BEARING, LOWER CONTACT

FORWARD, HAVE COURAGE

ENDURANCE TEST NO. 2
OIL = APIFZON A +ANTI +LEAD NAPH
BEARING THICKNESS = STD
INITIAL OIL FILM THICKNESS = THICK
LOAD(N) = 200
SPEED(RPM) = 100
CENTRAL OUTER CONTACTS = CENTRAL INNER CONTACTS MULTIPLIED BY 1.04432
MINIMUM OUTER CONTACTS = MINIMUM INNER CONTACTS MULTIPLIED BY 1.10109

FILM THICKNESSES ARE IN MICROMETERS																		
AFT BEARING, INNER CONTACTS										FORWARD BEARING, INNER CONTACTS								
TEST	TIME (HR)	PRESSURE (PASCAL)	TORQUE (N-m)	SPEED (RPM)	TEMPA (C)	BHCAI	XCENI	TCENI	RHMAI	XMINI	TMINI	TEMPF (C)	HMCFI	XCENI	TCENI	RHMFI	TMINI	
	0	1.3E-04	.297	24.00	25.0	.068	.095	.192	.060	.087	.163	25.0	.068	.095	.192	.060	.087	.163
	2	1.3E-04	.191	28.00	25.6	.074	.109	.187	.055	.100	.159	26.1	.072	.106	.182	.044	.098	.155
	4	1.6E-04	.205	15.00	27.2	.043	.065	.173	.039	.061	.148	28.9	.040	.061	.160	.037	.057	.138
	24	2.1E-04	.233	23.00	28.3	.054	.090	.164	.050	.084	.141	30.6	.051	.081	.148	.054	.084	.124
	30	1.6E-04	.164	30.00	28.3	.068	.105	.164	.061	.097	.141	30.6	.062	.095	.148	.055	.084	.124
	48	1.6E-04	.134	21.00	27.8	.054	.076	.168	.048	.071	.144	30.0	.049	.064	.152	.044	.064	.132
	76	1.3E-04	.177	18.00	27.8	.048	.079	.168	.043	.074	.144	30.0	.043	.071	.152	.040	.074	.132
	144	1.3E-04	.164	40.00	28.3	.084	.143	.164	.074	.133	.141	30.6	.076	.129	.148	.068	.121	.124
	168	1.2E-04	.162	28.00	27.8	.066	.092	.168	.059	.085	.144	31.1	.057	.079	.145	.052	.074	.126
	192	1.4E-04	.191	26.00	28.9	.060	.108	.160	.054	.101	.138	31.7	.053	.094	.141	.048	.098	.123
	216	1.3E-04	.177	28.00	29.4	.062	.104	.156	.055	.097	.135	31.7	.056	.094	.141	.050	.084	.123
	288	1.2E-04	.198	26.00	31.1	.054	.108	.145	.049	.102	.126	33.4	.048	.096	.128	.044	.094	.113
	312	1.1E-04	.177	30.00	30.6	.062	.115	.148	.055	.108	.129	32.8	.056	.104	.135	.051	.098	.118
	336	1.3E-04	.160	36.00	28.3	.078	.128	.164	.064	.128	.141	31.1	.064	.121	.145	.061	.114	.126
	360	1.2E-04	.127	36.00	27.8	.070	.130	.168	.042	.121	.144	30.6	.070	.108	.148	.063	.101	.124
	384	1.2E-04	.162	30.00	27.8	.065	.094	.168	.058	.092	.144	30.6	.062	.114	.148	.055	.104	.124
	456	9.5E-05	.162	27.00	27.8	.065	.123	.168	.058	.092	.144	31.1	.056	.095	.145	.050	.084	.126
	480	1.1E-04	.134	30.00	27.8	.070	.123	.168	.062	.115	.144	30.0	.063	.111	.152	.057	.105	.132
	504	1.1E-04	.191	10.00	26.7	.033	.083	.177	.030	.083	.152	28.3	.031	.079	.164	.028	.077	.141
	528	9.3E-05	.191	28.00	26.1	.072	.125	.182	.064	.116	.155	27.8	.066	.115	.168	.059	.104	.144
	552	8.8E-05	.198	29.00	26.7	.072	.123	.177	.064	.163	.152	28.9	.065	.155	.160	.058	.149	.138
	624	8.7E-05	.191	30.00	27.2	.087	.182	.173	.077	.171	.188	29.4	.078	.165	.156	.070	.154	.135
	672	9.1E-05	.113	24.00	27.2	.061	.184	.173	.054	.047	.138	30.0	.054	.091	.152	.048	.086	.132
	720	8.4E-05	.134	30.00	28.9	.066	.134	.160	.054	.131	.138	31.1	.060	.126	.145	.054	.120	.124
	792	8.8E-05	.134	32.00	27.8	.073	.104	.168	.065	.100	.144	32.2	.074	.089	.148	.054	.084	.120
	840	7.7E-05	.155	36.00	27.2	.082	.141	.173	.072	.150	.148	29.4	.074	.145	.154	.066	.134	.135
	888	7.5E-05	.106	28.00	27.8	.066	.141	.168	.054	.133	.144	31.1	.057	.121	.145	.052	.116	.126
	970	7.2E-05	.191	30.00	30.0	.063	.131	.152	.057	.124	.132	30.8	.046	.116	.135	.041	.111	.118
	1018	8.0E-05	.184	31.00	28.3	.070	.184	.164	.062	.141	.141	31.1	.062	.132	.145	.055	.125	.126
	1066	6.7E-05	.191	30.00	27.8	.077	.156	.168	.068	.147	.144	30.6	.047	.138	.148	.060	.130	.124
	1138	6.7E-05	.134	19.00	26.7	.053	.154	.177	.047	.150	.152	28.9	.048	.141	.160	.043	.134	.138
	1186	7.7E-05	.191	14.00	26.1	.054	.150	.182	.047	.143	.155	28.3	.044	.135	.164	.044	.130	.141
	1234	6.7E-05	.134	22.00	28.9	.053	.148	.160	.048	.142	.138	31.1	.048	.134	.145	.044	.124	.126
	1306	6.7E-05	.198	25.00	27.8	.061	.168	.168	.055	.159	.144	31.1	.053	.144	.145	.048	.134	.124
	1354	5.4E-05	.094	25.00	30.0	.055	.160	.142	.050	.154	.132	32.8	.049	.142	.145	.045	.132	.118
	1402	6.0E-05	.113	25.00	32.2	.050	.129	.138	.046	.124	.120	35.0	.045	.115	.123	.041	.111	.104
	1488	6.0E-05	.120	20.00	35.0	.038	.143	.123	.035	.138	.108	37.8	.034	.127	.110	.032	.124	.097
	1560	5.4E-05	.190	24.00	30.0	.054	.127	.152	.048	.121	.132	35.8	.047	.113	.135	.043	.104	.118
	1632	4.8E-05	.095	29.00	29.4	.063	.160	.156	.057	.152	.135	32.2	.056	.141	.138	.051	.135	.120

ENDURANCE TEST NO. 2
OIL = APIFZON A +ANTI +LEAD NAPH
RESIST- C RUGHNESS = STD
INITIAL OIL FILM THICKNESS = THICK
LOAD(N) = 890
SPEED(RPM) = 100
CENTRAL OUTER CONTACTS = CENTRAL INNER CONTACTS MULTIPLIED BY 1.08432
MINIMUM OUTER CONTACTS = MINIMUM INNER CONTACTS MULTIPLIED BY 1.10109

FILM THICKNESSES ARE IN MICROMETERS

4FT BEARING, INNER CONTACTS										FORWARD BEARING, INNER CONTACTS											
TEST TIME		PRESSURE (N-M)		TORQUE (N-M)		BASE SPEED (RPM)		TEMP (C)		HMCAI		XCENI		TCENI		BHMEI		XMENI		TMENI	
1228		4.71-05		.113		32.00		30.0		.054		.145		.152		.059		.132		.118	
1800		4.51-05		.134		24.00		26.7		.053		.165		.173		.054		.158		.132	
1846		4.71-05		.177		24.00		27.2		.070		.174		.173		.062		.165		.148	
2040		4.31-05		.106		20.00		26.7		.055		.134		.177		.049		.128		.152	
2160		4.71-05		.099		25.00		26.7		.065		.184		.177		.057		.175		.152	
2304		3.61-05		.120		22.00		26.1		.060		.138		.182		.054		.130		.155	
2400		3.71-05		.106		26.00		26.1		.068		.135		.182		.061		.127		.155	
2446		3.51-05		.092		17.00		26.1		.050		.117		.182		.045		.111		.155	
2568		4.01-05		.085		26.00		27.8		.063		.151		.168		.054		.154		.144	
2648		3.21-05		.092		20.00		26.1		.056		.134		.182		.050		.127		.155	
2808		3.31-05		.092		24.00		26.1		.064		.178		.182		.057		.170		.155	
2904		2.71-05		.092		16.00		25.0		.051		.112		.192		.045		.111		.163	
3048		2.91-05		.099		21.00		26.7		.057		.124		.177		.051		.117		.152	
3182		2.91-05		.106		22.00		26.7		.059		.101		.177		.053		.094		.152	
3336		2.81-05		.094		22.00		27.2		.057		.109		.173		.051		.103		.148	
3576		2.91-05		.127		26.00		26.7		.066		.134		.177		.059		.126		.152	
3816		2.91-05		.092		21.00		27.2		.055		.104		.173		.050		.097		.148	
3912		2.01-05		.106		22.00		26.7		.059		.101		.177		.053		.094		.152	
4056		2.71-05		.099		15.00		27.2		.043		.127		.173		.039		.122		.149	
4200		2.41-05		.085		15.00		27.2		.043		.121		.173		.039		.116		.148	

ENDURANCE TEST NO. 2
OIL = APIECON A 40WT 4LEAD NAPH
WEARING SURFACES = STN
INITIAL OIL FILM THICKNESS = THICK
LOAD(LBS) = 200
SPEED(RPM) = 100
CENTRAL OUTER CONTACTS = CENTRAL INNER CONTACTS MULTIPLIED BY 1.08432
MINIMUM OUTER CONTACTS = MINIMUM INNER CONTACTS MULTIPLIED BY 1.10109

FILM THICKNESSES ARE IN MICROINCHES									
AFT BEARING, INNER CONTACTS					FORWARD BEARING, INNER CONTACTS				
TEST TIME (HR)	PRESSURE (T-MIN)	TORQUE (OZ-IN)	SPEED (RPM)	TEMP (F)	BMCFI	XCENI	TCENI	YMINI	YMAXI
0 1.0E-04	42.00	24.00	24.00	77.0	2.67	3.71	7.58	6.43	2.37
2 1.0E-04	24.00	24.00	24.00	78.0	2.91	3.49	7.37	6.27	2.51
4 1.0E-04	24.00	24.00	24.00	81.0	1.70	2.57	6.80	5.83	1.94
6 1.0E-04	24.00	24.00	24.00	83.0	2.21	3.30	6.46	5.55	2.34
8 1.0E-04	24.00	24.00	24.00	83.0	2.68	3.81	6.46	5.55	2.74
10 1.0E-04	24.00	24.00	24.00	82.0	2.12	3.39	6.63	5.69	2.19
12 1.0E-04	24.00	24.00	24.00	82.0	1.40	2.70	6.63	5.69	1.56
14 1.0E-04	24.00	24.00	24.00	83.0	3.31	3.91	6.63	5.55	3.26
16 1.0E-04	24.00	24.00	24.00	82.0	2.62	3.33	6.63	5.55	2.62
18 1.0E-04	24.00	24.00	24.00	82.0	2.35	3.48	6.24	5.42	2.35
20 1.0E-04	24.00	24.00	24.00	82.0	2.62	3.81	6.14	5.30	2.62
22 1.0E-04	24.00	24.00	24.00	83.0	2.13	3.03	6.24	5.42	2.13
24 1.0E-04	24.00	24.00	24.00	83.0	2.92	3.72	6.46	5.55	2.92
26 1.0E-04	24.00	24.00	24.00	83.0	3.06	3.72	6.46	5.55	3.06
28 1.0E-04	24.00	24.00	24.00	82.0	2.75	3.42	6.63	5.69	2.75
30 1.0E-04	24.00	24.00	24.00	82.0	2.55	3.27	6.63	5.69	2.55
32 1.0E-04	24.00	24.00	24.00	82.0	2.75	3.42	6.46	5.42	2.75
34 1.0E-04	24.00	24.00	24.00	82.0	1.30	3.25	6.46	5.42	1.30
36 1.0E-04	24.00	24.00	24.00	82.0	2.83	3.57	6.46	5.42	2.83
38 1.0E-04	24.00	24.00	24.00	82.0	2.83	3.57	6.46	5.42	2.83
40 1.0E-04	24.00	24.00	24.00	81.0	3.42	3.81	6.46	5.42	3.42
42 1.0E-04	24.00	24.00	24.00	81.0	2.90	3.42	6.46	5.42	2.90
44 1.0E-04	24.00	24.00	24.00	82.0	2.61	3.24	6.24	5.42	2.61
46 1.0E-04	24.00	24.00	24.00	82.0	2.84	3.54	6.63	5.69	2.84
48 1.0E-04	24.00	24.00	24.00	82.0	2.23	3.23	6.63	5.69	2.23
50 1.0E-04	24.00	24.00	24.00	82.0	2.75	3.42	6.46	5.42	2.75
52 1.0E-04	24.00	24.00	24.00	82.0	3.02	3.67	6.63	5.69	3.02
54 1.0E-04	24.00	24.00	24.00	82.0	2.08	3.01	6.46	5.42	2.08
56 1.0E-04	24.00	24.00	24.00	82.0	2.13	3.01	6.46	5.42	2.13
58 1.0E-04	24.00	24.00	24.00	82.0	2.08	3.01	6.46	5.42	2.08
60 1.0E-04	24.00	24.00	24.00	82.0	2.08	3.01	6.46	5.42	2.08
62 1.0E-04	24.00	24.00	24.00	82.0	2.08	3.01	6.46	5.42	2.08
64 1.0E-04	24.00	24.00	24.00	82.0	2.08	3.01	6.46	5.42	2.08
66 1.0E-04	24.00	24.00	24.00	82.0	2.08	3.01	6.46	5.42	2.08
68 1.0E-04	24.00	24.00	24.00	82.0	2.08	3.01	6.46	5.42	2.08
70 1.0E-04	24.00	24.00	24.00	82.0	2.08	3.01	6.46	5.42	2.08
72 1.0E-04	24.00	24.00	24.00	82.0	2.08	3.01	6.46	5.42	2.08
74 1.0E-04	24.00	24.00	24.00	82.0	2.08	3.01	6.46	5.42	2.08
76 1.0E-04	24.00	24.00	24.00	82.0	2.08	3.01	6.46	5.42	2.08
78 1.0E-04	24.00	24.00	24.00	82.0	2.08	3.01	6.46	5.42	2.08
80 1.0E-04	24.00	24.00	24.00	82.0	2.08	3.01	6.46	5.42	2.08
82 1.0E-04	24.00	24.00	24.00	82.0	2.08	3.01	6.46	5.42	2.08
84 1.0E-04	24.00	24.00	24.00	82.0	2.08	3.01	6.46	5.42	2.08
86 1.0E-04	24.00	24.00	24.00	82.0	2.08	3.01	6.46	5.42	2.08
88 1.0E-04	24.00	24.00	24.00	82.0	2.08	3.01	6.46	5.42	2.08
90 1.0E-04	24.00	24.00	24.00	82.0	2.08	3.01	6.46	5.42	2.08
92 1.0E-04	24.00	24.00	24.00	82.0	2.08	3.01	6.46	5.42	2.08
94 1.0E-04	24.00	24.00	24.00	82.0	2.08	3.01	6.46	5.42	2.08
96 1.0E-04	24.00	24.00	24.00	82.0	2.08	3.01	6.46	5.42	2.08
98 1.0E-04	24.00	24.00	24.00	82.0	2.08	3.01	6.46	5.42	2.08
100 1.0E-04	24.00	24.00	24.00	82.0	2.08	3.01	6.46	5.42	2.08

Endurance Test No. 2
Oil & Spiffon & Anti-Oxidant
Operating Conditions & STD
Initial Oil Film Thickness & TWICA
(Initial) & 200
Speed (rpm) & 180
Central Outer Contacts & Central Inner Contacts Multiplied by 1.00432
Minimum C-Ten Contacts & Minimum Inner Contacts Multiplied by 1.10104

FILM THICKNESSES ARE IN MICRONS

TEST TIME (mm)	PRESSURE (lb-in)	TORQUE (lb-in)	WAVE SPREAD (mm)	AFT BEARING, INNER CONTACTS				FORWARD BEARING, INNER CONTACTS									
				BMCAI	ICCAI	TCMAI	RMCAI	RMIMI	TMIMI	TEMP (°F)	HMCAI	ICCAI	TCMAI	RMCAI	RMIMI	TMIMI	TEMP (°F)
1720	1.54-07	14.00	12.00	2.40	5.72	5.98	2.33	5.91	5.18	41.0	2.31	5.06	5.40	2.14	2.14	5.06	5.63
1800	1.01-07	14.00	24.00	2.46	6.55	6.94	2.20	6.20	5.97	64.0	2.11	5.61	5.48	1.41	1.41	5.38	5.18
1800	2.01-07	25.00	24.00	2.76	6.34	6.80	2.55	6.04	5.83	85.0	2.04	6.17	6.14	2.23	2.23	5.91	5.30
2000	1.21-07	14.00	24.00	2.16	5.24	6.44	1.93	5.03	5.97	85.0	1.90	6.45	6.14	1.22	1.22	6.87	5.30
2100	2.51-07	14.00	25.00	2.54	7.24	6.44	2.26	6.44	5.97	83.0	2.35	6.70	6.14	2.10	2.10	6.91	5.55
2100	2.51-07	17.00	25.00	2.30	5.93	7.18	2.12	5.14	6.12	82.0	2.14	5.02	6.23	1.97	1.97	6.78	5.64
2100	2.51-07	15.00	26.00	2.68	5.31	7.18	2.38	5.01	6.12	83.0	2.92	6.80	6.63	2.14	2.14	6.55	5.55
2100	2.51-07	13.00	17.00	1.97	6.60	7.18	1.77	6.36	6.12	84.0	2.35	6.04	6.24	1.11	1.11	5.77	5.62
2100	2.51-07	12.00	26.00	2.08	6.36	6.63	2.21	6.05	5.64	84.0	2.35	6.04	6.24	1.65	1.65	5.95	5.55
2100	2.51-07	13.00	24.00	2.22	5.27	7.18	1.98	6.00	6.12	82.0	2.05	6.87	6.43	1.44	1.44	6.44	5.64
2100	2.51-07	13.00	24.00	2.53	7.00	7.18	2.25	6.44	6.12	82.0	2.34	6.47	6.43	2.04	2.04	6.22	5.64
2100	2.51-07	13.00	14.00	1.94	6.62	7.58	1.78	6.37	6.43	80.0	1.83	6.24	6.44	1.44	1.44	6.06	5.97
2100	2.51-07	16.00	14.00	2.20	6.86	6.44	2.00	6.54	5.97	83.0	2.07	6.50	6.44	1.44	1.44	6.27	5.55
2100	2.51-07	15.00	22.00	2.31	3.97	6.44	2.07	3.70	5.97	83.0	2.08	3.54	6.24	1.44	1.44	1.37	5.55
2200	2.51-07	16.00	22.00	2.25	9.24	6.44	2.02	6.04	5.83	84.0	2.35	6.74	6.24	1.44	1.44	1.37	5.55
2200	2.51-07	16.00	24.00	2.61	5.26	6.44	2.32	6.04	5.97	83.0	2.14	6.08	6.24	1.44	1.44	1.37	5.55
2200	2.51-07	16.00	24.00	2.18	11.48	6.44	1.95	11.68	5.83	84.0	2.01	11.04	6.24	1.44	1.44	1.37	5.55
2200	2.51-07	13.00	22.00	2.31	3.97	6.44	2.07	3.70	5.97	84.0	2.08	3.58	6.24	1.44	1.44	1.37	5.55
2200	2.51-07	15.00	22.00	1.70	5.01	6.44	1.54	6.82	5.83	84.0	1.54	6.52	6.14	1.44	1.44	1.37	5.55
2300	2.51-07	16.00	15.00	2.00	6.00	6.44	1.54	6.82	5.83	85.0	1.54	6.52	6.14	1.44	1.44	1.37	5.55
2300	2.51-07	16.00	15.00	1.70	9.76	6.44	1.54	6.82	5.83	84.0	1.58	6.50	6.24	1.44	1.44	1.37	5.55

CENTRAL OVER CONTACTS = CENTRAL INNER CONTACTS MULTIPLIED BY 1.08432
 MINIMUM 0.750 CONTACTS = MINIMUM INNER CONTACTS MULTIPLIED BY 1.10109

FORWARD BEARING, INNER CONTACTS

118

ENDURANCE TEST NO. 3
OIL = RMC 36233
BEARING THICKNESS = .0015
INITIAL OIL FILM THICKNESS = .0015
LOAD(?) = 800
SPEED(RPM) = 100
CENTRAL INNER CONTACTS = CENTRAL INNER CONTACTS MULTIPLIED BY 1.08432
MINIMUM OUTER CONTACTS = MINIMUM INNER CONTACTS MULTIPLIED BY 1.10104

FILM THICKNESSES ARE IN MICROMETERS

TEST				AFT BEARING, INNER CONTACTS				FORWARD BEARING, INNER CONTACTS									
TIME (HRS)	PRESSURE (PSI)	TORQUE (IN-CH)	RPM	TEMPA (C)	RMCAI	XCENI	TCENI	BMCAI	XMCAI	TMCAI	TEMPF (C)	RMCFI	XCENI	TCENI	BMCFI	XMCFI	TMCFI
6004	75-06	.127	25.00	27.8	.166	.337	.458	.143	.311	.378	30.6	.146	.296	.403	.127	.274	.335
6168	75-06	.127	25.00	30.0	.146	.303	.413	.126	.282	.343	33.3	.126	.262	.357	.110	.224	.297
6266	75-06	.155	25.00	30.0	.146	.273	.413	.126	.253	.343	32.8	.124	.262	.365	.112	.224	.304
6360	75-06	.141	25.00	29.4	.150	.245	.424	.137	.271	.351	32.2	.140	.260	.374	.121	.241	.312
6432	75-06	.141	30.00	29.4	.174	.306	.424	.151	.281	.351	33.3	.140	.260	.357	.124	.241	.312
6526	75-06	.177	35.00	29.4	.147	.333	.424	.148	.303	.343	32.2	.140	.260	.374	.104	.264	.312
6600	75-06	.154	25.00	30.0	.137	.274	.413	.114	.255	.343	33.3	.118	.247	.357	.103	.221	.297
6720	75-06	.198	25.00	29.4	.143	.313	.435	.140	.288	.360	31.7	.143	.271	.383	.124	.256	.314
6768	75-06	.106	25.00	29.4	.154	.244	.424	.133	.277	.351	31.7	.149	.271	.383	.121	.252	.314
6800	75-06	.162	25.00	32.0	.137	.261	.365	.114	.241	.304	30.7	.114	.222	.310	.101	.204	.260
6916	75-06	.120	23.00	30.4	.138	.231	.403	.120	.212	.335	33.3	.122	.205	.357	.106	.184	.247
7032	75-06	.092	25.00	31.1	.147	.315	.393	.127	.243	.327	33.3	.133	.206	.357	.116	.267	.297

ENDURANCE TEST NO. 3
 OIL = PHRC 3623
 BEARING RUGHOSS = ROUGH
 INITIAL OIL FILM THICKNESS = THICK
 LOAD(LR) = 200
 SPEED(RPM) = 100
 CENTRAL OUTER CONTACTS = CENTRAL INNER CONTACTS MULTIPLIED BY 1.0832
 MINIMUM OUTER CONTACTS = MINIMUM INNER CONTACTS MULTIPLIED BY 1.10109

FILM THICKNESSES ARE IN MICROINCHES

TEST				AFT BEARING, INNER CONTACTS								FORWARD BEARING, INNER CONTACTS							
TIME (HR)	PRESSURE (T/MIN)	TORQUE (OZ-IN)	SPEED (RPM)	TEMPA (F)	BMCAI	XCENI	TCENI	HMCAI	XMCAI	TMINI	TEMPF (F)	BMCFI	XCENI	TCENI	HMCFI	XMCFI	TMCFI		
0	9.35-07	75.00	16.00	77.0	5.40	12.84	20.57	4.54	12.09	16.91	77.0	5.40	12.84	20.57	4.54	12.09	16.91		
1	1.05-06	98.00	16.00	84.0	4.94	9.51	17.11	3.93	8.41	14.17	84.0	4.94	9.51	17.11	3.93	8.41	14.17		
2	1.25-06	38.00	22.00	98.0	4.88	9.12	14.73	3.25	8.95	12.27	95.0	4.33	8.04	13.08	3.74	7.53	10.44		
25	1.45-06	30.00	24.00	94.0	3.45	7.28	11.93	3.47	6.76	10.01	104.0	3.53	6.51	10.47	3.12	6.08	9.00		
42	1.45-06	21.00	14.00	94.0	3.55	8.10	11.93	3.13	7.44	10.01	104.0	3.14	7.25	10.47	2.41	6.47	9.00		
98	1.25-06	21.00	20.00	97.0	3.86	6.76	12.48	3.34	6.25	10.96	102.0	3.44	6.02	11.15	3.04	5.61	9.34		
76	1.05-06	30.00	16.00	96.0	3.35	6.23	12.78	2.47	5.85	10.70	102.0	2.43	5.48	11.15	2.60	5.13	9.34		
104	1.05-06	24.00	24.00	94.0	4.72	4.16	13.34	4.12	4.51	11.14	94.0	4.21	4.16	11.43	3.64	7.62	10.01		
148	1.05-07	31.00	22.00	95.0	4.33	4.30	13.08	3.74	4.12	10.44	101.0	3.78	4.46	11.40	3.32	8.00	9.54		
142	1.25-06	25.00	12.00	97.0	4.42	7.28	12.48	3.43	6.84	10.96	104.0	2.43	6.23	10.47	2.60	5.84	9.00		
214	1.05-07	27.00	22.00	96.0	4.23	4.31	12.78	3.71	7.77	10.70	103.0	3.61	7.10	10.41	3.14	6.66	9.14		
288	1.25-07	24.00	24.00	95.0	4.84	12.74	13.08	4.26	12.01	10.44	98.0	4.56	11.84	12.20	3.94	11.24	10.23		
312	1.25-07	24.00	22.00	94.0	3.45	10.10	11.93	3.77	9.58	10.01	105.0	3.46	8.85	10.45	3.05	8.43	8.81		
334	1.05-06	24.00	14.00	95.0	3.84	10.28	13.08	3.42	9.77	10.44	101.0	3.34	8.46	11.40	3.00	8.54	9.54		
340	1.05-07	24.00	22.00	95.0	4.34	4.51	13.08	3.74	7.83	10.44	102.0	3.64	7.17	11.15	3.24	8.22	9.34		
345	1.05-07	27.00	24.00	95.0	5.10	10.75	13.08	4.60	4.47	10.44	102.0	4.52	9.17	11.15	3.45	8.54	9.34		
456	1.15-07	31.00	25.00	93.0	4.98	10.42	13.71	4.34	10.14	11.94	94.0	4.63	9.42	11.43	3.74	8.67	10.01		
480	1.05-07	31.00	20.00	93.0	4.23	10.42	12.71	3.71	10.66	11.94	94.0	3.68	9.24	11.43	3.24	8.60	10.01		
504	1.05-07	28.00	14.00	92.0	3.34	4.03	14.04	2.64	5.56	11.71	94.0	2.84	7.67	11.43	2.54	7.32	10.01		
528	1.05-07	24.00	24.00	92.0	5.44	11.60	14.04	4.47	10.74	11.71	94.0	4.83	9.42	11.43	4.21	9.20	10.01		
552	1.05-07	27.00	24.00	93.0	4.84	11.22	13.71	4.21	10.56	11.94	94.0	4.21	9.77	11.43	3.64	9.24	10.01		
624	1.05-07	34.00	24.00	92.0	4.54	11.54	14.14	4.14	10.82	11.71	94.0	4.21	9.40	11.43	3.64	9.25	10.01		
672	1.05-07	30.00	22.00	94.0	4.54	4.54	13.71	3.77	9.38	11.94	100.0	3.66	8.50	11.46	3.44	8.43	9.80		
720	1.05-07	24.00	21.00	94.0	4.28	10.12	13.34	3.75	9.51	11.14	100.0	3.73	8.82	11.46	3.24	8.43	9.80		
744	1.05-07	32.00	14.00	95.0	3.84	4.50	13.08	3.42	8.44	10.44	101.0	3.27	8.44	11.43	3.00	7.84	9.54		
800	1.05-07	26.00	17.00	95.0	3.54	4.31	13.08	3.16	8.41	10.44	94.0	3.27	8.44	11.43	2.40	8.04	10.01		
888	1.05-07	23.00	14.00	94.0	2.64	6.74	11.93	2.40	6.60	10.01	111.0	2.08	5.38	9.20	1.47	5.14	7.80		
976	1.05-07	25.00	14.00	94.0	3.64	7.44	12.20	3.20	7.02	10.23	104.0	3.11	6.41	10.45	2.74	6.04	8.01		
1018	1.05-07	24.00	13.00	94.0	3.02	8.44	13.34	2.68	8.52	11.14	101.0	2.57	7.61	11.40	2.34	7.40	9.54		
1066	1.05-07	24.00	14.00	97.0	3.34	4.21	14.04	2.46	9.34	11.71	94.0	2.49	8.33	11.43	2.53	7.40	10.01		
1130	1.05-07	44.00	22.00	94.0	5.67	14.22	17.11	4.91	13.38	14.17	90.0	4.08	12.24	14.73	4.25	11.54	12.27		
1144	1.05-07	24.00	20.00	85.0	5.15	12.24	16.48	4.98	11.44	13.82	92.0	4.34	10.30	14.04	3.80	9.74	11.71		
1214	1.05-07	53.00	14.00	82.0	5.16	10.24	10.02	4.45	17.74	14.84	92.0	5.36	14.60	18.02	4.65	12.74	14.84		
1246	1.05-07	31.00	22.00	84.0	5.12	10.42	15.47	4.46	10.14	12.84	93.0	4.54	9.68	13.71	4.47	9.04	11.94		
1354	1.05-07	25.00	14.00	93.0	7.55	9.44	13.71	2.28	9.44	11.44	104.0	4.22	8.54	11.43	2.00	8.14	1.71		
1442	1.05-07	25.00	14.00	92.0	3.24	11.24	12.44	2.40	10.83	10.44	104.0	2.80	9.65	10.47	2.44	9.32	9.00		
1488	1.05-07	24.00	17.00	102.0	3.06	4.06	11.15	2.42	8.63	9.34	104.0	2.63	7.74	9.54	2.35	7.97	8.12		
1560	1.05-07	24.00	14.00	94.0	3.04	4.51	12.78	2.70	9.04	10.70	103.0	2.60	8.12	10.41	2.32	7.61	9.14		
1632	1.05-07	25.00	22.00	98.0	4.04	4.91	12.20	3.55	8.88	10.23	104.0	3.53	8.23	10.47	3.12	7.61	9.00		

UNCLASSIFIED//FOR OFFICIAL USE ONLY

543810M31x 41 47V \$3534,021=1 m71f

[illegible]

LIST OF REFERENCES

1. Tyler, J. C., Carper, H. J., Brown, R. D., and Ku, P. M., "Analysis of Film Thickness Effect in Slow-Speed Lightly-Loaded Elastohydrodynamic Contacts," AFML-TR-74-189, Part I, December 1974.
2. Carper, H. J., and Tyler, J. C., "Elastohydrodynamic Film Thickness and Friction in Counterformal Conjunctions," SwRI Rept. RS-595, July 1972.
3. Archard, J. F., and Cowking, E. W., "Elastohydrodynamic Lubrication at Point Contacts," Elastohydrodynamic Lubrication, Proc. IMechE, Vol. 180, Pt. 3B, 1965-66.
4. Westlake, F. J., and Cameron, A., "Interference Study of Point Contact Lubrication," Elastohydrodynamic Lubrication, 1972 Symposium, IMechE, 1972.
5. Cheng, H. S., "Calculation of Elastohydrodynamic Film Thickness in High-Speed Rolling and Sliding Contacts," MTI Rept. 67-24, 1967.
6. Grubin, A. N., and Vinogradova, I. Y. E., "Fundamentals of the Hydrodynamic Theory of Lubrication of Heavily Loaded Cylindrical Surfaces" (in Russian), Gozud, Nauch. Tekh. Izdat. Mashin. Lit., Book No. 30, 1949.
7. Dowson, D., "Elastohydrodynamic Lubrication," Interdisciplinary Approach to the Lubrication of Concentrated Contacts, P. M. Ku, ed., NASA SP-237, 1970.
8. Ku, P. M., and Carper, H. J., "Elements of Elastohydrodynamic Analysis," SwRI Rept. No. RS-601, 1973.
9. Jones, A. B., Analysis of Stresses and Deflections, Vols. I and II, New Departure Division, General Motors Corp., 1946.